

POLITECNICO DI TORINO

Department of Mechanical and Aerospace Engineering



MSc Thesis
in Mechanical Engineering

Finite element modelling of vehicles and human body models for passive safety

Supervisor

Prof. Eng. Alessandro Scattina

Candidate

Davide Soliman

October 2020

Index

Index of Figures	IV
Abstract	VIII
Preface.....	IX
Introduction.....	IX
Thesis purpose.....	IX
Thesis work roadmap	X
Chapter 1	1
1 Literature review	1
1.1 EuroNCAP [3].....	1
1.2 Frontal Full-Width EuroNCAP test	4
1.2.1 Introduction.....	4
1.2.2 Crash test description [6]	4
1.3 Mechanic of the impact and passive safety devices.....	9
Chapter 2.....	10
2 Finite Element models.....	10
2.1 Full-scale 2012 Toyota Camry model.....	10
2.1.1 Introduction [8] [9]	10
2.1.2 Model description [8] [9].....	11
2.1.3 Full-scale EuroNCAP model.....	14
2.2 Sled model.....	17
2.2.1 Introduction.....	17
2.2.2 Sled model description.....	18
2.2.3 Sled environment	19
2.2.4 Sled kinematic.....	32
2.2.5 Sled set-up.....	39

2.3	Human Body Model.....	40
2.3.1	Introduction [12].....	40
2.3.2	THUMS model [13]	41
2.3.3	THUMS instrumentation [14].....	44
2.4	Seatbelt model.....	47
2.4.1	Introduction.....	47
2.4.2	FE seatbelt.....	47
Chapter 3.....		60
3	Pre-simulation processes.....	60
3.1	Introduction.....	60
3.2	Positioning	62
3.2.1	Introduction.....	62
3.2.2	Modelling with PIPER program [17][18][14]	62
3.2.3	Positioning simulation and final THUMS model.....	66
3.3	Sitting simulation	69
3.3.1	Introduction.....	69
3.3.2	Sitting simulation set-up and final seat model	70
3.4	Seatbelt routing	73
3.4.1	Introduction.....	73
3.4.2	Seat belt routing with LS-DYNA.....	73
Chapter 4.....		77
4	Impact test simulation results.....	77
4.1	Comparison between full-scale and sled model without occupant	77
4.1.1	Visual comparison.....	77
4.1.2	Energy balance.....	80
4.1.3	Acceleration comparison.....	81
4.2	Comparison between full-scale and sled model with HBM.....	83

4.2.1	Visual comparison.....	84
4.2.2	Energy balance.....	86
4.2.3	Vehicle kinematics comparison	88
4.2.4	THUMS acceleration comparison.....	91
4.2.5	Seatbelt forces comparison	95
	Conclusions.....	97
	Appendix A.....	99
	Dashboard constraining.....	99
	B-pillar stiffening.....	101
	References.....	102

Index of Figures

Figure 1.1 MPDB crash test [5]	2
Figure 1.2 EuroNCAP rating system	3
Figure 1.3 EuroNCAP - Frontal FW test [3].....	5
Figure 1.4 Vehicle instrumentation - sensors.....	6
Figure 1.5 Dummy instrumentation - sensors	7
Figure 1.6 Left and right foot position [6]	8
Figure 1.7 Seatbelt behaviour during a frontal impact [7]	9
Figure 2.1 Real NCAP crash test and NCAP simulation	10
Figure 2.2 Actual, FE model and details of a 2012 Toyota Camry sedan.....	11
Figure 2.3 Front suspension and steering subsystems.....	12
Figure 2.4 Rear suspension subsystem.....	12
Figure 2.5 Representation of vehicle interior components	13
Figure 2.6 Simple occupant models	14
Figure 2.7 Driver Accelerometer	15
Figure 2.8 Footrest model	16
Figure 2.9 Real sled device	17
Figure 2.10 Vehicle model after disassembling	20
Figure 2.11 Vehicle model after cutting	21
Figure 2.12 Sled structure	23
Figure 2.13 Sled dashboard.....	24
Figure 2.14 Foam cushions	25
Figure 2.15 Foam material curve	25
Figure 2.16 Seat spring frames.....	26
Figure 2.17 Seat frame	26
Figure 2.18 Driver seat.....	27
Figure 2.19 Detail of the front stiffened region	28
Figure 2.20 Detail of the stiffened A-pillar and B-pillar.....	28
Figure 2.21 Detail of the rear stiffened region with respect to the rigid sections	28
Figure 2.22 Rigid section positions.....	29
Figure 2.23 Details of front (a) and rear (b) rigid sections of the left side.....	30
Figure 2.24 Sled model - final configuration	31
Figure 2.25 Detail of rigid sections position in Rigidparts model	32

Figure 2.26 Original EuroNCAP model vs Rigidparts model - Energy balance	33
Figure 2.27 Original EuroNCAP model vs Rigidparts model - Driver sensor - x acceleration ..	33
Figure 2.28 Original EuroNCAP model vs Rigidparts model - Driver sensor - y acceleration ..	34
Figure 2.29 Original EuroNCAP model vs Rigidparts model - Driver sensor - z acceleration ..	34
Figure 2.30 Original EuroNCAP model vs Rigidparts model - velocity FL node	35
Figure 2.31 Original EuroNCAP model vs Rigidparts model - velocity FR node	35
Figure 2.32 Original EuroNCAP model vs Rigidparts model - velocity RL node	36
Figure 2.33 Original EuroNCAP model vs Rigidparts model - velocity RR node	36
Figure 2.34 Rigidparts model - FL rigid section velocity	37
Figure 2.35 Rigidparts model - FR rigid section velocity	37
Figure 2.36 Rigidparts model - RL rigid section velocity	38
Figure 2.37 Rigidparts model - RR rigid section velocity	38
Figure 2.38 Sled model - Driver accelerometer	39
Figure 2.39 Different models of HBM [13]	40
Figure 2.40 THUMS - initial sitting position [13]	41
Figure 2.41 THUMS - head model [13]	42
Figure 2.42 THUMS - Skeletal parts in torso model (with Neck Model) [13]	42
Figure 2.43 THUMS - Soft tissue parts in torso model [13]	43
Figure 2.44 THUMS - Extremity models [13]	43
Figure 2.45 THUMS - Joint model [13]	44
Figure 2.46 Head accelerometer	45
Figure 2.47 Vertebrae accelerometers and detail of the T4 vertebra	45
Figure 2.48 Pelvis accelerometer	46
Figure 2.49 Seatbelt model	48
Figure 2.50 Comparison between actual and FE end belt anchor	50
Figure 2.51 Comparison between actual and FE buckler position	50
Figure 2.52 Comparison between actual and FE D-ring position	51
Figure 2.53 Comparison between actual and FE retractor position	51
Figure 2.54 Segment belt curve	52
Figure 2.55 Main axes of the mesh element in fabric belt model	53
Figure 2.56 Longitudinal curve of the fabric belt model	54
Figure 2.57 lateral curve of the fabric belt model	54
Figure 2.58 Retractor curve	57
Figure 2.59 Pretensioner curve	59

Figure 3.1 original THUMS in vehicle model - side (upper) and section (lower) views.....	60
Figure 3.2 THUMS, seat and seatbelt in final configuration	61
Figure 3.3 Vehicle environment for positioning in PIPER	63
Figure 3.4 THUMS and vehicle environment.....	63
Figure 3.5 Positioning of the THUMS	64
Figure 3.6 THUMS final posture	65
Figure 3.7 THUMS final position	66
Figure 3.8 Details of positioned THUMS in vehicle environment	67
Figure 3.9 Details of the final posture.....	67
Figure 3.10 Initial vs final THUMS position - overlapped view	68
Figure 3.11 Penetration regions between THUMS and driver seat.....	69
Figure 3.12 Comparison between THUMS and simplified skin model.....	70
Figure 3.13 Sitting simulation - initial (upper) and final (lower) simulation step - side and section views	71
Figure 3.14 Sitting simulation and detail of the deformed seat cushion	72
Figure 3.15 THUMS and seat - section view	72
Figure 3.16 Structure, seat, THUMS and seatbelt anchors - FE configuration before routing... ..	74
Figure 3.17 Graphic interface of the Seatbelt Fitting command.....	75
Figure 3.18 Seatbelt details.....	75
Figure 3.19 Seatbelt model at the end of the routing	76
Figure 4.1 Full-scale and sled model - side view - 0 ms.....	77
Figure 4.2 Full-scale and sled model - side view - 20 ms.....	78
Figure 4.3 Full-scale and sled model - side view - 40 ms.....	78
Figure 4.4 Full-scale and sled model - side view - 60 ms.....	78
Figure 4.5 Full-scale and sled model - side view - 80 ms.....	79
Figure 4.6 Full-scale and sled model - side view - 100 ms.....	79
Figure 4.7 Full-scale and sled model - side view - 120 ms.....	79
Figure 4.8 Full-scale model - Global energy plot	80
Figure 4.9 Sled model - Global Energy plot	80
Figure 4.10 Table energy comparison.....	81
Figure 4.11 Sensor - x acceleration.....	81
Figure 4.12 Sensor - y acceleration.....	82
Figure 4.13 Sensor - z acceleration.....	82
Figure 4.14 Sled (upper) and full-scale (lower) model with THUMS	83

Figure 4.15 Full-scale and sled model with THUMS - side section view - 0 ms.....	84
Figure 4.16 Full-scale and sled model with THUMS - side section view - 20 ms.....	84
Figure 4.17 Full-scale and sled model with THUMS - side section view - 40 ms.....	85
Figure 4.18 Full-scale and sled model with THUMS - side section view - 60 ms.....	85
Figure 4.19 Full-scale and sled model with THUMS - side section view - 80 ms.....	85
Figure 4.20 Full-scale and sled model with THUMS - side section view - 100 ms.....	86
Figure 4.21 Full-scale and sled model with THUMS - side section view - 110 ms.....	86
Figure 4.22 Full-scale model - Global energy plot	87
Figure 4.23 Sled model - Global energy plot.....	87
Figure 4.24 Table energy comparison.....	87
Figure 4.25 Velocity in Frontal Left section area	88
Figure 4.26 Velocity in Rear Left section area	88
Figure 4.27 Velocity in Front Right section area.....	89
Figure 4.28 Velocity in Rear Right section area	89
Figure 4.29 Sensor - x acceleration.....	89
Figure 4.30 Sensor - y acceleration.....	90
Figure 4.31 Sensor - z acceleration.....	90
Figure 4.32 Head accelerometer - x acceleration.....	91
Figure 4.33 Head accelerometer - y acceleration.....	91
Figure 4.34 Head accelerometer - z acceleration	92
Figure 4.35 Head accelerometer - resultant acceleration	92
Figure 4.36 Head accelerometer - x rotational acceleration.....	92
Figure 4.37 Head accelerometer - y rotational acceleration.....	93
Figure 4.38 Head accelerometer - z rotational acceleration.....	93
Figure 4.39 Head accelerometer - resultant rotational acceleration.....	93
Figure 4.40 Thorax T1 accelerometer - x acceleration	94
Figure 4.41 Thorax T4 accelerometer - x acceleration	94
Figure 4.42 Thorax T12 accelerometer - x acceleration	94
Figure 4.43 Pelvis accelerometer - x acceleration.....	95
Figure 4.44 Lap belt force.....	95
Figure 4.45 Shoulder belt force.....	96

Abstract

In this thesis, a simplified FE system was modelled in order to reproduce a frontal full-width impact test of a mid-size sedan, according to EuroNCAP regulation. The FE environment simulates the interior of a 2012 Toyota Camry and can accommodate a driver Human Body Model (HBM). Starting from a full-scale vehicle model provided by CCSA, a modelling effort was performed in order to simulate an actual reverse-firing sled with detailed interiors. In particular, the pulse motion of the system was derived from the kinematics of the complete car, monitoring them over the crash test. The model was validated performing two comparisons between the sled and full-scale model in different scenarios: with and without a human model in driver configuration. Before including the HBM into the simulation, several steps were performed in order to set up the simulations properly. The human body was positioned in standard driver posture inside the vehicle, then, the sitting footprint was created on the seat and finally, the seatbelt was fitted to secure the driver occupant. In the first comparison, a high similarity in behaviour of model structures was found. The second comparison showed a good correspondence between models even if a slight difference in human motion is detected. Overall, the sled system behaves in a realistic way with respect to the complete vehicle model, making it a good tool for the evaluation of safety devices and the prediction of injuries and trauma on human body. Moreover, this model allows to reduce computational time of the simulation with respect to a full-scale model and allows to change set-up of the vehicle in the easiest way.

Preface

Introduction

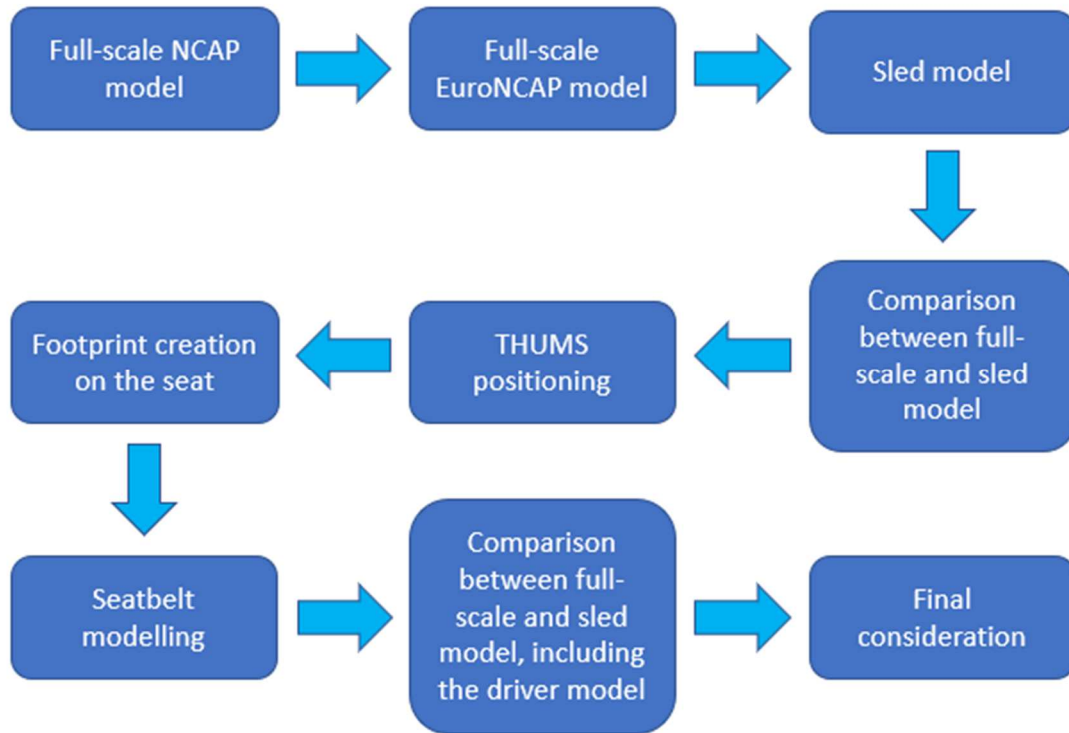
In the last few years, the efforts made by the car manufacturers and the sensitivity of the legislator on road safety issues have allowed a big step forward in the road safety field, in particular, in the active and passive safety of vehicles [1]. In Europe, the sales of safer vehicles have led to a decrease of the accidents number with injuries to persons and/or things but the development of safety devices included in new car is constantly evolving. However, in order to evaluate the safety devices and the crashworthiness of a vehicle in different scenarios, several crash tests were developed by car manufactures and organisations, such as EuroNCAP. These tests are standardized and highly expensive (destructive tests) but they are necessary to assess objectively the vehicle safety properties [2]. The costs and time required for the testing limit the number of scenarios to study therefore, FE simulations have become more and more popular. The numerical simulation allows to analyse the crash behaviour of the vehicle and the biomechanical parameters of occupants in a wide variety of configurations, saving time and costs. In addition, Human Body Models (HBM) have increased their accuracy in the last twenty years, becoming even more realistic than dummies used in crash test. This powerful tool cannot yet be used to assess vehicle properties, but it represents an important resource for car manufacturers and research groups in car safety field.

Thesis purpose

The aim of this thesis is to realize a simplified Finite Element (FE) model which is able to reproduce the interior environment of a mid-size passenger sedan over a frontal Full Width crash test, according to EuroNCAP regulation. This model will be used for future studies in passive safety therefore, it must be able to include into the simulation a HBM in driver configuration. The model environment is inspired by actual reverse-firing sled used in passive components testing, in particular by a FE model used in a well-known car manufacturer. The validation of the model has been performed comparing the kinematics of the sled structure with those taken out from the full-scale model in the same condition, with and without the presence of the driver. Moreover, the biomechanical information of the occupant is compared in order to verify the similarity of the two FE model. The simulations have been executed using LS-DYNA Finite Element explicit code.

Thesis work roadmap

The main thesis steps are represented in Figure 1 and a brief description are provided below.



Preface 1 Thesis work roadmap

The starting FE model represents a frontal full-width crash test involving a 2012 Toyota Camry sedan, according to American NCAP regulation. Changing some test parameters, the initial model is set in order to perform a frontal FW crash collision respecting EuroNCAP protocol. Then, a modelling effort is performed to simplify the FE environment, obtaining the sled model. The kinematics of the full-scale vehicle are monitored and enforced to sled structure, simulating the car environment during the impact. A first comparison was performed between the full-scale and sled model without considering the presence of the driver occupant. In order to include the driver into the FE environment, the THUMS is positioned in a proper sitting posture, the driver seat is deformed obtaining the footprint of the HBM on the model and the seatbelt system is included in the simulations. The final comparison is performed between the complete vehicle and the simplified environment including the THUMS in driver position. The final considerations are made observing the two comparison.

Chapter 1

1 Literature review

1.1 EuroNCAP [3]

The European New Car Assessment Program is a voluntary (non-profit) assessment project in car safety field which was founded in 1996. It is based in Leuven (Belgium) and its slogan is "For Safer Cars". The program was inspired by the New Car Assessment Program, introduced 1979 by the US National Highway Traffic Safety Administration. The aim of this program is the publication of safety reports on new car which are based on the performance of the vehicles in a variety of crash tests. It is important understand that in Europe new cars are certified as legal for sale under the Whole Vehicle Type Approval regimen which differs from EuroNCAP regulation. While legislation sets a minimum compulsory standard, the EuroNCAP is concerned with best possible current practice. Moreover, this program provides a continuing incentive by regularly enhancing its assessment procedures to stimulate further improvements in vehicle safety. The purpose of this regulation is to incentivize car manufacturers to improve vehicle equipment and raise safety standards for their vehicles [4]. EuroNCAP also introduced a vehicle rating system in order to provide European consumers with information regarding the safety of passenger vehicles. This rating is based on assessments in four different areas:

- **Adult Occupant Protection (for the driver and passenger)**
Frontal impact tests (Mobile Progressive Deformable Barrier test and Full Width Rigid Barrier), lateral impact tests (Side Mobile Barrier, Side Pole and Far-Side Impact) and whiplash test are performed to evaluate the protection of adult driver and passengers offered by the vehicle. Also, the car undergoes to rescue and extrication test.
- **Child Occupant Protection**
In this field is evaluated: the protection offered by the child restraint systems in the frontal and side impact tests (Child Restraint System performance), the vehicle's ability to accommodate child restraints of various sizes and designs (CRS Installation Check), and the availability of provisions for safe transport of children in the car.

- Vulnerable Road User (VRU) protection for pedestrians and cyclists
In order to assess how well cars protect vulnerable road users with whom they might collide, some test representing body part impact are developed (Head Impact, Upper Leg Impact and Lower Leg Impact). In addition, the Autonomous Emergency Braking can be tested (AEB Pedestrian test and AEB Cyclist test)
- Safety Assist, which evaluated driver-assistance and crash-avoidance technologies
AEB car-to-car, Occupant Status Monitoring, Speed Assistance, Lane support are tested in order to assess the systems functionality and/or performance during normal driving and in typical accident scenarios.

A brief description of the frontal impact in adult occupant protection is given below:

- Mobile Progressive Deformable Barrier (MPDB, Figure 1.1)
In this test, the car is driven at 50 km/h and with 50 percent overlap into a deformable barrier mounted on an oncoming 1400 kg trolley, also travelling at 50 km/h. During the collision, the barrier gets progressively stiffer the more it is deformed in order to simulate the behaviour of the front end of another vehicle. Two frontal impact dummies representing the average male are seated in the front and child dummies are placed in child restraints in the rear seats. The aims of this test are to evaluate the crashworthiness of the vehicle, observing the crash behaviour in crumple zone, and detect how efficiently car and trolley interact.

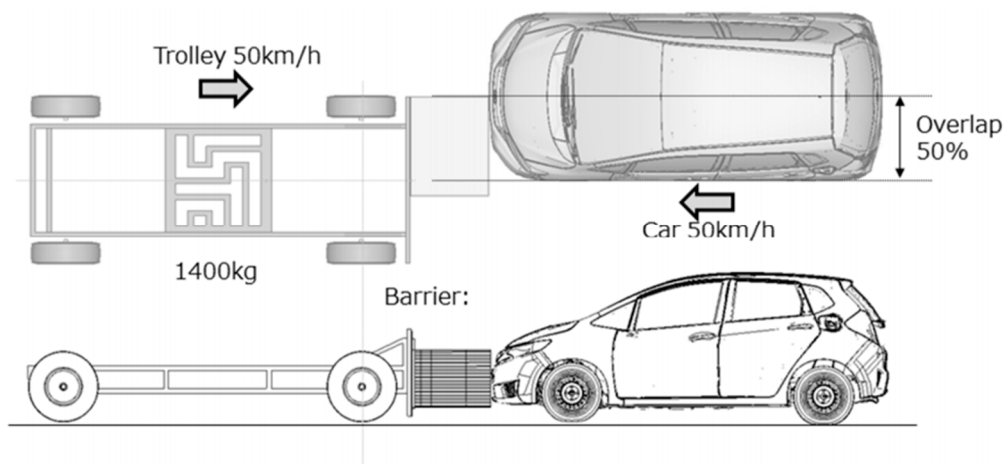


Figure 1.1 MPDB crash test [5]

- Full Width Rigid Barrier (FW)

In this test, the car crashes against a rigid barrier with full overlap at a test speed of 50 km/h. A small female frontal impact dummy is seated in the front driver’s seat and in the rear passenger side seat. The purpose of this test is mainly to evaluate the efficiency of the restrain system. This crash test is better explained in the following section §1.2.

The vehicles tested are usually relevant to the domestic market of EuroNCAP member organisations or they are important in a certain market segment. In addition, vehicle manufacturers can sponsor their own cars to be tested. The vehicle rating system (five-stars rating) allows to help families and business compare vehicles more easily and to help them identify the safest choice for their needs. The number of stars reflects how well the car performs in EuroNCAP tests, but it is also influenced by what safety equipment the vehicle manufacturer is offering in each market. The star rating goes beyond the legal requirements and not all new vehicles need to be tested for this regulation. Therefore, if a car is rated poorly is not necessarily unsafe, but it is not as safe as its competitors that were rated better. Some cars can be evaluated in two different configurations: vehicle with standard safety equipment and, if available, with an additional “safety pack”, that may be offered as an add-on option to consumers. In the Figure 1.2 are exposed some general guidance as to what safety performance the stars refer to in today's system.



Figure 1.2 EuroNCAP rating system

1.2 Frontal Full-Width EuroNCAP test

1.2.1 Introduction

Frontal collision are the most frequent car accidents therefore, it is important to design passive safety devices in order to minimize the risk of injuries in this scenario. By means of frontal crash test it is possible to evaluate the effectiveness of these vehicle component and take out important biomechanical data of the occupants including crash dummies. For this purpose, EuroNCAP developed two tests: Frontal Full Width (FW) test and Frontal Mobile Progressive Deformable Barrier (MPDB) test. The second one differs about the obstacle against the crash occurs which is mobile and deformable (trolley) oppose to the wall that is used in FW test that is rigid and firm. Moreover, whereas the FW collision involves the whole lateral dimension of the vehicle, in MPDB the overlap between car and trolley is 50 percent. Therefore, the FW impact represents a less dangerous situation since all structural parts located on the frontal side of the vehicle contribute to the energy dissipation through their deformation, decreasing the risk of cockpit intrusions. In this thesis only the Frontal FW test, which simulates a collision between two similar vehicles with the same weight moving at identical speed, is considered. This test is characterized by the impact of the car under study against a rigid barrier in a controlled environment and using registered parameters for speed, weight, and characteristics of the car.

1.2.2 Crash test description [6]

In the Frontal full-width test (Figure 1.3), according with EuroNCAP regulation, the car crashes against a rigid and non-deformable barrier at the speed of 50 ± 1 km/h. In real lab test, this speed is measured as near as possible to the impact point and the vehicle is moved long the axis of the run-up track until the crash. The rigid barrier consists of a block of reinforced concrete not less than 3 m wide in front and not less than 1.5 m high. The barrier shall be of such thickness that it weighs at least 70 metric tons. The front face must be flat, vertical and perpendicular to the axis of the run-up track. It is possible to install a high resolution loadcell wall (LCW) on the concrete block. The barrier must be covered with plywood boards 20 ± 2 mm thick, in good condition. In order to evaluate biomechanical information about occupant during the test, two small female dummies (Hybrid III 5%) are seated in the front driver's seat and in the rear passenger side seat. Before the impact, several steps must be performed to set up the test. Following a brief

presentation of the pre-test set-ups are reported, describing mainly the information useful for FE modelling.



Figure 1.3 EuroNCAP - Frontal FW test [3]

1.2.2.1 Vehicle set-up

Before testing it is necessary to control and standardize the parameters of the car. The first step is represented by calculation of the unladen kerb mass of the vehicle. Concerning the fuel tank, the protocol demands to know the total volume of the fuel tank and the mass of the fluid within it. In particular, the volume must be indicated by the manufacturer and the mass can be computed assuming for density 0,745 kg/l for petrol and 0,840 kg/l for diesel. First of all, the tank must be emptied of the fuel by syphoning it and then with the running of the car until the complete running out of the fuel. To measure the unladen kerb mass, the tank has to be filled of water or ballast in order to reach the same weight as the tank full of fuel, while oil and other fluids must be at the maximum level. Only spare wheel and tools supplied with the vehicle must be on board while the tyres have to be inflated for the half load indicated by the manufacturer. It is necessary to measure the front and rear axle weights, determine the total weight of the vehicle and also the car height from the ground. The total weight is the unladen kerb mass of the vehicle. The second step requires to compute the reference loads. The collision is performed considering 90 percent of the fuel tank capacity therefore, 10 percent of the water into the reservoir is removed. An equivalent mass of the Hybrid III 05F dummy (57 kg) is placed of the front driver seat and on the rear passenger seat at the opposite side, whereas 36 kg are added in luggage compartment of the

vehicle. Then, the axes reference loads and the total reference mass are measured. In order to prepare the vehicle for the collision, it is necessary to remove the luggage area carpeting (and the added mass), spare wheel and any tools or jack from the car, while an emergency abort braking system may be fitted to the vehicle. The spare wheel can be removed only if it will not affect the crash performance. The on-board equipment for the data acquisition is fitted in the boot of the car. The vehicle has to be fitted with an accelerometer on the sill directly below each B-post and lightweight seatbelt loadcell must be attached to the shoulder section of the driver and passenger seatbelts. The loadcell must be placed far enough away from the D-loop in order to ensure there is no interaction as the pretensioner fires. The Figure 1.4 show the instrumentation that must be included into the vehicle. This equipment will be triggered by a contact plate at the point of first contact ($t=0$) and will record digital information at a sample rate of 20kHz (alternatively a sample rate of 10kHz may be used). The equipment conforms to SAE J211. At the end of these procedures, the front and rear axle weights of the vehicle must be weighed considering also the occupant masses in their position. The maximal weight difference between axle reference loads and the vehicle prepared for the impact can be of 5 % or 20 kg. If the test vehicle differs more than the limits it is necessary to add or remove ballast or non-structural items in order to adjust the weight.

Location	Parameter	Minimum Amplitude	No of channels
B-Post LHS	Accelerations, A_x	150g	1
B-Post RHS	Accelerations, A_x	150g	1
Driver Seatbelt Shoulder Section	Force, $F_{diagonal}$	16kN	1
Rear Passenger Seatbelt Shoulder Section	Force, $F_{diagonal}$	16kN	1
Battery (including any secondary batteries)	Supply voltage, V	15V	1
Total Channels per Vehicle			5

Figure 1.4 Vehicle instrumentation - sensors

1.2.2.2 Dummy set-up

Hybrid III 05F test dummies should be used for the front driver seat and the rear passenger seat, on the opposite side to the driver. They should conform to U.S. Department of transportation; Code of Federal Regulations Part 572 Subpart O. Dummies are clothes by cotton garments that do not cover dummy's elbows and knees. Furthermore, each dummy wear specific and regulate shoes. The dummy must have a temperature between 19°C and 22°C. It is important set properly the constant friction joint of the dummy, adjusting them thanks to the tensioning screw or bolt. The dummy should have painted tape in specific body and face areas. In particular, eyebrows, nose, chin and top of the head are painted for the face, knees and tibia for the body. All instrumentation must be calibrated before the test programme.

Location	Parameter	Minimum Amplitude	Driver No of channels	Rear Passenger No of channels
Head	Accelerations, $A_x A_y A_z$	250g	3	3
Neck	Forces	$F_x F_y$	2	2
		F_z	1	1
	Moments, $M_x M_y M_z$	290Nm	3	3
Chest	Accelerations, $A_x A_y A_z$	150g	3	3
	Deflection, D_{chest}	100mm	1	1
Pelvis	Accelerations, $A_x A_y A_z$	150g	3	3
Iliac (L & R)	Force, F_x	9kN	2	2
	Moment, M_y	220Nm	2	2
Lumbar Spine	Force, $F_x F_z$	13kN	2	2
	Moment, M_y	500Nm	1	1
Femurs (L & R)	Forces, F_z	20kN	2	2
Knees (L & R)	Displacements, D_{knee}	19mm	2	
Upper Tibia (L & R)	Forces, $F_x F_z$	12kN	4	
	Moments, $M_x M_y$	400Nm	4	
Lower Tibia ¹ (L & R)	Forces, $F_x F_z (F_y)$	12kN	4	
	Moments, $M_x M_y$	400Nm	4	
Total Channels per Dummy			43	25
Total Channels			68	

Figure 1.5 Dummy instrumentation - sensors

The Channel Amplitude Class (CAC) for each transducer must be chosen to cover the Minimum Amplitude listed in the Figure 1.5. To fully understand, the CAC number is numerically equal to the upper limit of the measurement range (that is, equivalent to the data channel full scale). An extremely important process for the test is the positioning of the crash dummies inside the vehicle but only the driver position is interested in this work. This process is characterized by the following body part positions:

- The dummy's backs should be in contact with the seat back and the centre line of the occupant should be lined up with the centre line of its respective seats.
- The hands shall have their palms placed against the steering wheel at a position of a quarter to three. The thumbs should be lightly taped to the wheel.
- The upper legs of the dummy shall be in contact with the seat cushion as far as possible. The legs should be in vertical longitudinal planes as far as is possible.
- The driver dummy's right foot shall be placed on the undepressed accelerator pedal with the heel on the floor. The right foot should overlap the accelerator pedal with at least 20mm (Figure 1.6).
- The left foot should be placed as flat as possible on the toe-board parallel to the centre line of the vehicle. If any part of the left foot is in contact with a footrest or wheel arch when in this position, then place the foot fully on this rest providing a normal seating position can still be achieved (Figure 1.6).

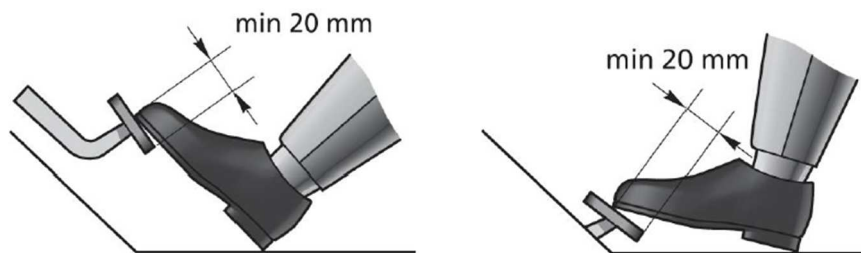


Figure 1.6 Left and right foot position [6]

Another important factor in crash test is the position of the seatbelt. It is necessary to place carefully the seat belt across the dummy and lock as normal and the route of the lap belt should be as natural as possible. The position of the upper seat belt anchorage must be set in the manufacturers 5th percentile design position. If no design position is provided, set the adjustable upper anchorage to the lowest position. Immediately after the test the dummies must be visually inspected. Any damage of the dummy has to be noted.

1.3 Mechanic of the impact and passive safety devices

The frontal FW test previous described can be considered as an impact against a rigid barrier of infinite mass. In this scenario, the vehicle crashes against a fixed barrier at prescribe velocity (50 km/h for EuroNCAP regulation), reaching the full stop almost instantly. At initial time instant ($t=0$), the bumper hits the wall and the car structure starts to deform. The force acting on the vehicle does not dissipate energy as the surface of the barrier is not moving at all, therefore, the initial kinetic energy of the vehicle is transformed into plastic strain energy. During the crash, the kinetic energy is dissipated by the car structure with the plastic deformation of its front structure, increasing the vehicle internal energy. During the deformation of the front structure, folding (stable plastic collapses), bending (unstable plastic collapses) phenomena, and contacts between parts in engine compartment occur, thus the deceleration profile of the vehicle is highly tormented. The end of the impact is considered when the rebound of the vehicle occurs (time instant is about 100 ms). From the occupant point of view, at time $t=0$ he is moving at the same speed of the car. When the vehicle crash into the wall and starts to decelerate, the occupant tends to move at the same initial velocity. If no restrain system is included into the car, the driver body violently hits the steering wheel, the dashboard and could also be ejected from the car. For this reason, it is important introduce passive safety systems in passenger vehicles. Passive safety device are on-board systems which aim to limit/contain the injuries caused to occupants and pedestrians in the event of a street accident. Airbags, seatbelts, whiplash protection system (headrest) etc. are common passive safety devices deployed in vehicles nowadays. In particular, the seatbelts allow occupants to remain secure to their seat, reducing the possibility of collision against car interior and dissipating his kinetic energy (Figure 1.7).

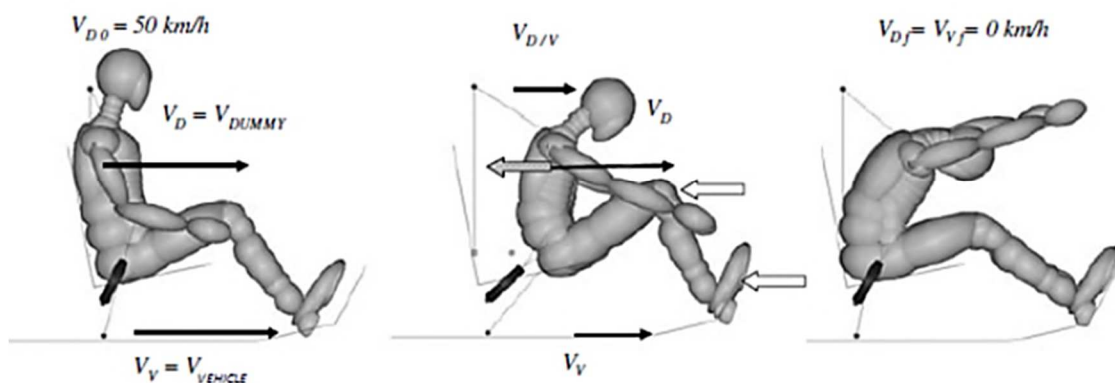


Figure 1.7 Seatbelt behaviour during a frontal impact [7]

Chapter 2

2 Finite Element models

2.1 Full-scale 2012 Toyota Camry model

2.1.1 Introduction [8][9]

In this work a Finite Element Model (FEM) of a mid-size passenger sedan is involved. The model is based on a 2012 Toyota Camry and was developed through the process of reverse engineering by the Center for Collision Safety and Analysis (CCSA) which researchers under a contract with the Federal Highway Administration (FHWA). It can be downloaded from the CCSA library of FE vehicle models developed to support crash simulation efforts [10]. The model is validated against the National Highway Traffic Safety Administration (NHTSA) frontal New Car Assessment Program (NCAP, American legislation) test for the corresponding vehicle. This vehicle conforms to the Manual for Assessing Safety Hardware (MASH) requirements for a 1500A test vehicle. The figure 2.1 shows the comparison between real and FE crash test of the car model.



Figure 2.1 Real NCAP crash test and NCAP simulation

This detailed model consists of over 2 million elements, includes representation of all vehicle structural components, suspensions, and steering subsystem. Moreover, a simple model of the driver, the front passenger and the rigid barrier are included. The FE numerical simulations were performed using the LS-DYNA (version: MPP s R9.3.1) non-linear explicit finite element code

during the whole thesis period. Since the model is extremely complex, it is divided in three different files in which is contained: the full-scale vehicle, the rigid barrier involved in the test and all settings necessary for the simulation. Another file combines all entities in a single simulation environment thanks to *INCLUDE command (*INCLUDE_TRANSFORM for the wall model) and set test instrumentations and outputs.

2.1.2 Model description [8] [9]

A production 2012 Toyota Camry four-door passenger sedan was used as starting model for this thesis work (Figure 2.2). The reverse engineering process performed by CCSA systematically disassembled the vehicle part by part and each component was catalogued, scanned to define its geometry, measured for thicknesses, and classified by material type. Material data for the major structural components was obtained from manufacturer specifications or determined through coupon testing from samples taken from the vehicle parts. This information was implemented into a finite element environment in order to model each part properly and so create a digital representation that reflected all the structural and mechanical features. The resulting finite element vehicle model has about 2.25 million elements and the average element size of the model is 6-8 mm with a minimum size of 4 mm.



Figure 2.2 Actual, FE model and details of a 2012 Toyota Camry sedan

This FE model was constructed to include full functional capabilities of the suspension and steering subsystems therefore, these moving parts were carefully detailed. In order to provide the capability to simulate a realistic behaviour in crash analyses, brackets and suspensions are

represented accurately in digital environment. No rolling friction is taken into account into wheel joints. The steering and suspension subsystem are exposed in Figure 2.3 and 2.4. Detailed representations of interior components of this vehicle are included and for this reason, the model can be used for simulations in which HBM, as in this thesis, or a crash test dummy are involved. In particular, the FE seats are very accurate, allowing to perform the footprint creation process (Sitting §3.2), while the complete dashboard reproduces a very realistic vehicle environment for the crash test. The Figure 2.5 shows the vehicle interiors. All components (except spot welded parts of the frame) connected each other thanks to the use of Constrain Nodal Rigid Body (CNRB) entities, simulating the fixing clamps and screws adopted in real vehicle. This command line requires a set of nodes (*SET_NODE_LIST) that belong to parts that must be bolted together in order to create a rigid bond between themselves, constraining their translation motions and rotations. As can be seen in appendix A, the upper part of the dashboard is not bonded correctly but the presence of windshield ensures an acceptable behaviour over the whole simulation. The vehicle presents an automatic transmission so only brake, handbrake and accelerator pedals are represented on the lower part of the dashboard.

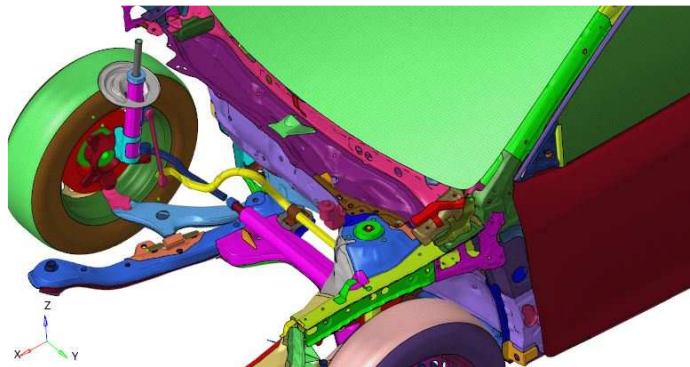


Figure 2.3 Front suspension and steering subsystems

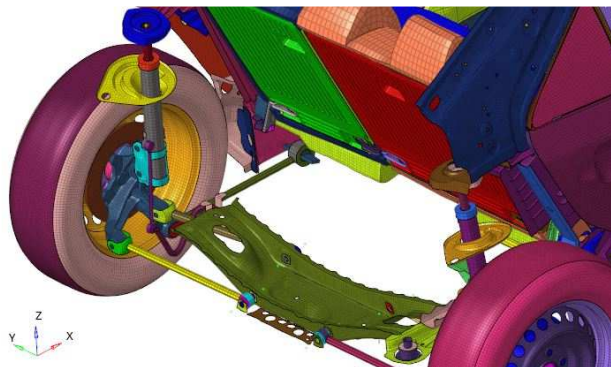


Figure 2.4 Rear suspension subsystem

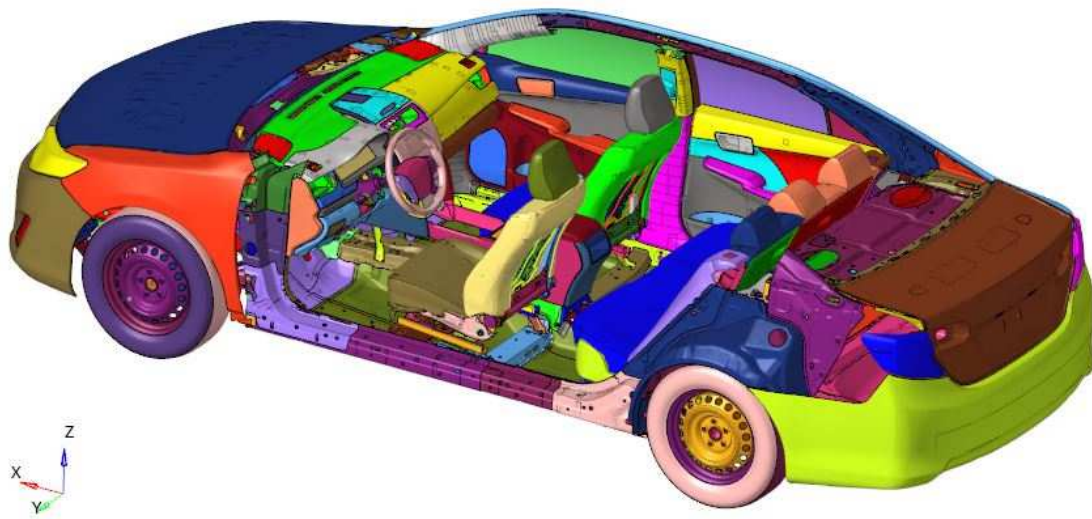


Figure 2.5 Representation of vehicle interior components

The original model is set to simulate a NCAP frontal full-width crash test. In this American test, a vehicle impacts into a fixed barrier at 35 mph (56.327 km/h) to represent a crash between two similar cars with same weight. The simulation starts when the vehicle touches the rigid barrier (included into the simulation) with the frontal bumper and end 120 ms later. Although the motor vehicle model is actually detailed, some masses are added because of missing components and test requirements. Indeed, the simulation takes into account the presence of fuel and luggage. The fuel mass is computed considering that gasoline weights about 6 pounds (2.72 kg) per US Gallon and the tank capacity of the vehicle is 15.5 Gallons ($15.5 \times 2.72 = 42.16$ kg) while NCAP provides a rated cargo mass (such as luggage) of 69.8 kg. The full-scale model includes two simple models representing an average-size adult male in driver seat and a small-size adult female in front passenger position, both secured on their seats as in a real NCAP test. The driver dummy is characterized by a lumped mass of 39.25 kg located in a central position over the lower cushion and it is connected with discrete elements to other four lumped mass of about 9.81 kg, each one situated in a node of the four CNRB that constrain the seat rails to the floor panel. There is another spring with the same stiffness which links the upper part of the B-pillar with the central mass. The total weight of the male occupant dummy is 78.5 kg, whereas, the passenger seat dummy weighs 62.2 kg and it has a similar model. These occupant subsystems are shown in Figure 2.6. Over the whole simulation time, the FE model takes into account the gravity effect.



Figure 2.6 Simple occupant models

2.1.3 Full-scale EuroNCAP model

In this thesis, the full-scale vehicle model is used to perform a EuroNCAP frontal full-width test in order to study the kinematic of the system and to be able to find out a comparison with the sled model described in section §2.3. For this reason, the original full-scale NCAP model must be suited to perform the desired assessment, modifying the test parameters. A substantial difference between the two legislations is the impact speed which corresponds to 50 ± 1 km/h for European legislation, while for the NCAP assessment the collision must occur at 56 km/h (35 mph). Therefore, `*INITIAL_VELOCITY` command is used to define the proper vehicle speed at the beginning of the simulation when the car hits the rigid barrier. In order to obtain an accurate comparison between the full-scale and the sled simulation, these models must be equipped with an appropriate instrumentation, but the original series of accelerometers result useless for this purpose. Therefore, an accelerometer is implemented in the FE environment and constrained on the frontal seat cross reinforcement, right under the driver position, to analyse the kinematic of that vehicle portion. The accelerometer is modelled as a single cube element which is characterized by:

- `*SECTION_SOLID`
- `*MAT_ELASTIC` with aluminium properties ($\rho=2.7 \cdot 10^3$ kg/m³, $E=70\,000$ MPa, $\nu=0.3$)

This element is constrained to the interested zone with a CNRB (all nodes of the cube are included in constrain definition) and *ELEMENT_SEATBELT_ACCELEROMETER is defined to avoid raw nodal acceleration due to considerable numerical noise. This command line uses 3 nodes (NID1, NID2, NID3) of the cube element to create a local reference frame for the accelerometer:

- Local **X** axis is defined from NID1 to NID2 and it is parallel to the vehicle center line
- Local **Z** axis is perpendicular to the plane containing NID1, NID2 and NID3
- Local **Y** axis is defined as $\mathbf{Y}=\mathbf{Z} \times \mathbf{X}$

The first specified node (NID1) is also defined in *DATABASE_HISTORY_NODE command which allows to output the node accelerations in the accelerometer local coordinates. The Figure 2.7 shows the position of the component and its local reference frame.

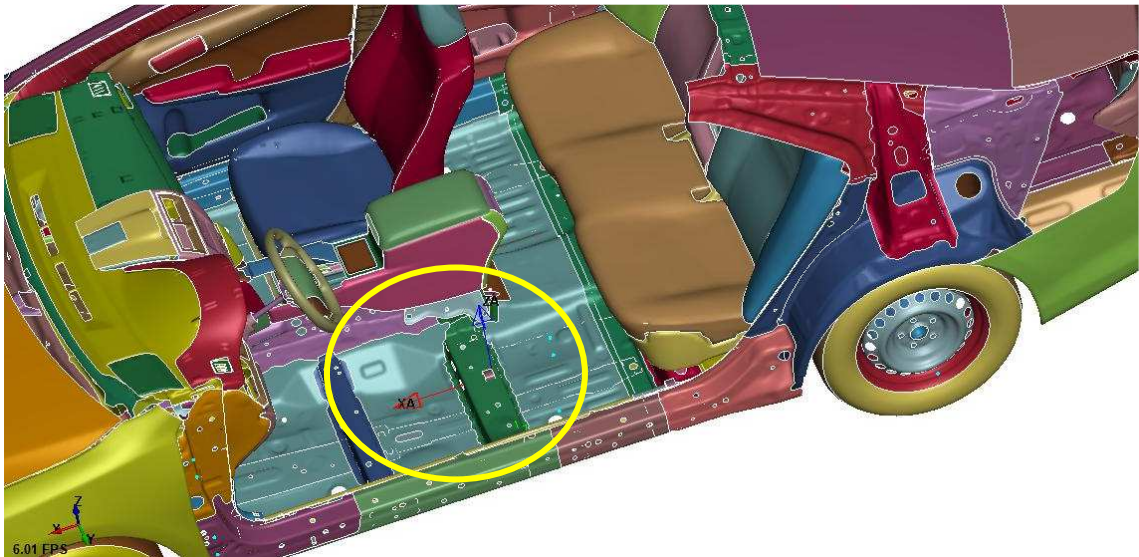


Figure 2.7 Driver Accelerometer

In the original model, the occupants are simulated as simple springs-masses systems, but they are not able to represent properly their crash behaviour as this work requires. Since for this thesis a human model is supplied by Polytechnic of Turin, original occupant models are deleted. As specified by EuroNCAP regulation, for real test the dummy must be positioned with the left foot on the vehicle footrest. Since in the original car model this component is not included, a simple footrest model is added in Sled environment to allow a proper positioning process. This part is made up by shell elements in structural steel and it is bolted to the structure thanks to six CNRB. To add this component on the Sled model, *Footrest.key* file is load on the simulation environment

using `*INCLUDE` command in *vehicle.key* file. The Figure 2.8 shows this part constrained on the structure.



Figure 2.8 Footrest model

Other changes regard the added mass for rated cargo which is reduced to 36 kg and the weight of fuel tank that is increased slightly to 43 kg in order to respect the European regulation. The weight of the tank is computed as 17 (tank capacity in US Gallons specified by the manufacturer) \times 3.785 (conversion factor US Gallons/Litre) \times 0.745 (density for petrol kg/l) \times 0.9 (standard for tank mass considered in the crash test) = 43 kg.

Since the whole full-scale EuroNCAP model is very complex to manage, it is divided in four different files:

- *Combine.key*: allows to perform the following files on LS-DYNA in a single simulation using `*INCLUDE` command (for the rigid barrier `*INCLUDE_TRANSFORMATION` is used), contains the control cards and in which output are defined as well. Also, it describes the contacts involved into the simulation.
- *Vehicle.key*: includes the full-scale vehicle model
- *Wall.key*: contains the rigid barrier model
- *Set.key*: provides the model instrumentation and the part sets for the contact definitions, allows also to set some test parameters (added masses, initial velocity, etc...).

2.2 Sled model

2.2.1 Introduction

This thesis aims to create a realistic finite element model that allows to simulate a frontal full-width test, according to European regulation. In particular, this model must represent accurately the driver side of a mid-size passenger sedan vehicle during the frontal collision. To facilitate future research projects, another important characteristic is also required: the model must be as simple as possible. Especially when multiple tests must be performed, this feature allows to reduce the chance of making mistakes for new users, avoid long simulation run time, also for complex setups, and ensures that LS-DYNA solver miscalculations do not occur. To achieve this goal, the basic concept is to realize a finite element sled model and for this reason is fundamental to understand how the machine works. The sled device (Figure 2.9) is a test equipment designed to reproduce the dynamic conditions in a full-scale motor vehicle during an impact. It is a cost-effective way of performing crash test based on the occupant's safety analysis, both in acceleration and deceleration condition. Testing of safety components such as airbags, seat belts and other restrain systems can be also carried out on this kind of equipment. Typically, the occupant compartment of a vehicle, referred to as a vehicle buck, is mounted to the test sled. The sled and buck can then be subjected to accelerations representative of a particular crash environment. This controlled acceleration is commonly referred to as a sled pulse and can be modelled after accelerometer data collected from actual crash testing. In this way, even complex crash events, such as those created by impacts involving two moving vehicles, can be replicated with sled tests. The two most common types of sled systems are reverse-firing sleds which are fired from a standstill, and decelerating sleds which are accelerated from a starting point and stopped in the crash area with a hydraulic ram [11]. In this thesis, a 2012 Toyota Camry sedan is used as reference to realize the sled in which reverse-firing kinematics are adopted.



Figure 2.9 Real sled device

2.2.2 Sled model description

The sled developed in this work is a simplified FE model which reproduces a EuroNCAP frontal full-width test, involving a mid-passenger sedan. This model is conceived to carry on experimental studies focused on passive safety system where HBM are included, therefore it has the following features:

- It simulates the internal vehicle environment in driver side and its motion during the test.
- It allows to include easily seat belts, airbags and other virtual restrain systems.
- It can hold a human model, allowing to create the seat footprint.
- It is an open source FE model, allowing to perform changes on the simulation environment or set different parameters.
- It is as simple as possible in order to reduce the computational run time of the simulation and the risk of errors.
- It is organized in an intuitive way, making it more user-friendly.

The process to model the sled can be divided in three big steps:

1. Sled environment modelling: it represents the structure which interacts with the HBM and other car equipment during the simulations. it is obtained from the full-scale model in order to be as realistic as possible.
2. Model kinematic definition: this process is aimed at providing the proper sled motion, simulating the designed crash test. For this reason, the kinematics of four area which are called *rigid sections* in this thesis are implemented through velocity curves definition.
3. Set-up of the model: this step ensures a proper execution of the simulation, modelling the required entities and setting adequate parameters.

At the end of the modelling process the sled is composed by several files:

- `Combine.key`: allows to include all following files on a single simulation
- `Structure.key`: contains the sled frame
- `Dashboard.key`: contains the detailed vehicle dashboard
- `Seat.key`: contains the driver seat
- `Dashboard_structure_constrain.key`: allows to constrain the dashboard on the frame
- `Seat_structure_constrain.key`: allows to constrain the seat on the sled frame
- `Velocity_curves.key`: contains the kinematic applied to the sled
- `Set.key`: defines contact entities and other set-up to perform a proper simulation

2.2.3 Sled environment

The sled environment modelled in this thesis is developed starting from a 2012 Toyota Camry sedan of which the complete full-scale FE model is provided by CCSA. Since the simplified model must simulate the driver conditions during a crash test, its structure is designed to represent precisely the interior environment of the car cockpit, especially on the driver side. As in a real sled, all unnecessary components are removed, such as engine and steering system, until only the main parts which can contact the driver body during the crash are left. Therefore, only the portion of the vehicle between the firewall and the B-pillar was considered, deleting the car roof and the central tunnel but taking into account in detail all the internal dimensions on the driver's side. The frame of the sled is adapted slightly to keep under control the strains in specific regions over the whole test. This model is designed for experimental purposes so that the interior setup of the vehicle can be changed as simple as possible. To enable easy and intuitive use of the model, the sled structure is organized in different subsystems (structure, dashboard and driver seat) that together make up the simulation environment. These subsystems can be readapted individually, depending about the subject of the studies, and then combine themselves in a single finite element model, beside specific files are included to introduce relationships between subsystems. To simulate the impact deceleration, the motion of the whole sled must be defined, for this reason, in four regions of the frame prescribed velocities are applied. The process to model the sled structure counts different steps:

1. Removing/deleting of unnecessary vehicle components
2. Cutting of vehicle frame to realize a compact structure
3. Model division into three subsystems: driver seat, dashboard, and structure
4. Stiffening free edges of cut parts
5. Definition of rigid sections which allow the simulate the motion
6. Stiffening of the B-pillar and footrest modelling

At the end of this process, the obtained structure represents the environment which interact with the human model and where the virtual restrain system is fixed.

2.2.3.1 Deleting the unnecessary components

The starting FE Camry model is actually detailed, especially the cockpit, and allows to perform simulations with a dummy or an HBM thanks to the possibility of deforming the seat foam cushions. In order to model the sled system, many components are disassembled, keeping only the functional parts for this purpose. The front and rear car side are removed, leaving the main frame components and the interior parts in front occupant area. This means the steering and suspension subsystem, the bumpers, the cool, the hood, the rear seats, the wheels, etc. are deleted from the original model. Since in this work only the crash behaviour of the driver is considered, also the central tunnel, the front passenger seat, and all covers that belongs to right side of the cockpit are disassembled, making the sled file leaner. For the same reason, also all the roof components and the windshield are removed. The Figure 2.10 shows the vehicle model after the disassembling process.

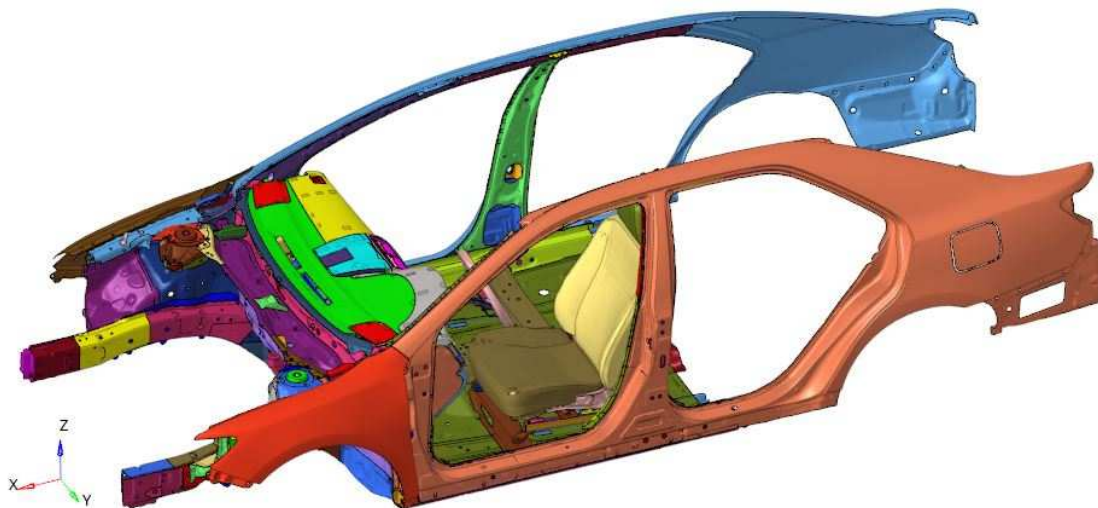


Figure 2.10 Vehicle model after disassembling

2.2.3.2 Cutting of the frame

At the end of the removing part process, the sled model is not compact enough because of the shape of vehicle frame, therefore it is necessary to cut the rough sled structure, as in a real sled device, in order to obtain an appropriate test model. During this process is useful to consider the next two steps: the stiffening of the free edges and the modelling of rigid sections on the structure. To ensure a proper stiffening, the edge shape of cut parts is really important, so the box-section

design of the front side members is exploited, cutting the front part of the car frame a few centimeters ahead of the firewall. On the other hand, the rear structure cut is performed taking into account the possibility to realize the back rigid sections, therefore also in this case few centimeters of sheet metal are kept over the B-pillar. The upper part of the A-pillar and B-pillar are cut to define a better free edge shape, simplifying the following steps. The cutting process is made by deleting structure shell elements shaping suitably the free edges. At the end of this step, a careful resolution of errors in the model is performed, modifying each entity in which deleted parts or elements are defined. In Figure 2.11, the Sled structure is exposed after cutting of the frame.

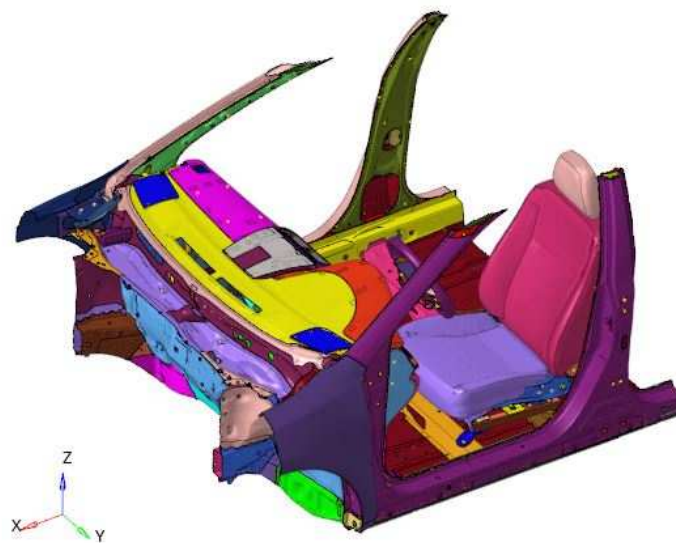


Figure 2.11 Vehicle model after cutting

2.2.3.3 Model division

Then the cutting step is performed, the sled model is almost complete from a structural point of view, but improvements of the frame are reported in the next sections. After the previous processes, the result of the modelling is a complex file in which all the parts that make up the test environment are included. This means if the model must be modified, changing some properties or deleting/adding components, a heavy modelling effort must be done and lots of mistakes could occur easily. To reduce the chance of error and simplify the model, the sled is divided into three subsystems: structure, dashboard, and seat.

These subsystems are obtained by isolating appropriate parts and saving them into three different files:

- *Structure.key*
- *Dashboard.key*
- *Seat.key*

This splitting makes the model more user-friendly and more intuitive to modify, giving the opportunity to manage separately each group of parts. To bolt the seat and the dashboard on the structure, other two files are needed:

- *Dashboard_structure_constrain.key*
- *Seat_structure_constrain.key*

These files include the constrains that allows to fix the related subsystem on the structure, simulating the fixing clamps and screws used in real vehicle. All connections are modelled as CNRB specifying proper nodes. The whole sled is assembled in FE environment, loading the subsystems and the constrains thanks to *INCLUDE command (no transformation is needed) in *Combine.key* file. The following sections describe in detail the three main subsystem and their constrain.

STRUCTURE

The sled structure is represented by what remains of vehicle frame after the cutting process. As in real vehicles it is made up by sheet metal parts connect each other with spot weld. In FE environment, each structural component is represented in detail through shell elements (*SECTION_SHELL) with proper thickness, whereas the part materials are modelled as *MAT_PIECEWISE_LINEAR_PLASTICITY with different properties depending on the component. The mesh properties are kept the same as in the original full-scale simulation. The LS-DYNA allows to represent massless spot weld using *CONSTRAINED_SPOTWELD and this command line creates a rigid beam with appropriate characteristics that connects two defined non-contiguous nodal pairs. After the previous deleting and cutting process, the contact entity *CONTACT_TIED_SHELL_EDGE_TO_SURFACE is modified, redefining the part sets specified into the command line. This constrain-based contact allows to tie parts with disparate meshes, and regulate their interactions, therefore in this model it is used to link the spot welds to the surface of structure components.

The original full-scale model represents a vehicle with an automatic transmission therefore the accelerator, the brake and the handbrake pedal are modelled. Since these components are represent in a simple way, they are included into the structure file in order to not complicate the combine file. The Figure 2.12 shows the Sled structure.

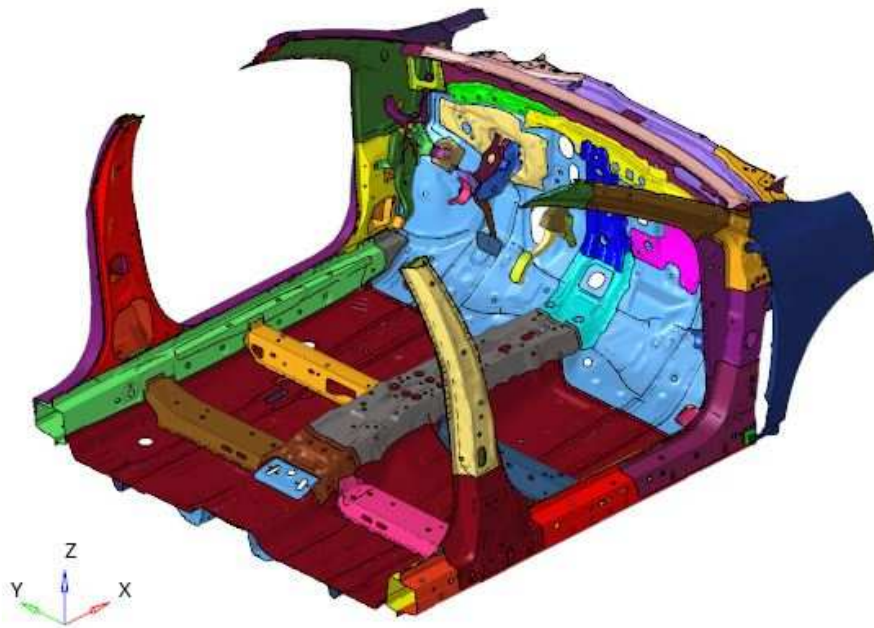


Figure 2.12 Sled structure

DASHBOARD

Thanks to the huge modelling effort performed by CCSA on the original full-scale model, the Sled dashboard results extremely detailed and complete in all its parts. The detailed representation of instrument panel allows to simulate in accurate manner the dimensions of internal components of the cockpit, making the analysis very realistic. Because of its simple structure is made up by parts bolted each other with CNRB, it is possible to easily modify the dashboard configuration, adding components such as the airbag and changing the set-up. All parts of the instrument panel are modelled by shell elements with different properties depending on the component. The Figure 2.13 exposes the dashboard subsystem. Thanks to the *Dashboard_structure_constraint.key* file loaded during the simulation, the dashboard is constrained properly with a series of CNRB to the brake pedal, the lower front pillars, and the firewall (all parts belong to the structure).

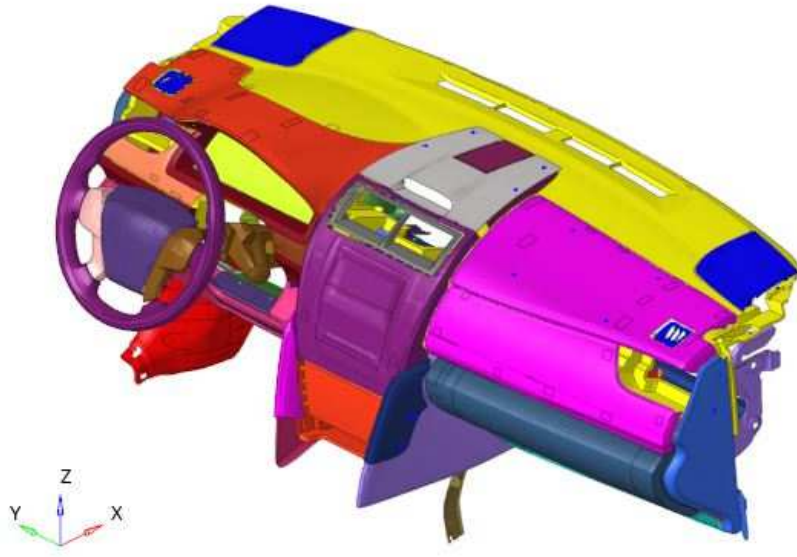


Figure 2.13 Sled dashboard

SEAT

The seat is one of the most important part of the FE model since it allows to perform the sitting simulation (section §3.3) of the occupant and this is due to the high accurate modelling that ensures a proper seat deformation. The model can be divided in:

- CUSHIONS

The upper (backrest), lower cushion and the headrest are included in the model (Figure 2.14), and they reproduce accurately the shape of the real vehicle parts. To allow a realistic footprint of the THUMS during the positioning, the elements that make up these components are modelled as:

- *SECTION_SOLID
- *MAT_LOW_DENSITY_FOAM, the following properties are set: $\rho=1.01 \cdot 10^2$ kg/m³, $E=4.16$ MPa (1.16 MPa for headrest), $\nu=0.3$, to describe the tensile behaviour, the stress-strain curve, exposed in Figure 2.15, is included while the hysteretic unloading factor of 0.01 and a large unloading shape factor of 10 are adopted to model the increase of energy dissipation when the forces are removed.

The cushions are constrained to the seat frame thanks to CNRB.

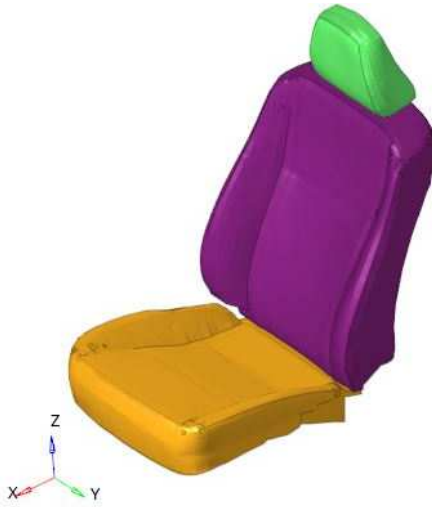


Figure 2.14 Foam cushions

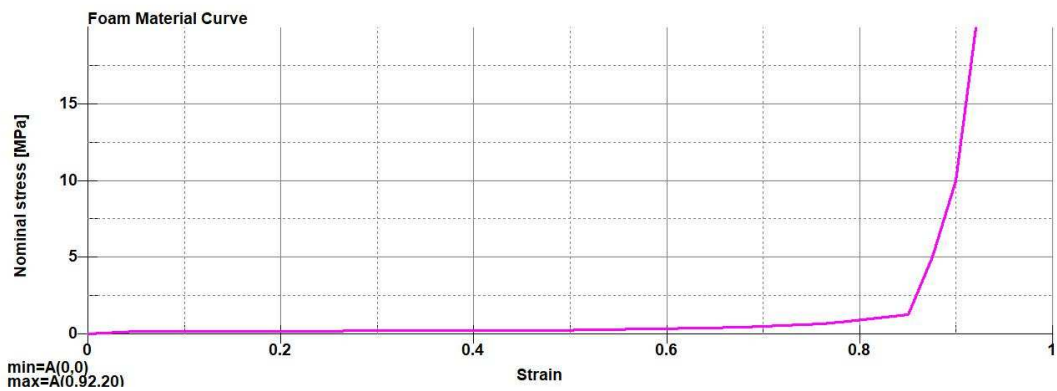


Figure 2.15 Foam material curve

- SPRING FRAMES

In the model, two spring frames are present to sustain the backrest and the lower cushion. They are made up by many elements modelled as:

- *SECTION_BEAM, with defined circular cross section and outer diameter of 3.1 mm
- *MAT_ELASTIC, modelled as steel with $\rho=7.89 \cdot 10^3 \text{ kg/m}^3$, $E=210\,000 \text{ MPa}$, $\nu=0.3$

The shape of the frames is represented carefully as in a real vehicle and they are connected to the seat frame thanks to CNRB. The Figure 2.16 shows the support of the cushions in which the spring frames are included.



Figure 2.16 Seat spring frames

- SEAT FRAME

The seat frame is modelled in detail (Figure 2.17), and all sheet metal components are represented through shell elements with proper thickness and material properties. It is linked to the structure with four CNRB, thanks to the *Seat_structure_constraint.key* file. These constraints bolt the base foot brackets (four brackets) of the seat frame to the front floor cross-members.



Figure 2.17 Seat frame

During the crash or sitting simulation, the seat components interact each other therefore, to avoid penetration between unmerged elements, a contact entity is added to the model as `*CONTACT_AUTOMATIC_SURFACE_TO_SURFACE`. This contact type is recommended by LS-DYNA for crash analysis since the model could be undergo large deformations. In this command, two part sets are defined: cushions as master set and seat frame as slave set. The Figure 2.18 exposes the whole seat subsystem.



Figure 2.18 Driver seat

2.2.3.4 Stiffening free edges

After the previous cutting process, the Sled structure has the appropriate final shape, but another problem must be solved. In this configuration, the model could exhibit an unrealistic behaviour at free edges of the sled frame during the test because of the weakening due to the previous modelling processes. This incorrect crashworthiness of the structure is solved by stiffening the area where the part cutting is performed thanks to the use of rigid elements. This means the elements which are located on the free edges in front and rear side of the frame and in the upper part of the A-pillar and B-pillar are modified, changing their properties to obtain a rigid border. In particular, these elements are modelled as:

- `*SECTION_SHELL` with a thickness of 1 mm
- `*MAT_RIGID` where $\rho=7.89 \cdot 10^3 \text{ kg/m}^3$, $E=210\,000$, $\nu=0.3$ (as a structural steel)

The 1-millimeter thickness is applied because it is the average measurement found between elements that belong to parts on the edges whereas the material is considered as a structural steel for inertia properties and contact analysis (as the other structural parts). This process is performed working only on the sled structure file presented in the previous division step, and thanks to the defined rigid elements of the free edges at the box-sections on front side members (Figure 2.19), pillars (Figure 2.20), and vehicle floor frame (Figure 2.21), the model results extremely stiffened, avoiding harmful distortions on the structure during the simulation. This stiffening process could cause a different stress distribution on the Sled frame but in this model the tension analysis is not so important.

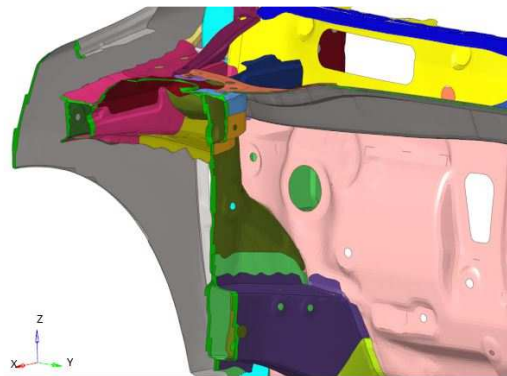


Figure 2.19 Detail of the front stiffened region

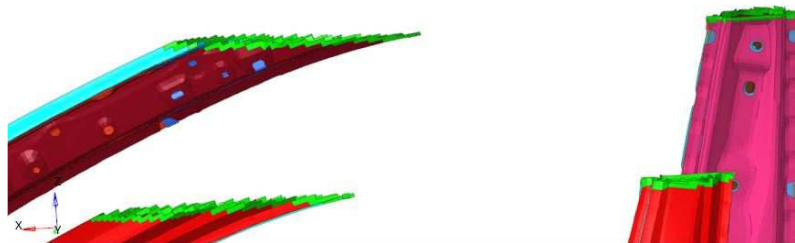


Figure 2.20 Detail of the stiffened A-pillar and B-pillar

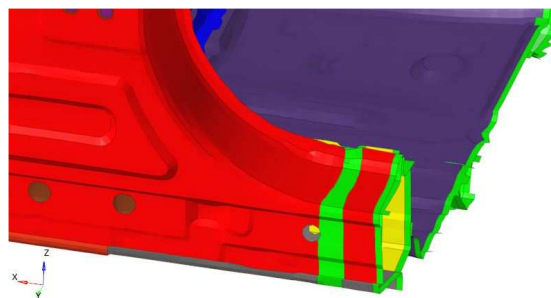


Figure 2.21 Detail of the rear stiffened region with respect to the rigid sections

2.2.3.5 Realization of rigid section

At this point it is necessary to understand how transmit the crash motion to the structure. In this thesis to characterize the sled kinematic, the motion is applied in four regions of the vehicle frame. If a prescribed motion is set on a single node for each region, the inertia effects could cause serious stress concentrations, bringing excessive and unrealistic distortions and for this reason four rigid parts are modelled on the structure. These parts are also called rigid sections because their shape goes through the box-section of the rockers and the width counts no more than four mesh elements. Defining a prescribe velocity curve on a rigid section it is possible to spread the motion upon the vehicle rocker, which is one of the most important components for the frame stiffness, transmitting the kinematic to the whole sled in a effective way. In the Sled model there are two frontal rigid sections and two rear ones, symmetrical with respect to the center line of the car (Figure 2.22). The rear sections cut the side panel and the rocker panels whereas the front rigid parts cut some sheet metal part of the A-Pillar as well. Each section is characterized by elements modelled as:

- *SECTION_SHELL, with a thickness of 1 mm
- * MAT_RIGID where $\rho=7.89 \cdot 10^3 \text{ kg/m}^3$, $E=210\,000$, $\nu=0.3$ (as a structural steel)

The 1-millimeter thickness is applied because it is the average measurement found between elements that belong to parts cut by the rigid sections whereas the material is considered as a structural steel for inertia properties and contact analysis (as the other structural parts that surround the sections). The Figure 2.23 shows the front and rear rigid sections in detail.

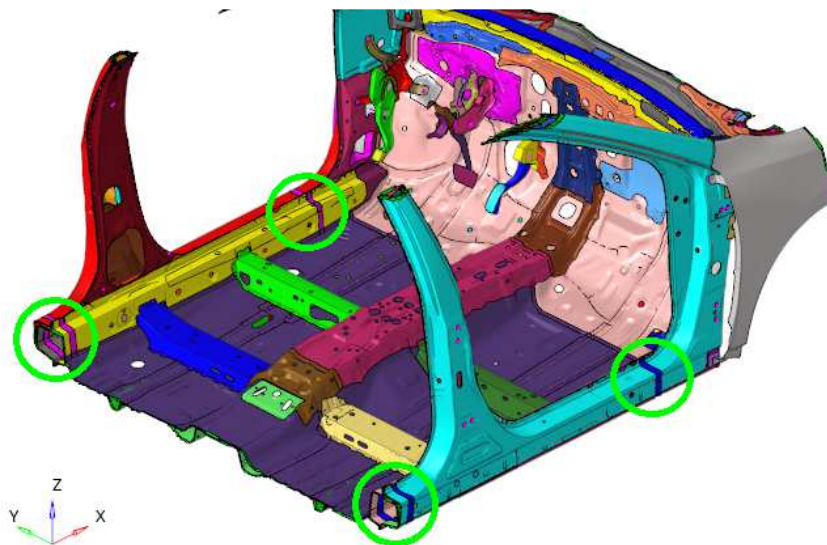


Figure 2.22 Rigid section positions

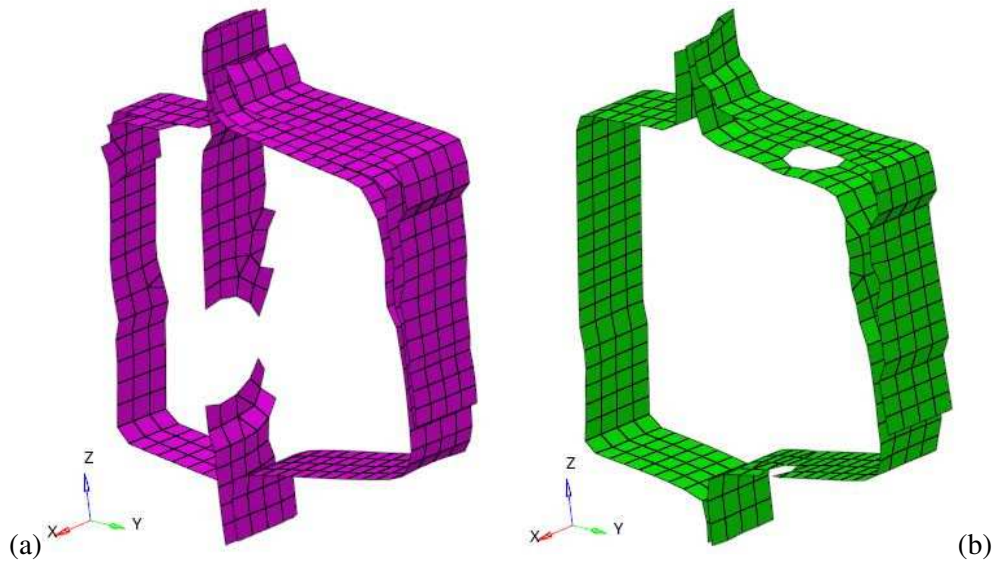


Figure 2.23 Details of front (a) and rear (b) rigid sections of the left side

2.2.3.6 Problems resolution

As can be seen in appendix A, the upper part of the dashboard is not bonded correctly therefore, after the windshield removing, an unrealistic behaviour due to dynamic phenomena is shown during the simulation. To solve the problem, five CNRB are located in proper positions, fixing the free edge. Another problem due to the weakening of the previous processes is represented by the excessive displacement on the upper part of the B-pillar during the test, as reported in appendix A. In order to stiffen the pillar structure, several elements are modified changing their properties to a rigid material with thickness of a 1 mm. This step allows to reduce the flexion of the B-pillar, keeping it under reasonable values. As specified in EuroNCAP regulation, the dummy must be positioned with the left foot on the footrest. Since in the original vehicle model of this component is not included, the same footrest model included into full-scale simulations is added in Sled environment to allow a proper positioning process. To add this component on the Sled model, *Footrest.key* file is load on the simulation environment using `*INCLUDE` command in *structure.key* file. The final sled environment is exposed in Figure 2.24.

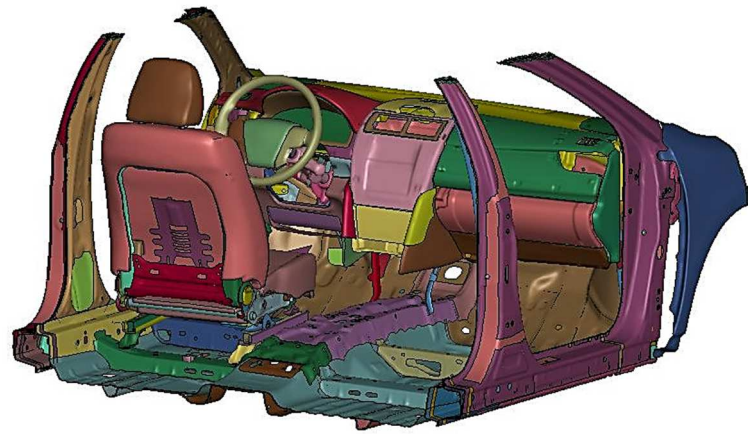


Figure 2.24 Sled model - final configuration

2.2.4 Sled kinematic

To simulate a EuroNCAP frontal full-width test, the proper motion must be supplied to the Sled model therefore, the equations of motion are implemented in four area of the Sled structure. Conceiving the system as a reverse-firing sled, the model must be accelerated properly from a standstill position, simulating the deceleration that occurs during a collision. To ensure a realistic crash kinematic of the Sled frame, four velocity curves (derived from the equations of motion that are taken out from full-scale vehicle simulations) are applied on the rigid sections described previously in section §2.2.3.5. The process to take out the pulse of the system follows several steps. Firstly, a full-scale vehicle model, in which the rigid sections are included, is modelled to simulate the crash impact in EuroNCAP standards. This model is previously validated, comparing it with the unmodified EuroNCAP model. The modified full-scale vehicle is adopted to get clearer velocity curves, facilitating the data mining. Then, the simulation results are evaluated, and the curves are suited to be included into Sled model.

2.2.4.1 Full-scale EuroNCAP model with rigid sections

The full-scale EuroNCAP model used during the velocity curve extrapolation is equipped with the same rigid sections modelled in the Sled model and for this reason it is also called *Rigidparts model*. The rigid sections are located at the same position with respect to the Sled frame as exposed in Figure 2.25, and they are made up of identical rigid material. Except for the inclusion of rigid sections, the model is the same as the full-scale EuroNCAP model described in section §2.1.3.



Figure 2.25 Detail of rigid sections position in Rigidparts model

This FE model is validated against the unmodified full-scale EuroNCAP model, comparing the energy balance curves and the accelerations measured in proximity to the driver seat thanks to the accelerometer included in both models.

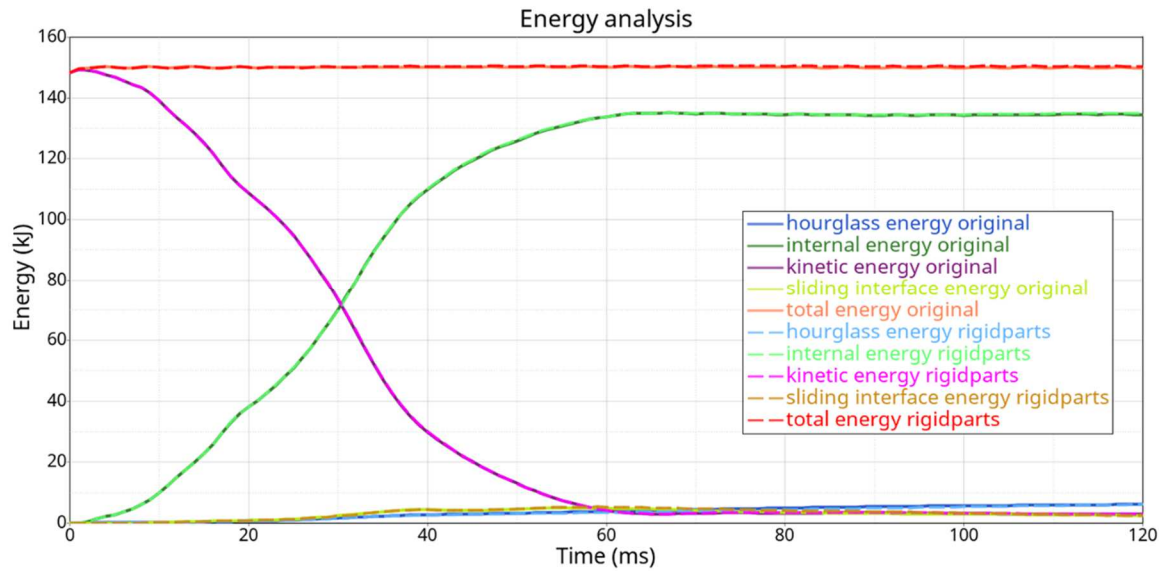


Figure 2.26 Original EuroNCAP model vs Rigidparts model - Energy balance

The Figure 2.26 exposes the global energy plots from the simulations. It can be seen that in both models there is energy balance throughout the simulation and the shape of the curves are identical. The Figures 2.27, 2.28 and 2.29 show similar accelerations measured during the simulation, indicating that the modified model provides a reasonably representation of the original vehicle crash behaviour.

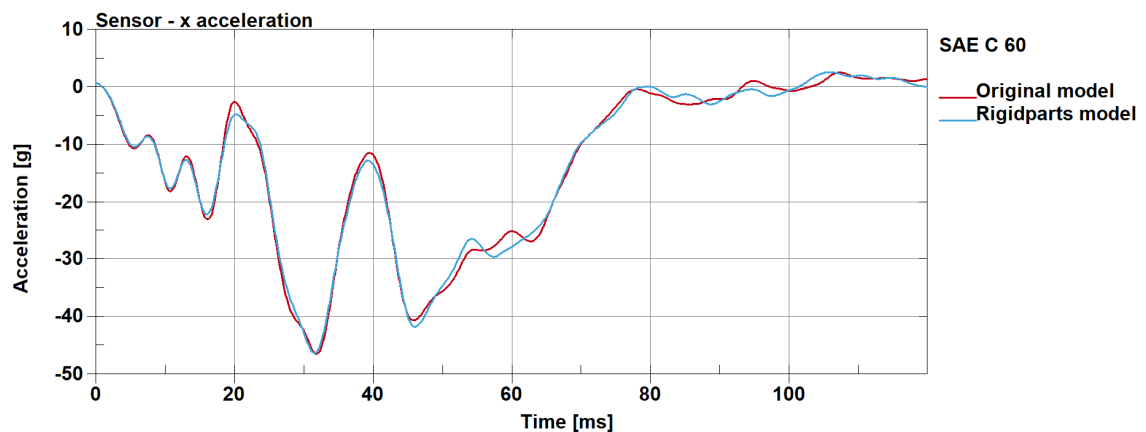


Figure 2.27 Original EuroNCAP model vs Rigidparts model - Driver sensor - x acceleration

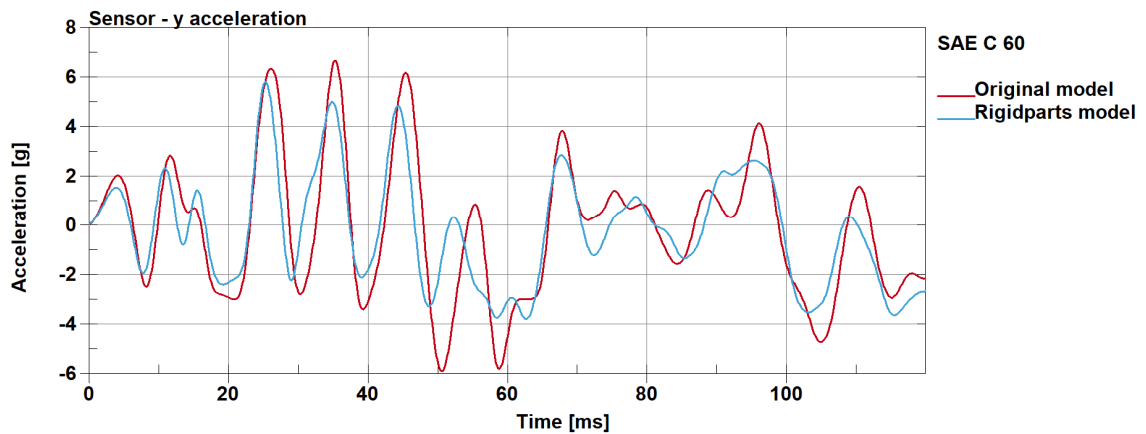


Figure 2.28 Original EuroNCAP model vs Rigidparts model - Driver sensor - y acceleration

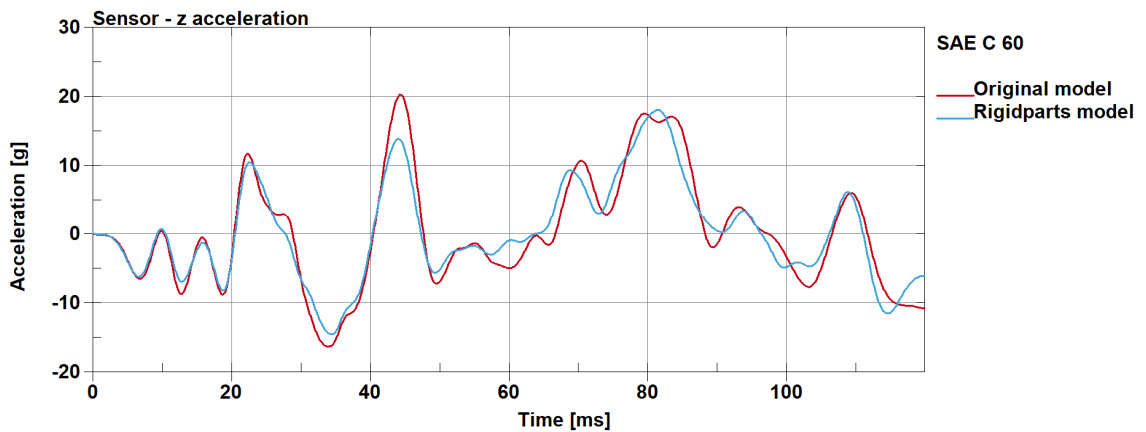


Figure 2.29 Original EuroNCAP model vs Rigidparts model - Driver sensor - z acceleration

The purpose of this model is to take out the velocity profiles of the rigid sections over the EuroNCAP crash test. To achieve this goal, four nodes are tracked (adding their identification number in *DATABASE_HYSTORY_NODE program section) to obtain their kinematics over the crash test:

- Front Right node: node 2999161 belonging to front right section (FR)
- Front Left node: node 2451780 belonging to front left section (FL)
- Rear Right node: node 2991038 belonging to rear right section (RR)
- Rear Left node: node 2424872 belonging to rear left section (RL)

The presence of the rigid material that surround the nodes in these areas allows to get clearer curves, reducing the numerical noise due to the elastic phenomena on the car structure and facilitating the Sled curves definition. A comparison between velocities of the same nodes tracked in Rigidpars model and in original EuroNCAP model is shown in the following figures (Figures 2.30-2.33).

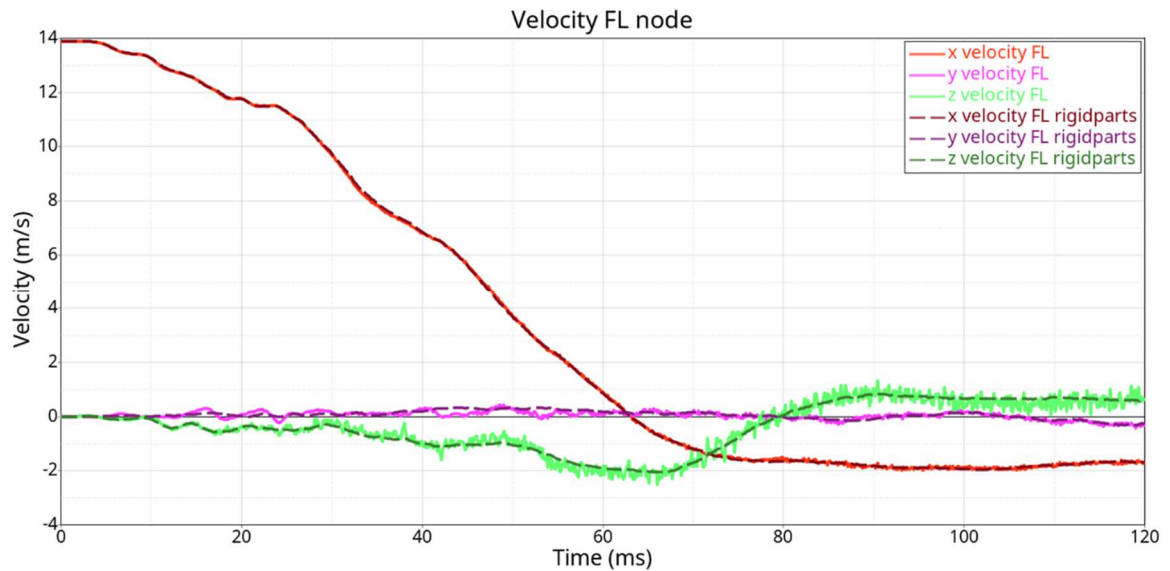


Figure 2.30 Original EuroNCAP model vs Rigidparts model - velocity FL node

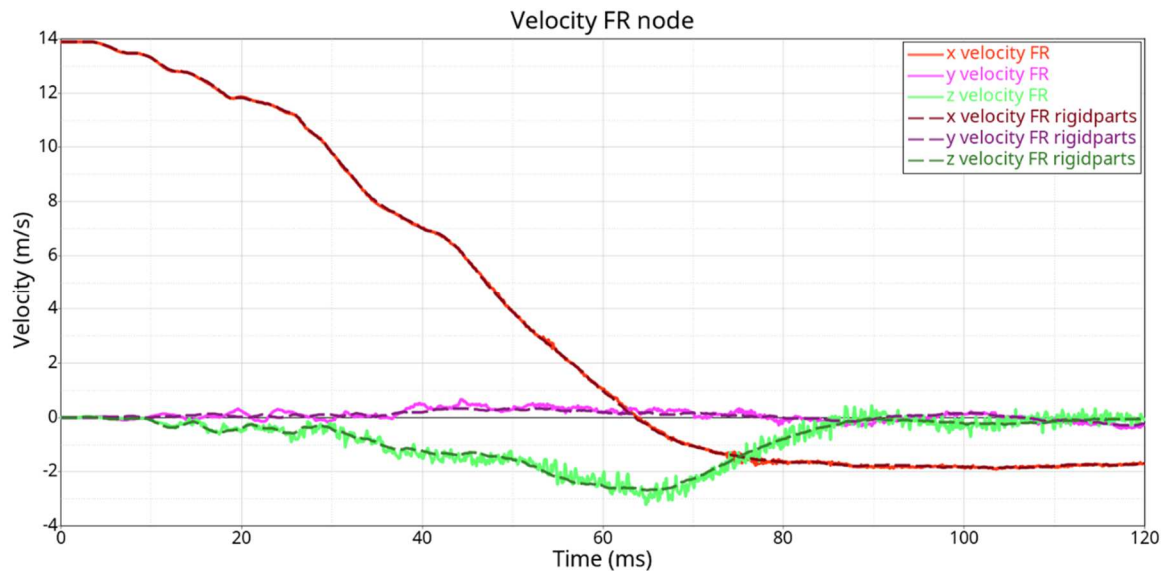


Figure 2.31 Original EuroNCAP model vs Rigidparts model - velocity FR node

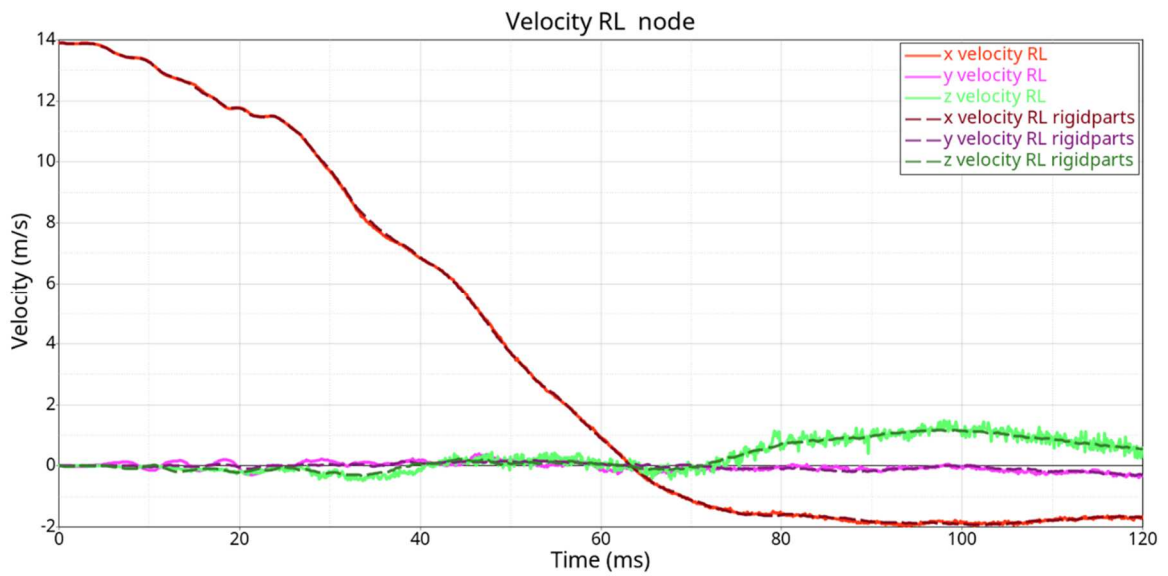


Figure 2.32 Original EuroNCAP model vs Rigidparts model - velocity RL node

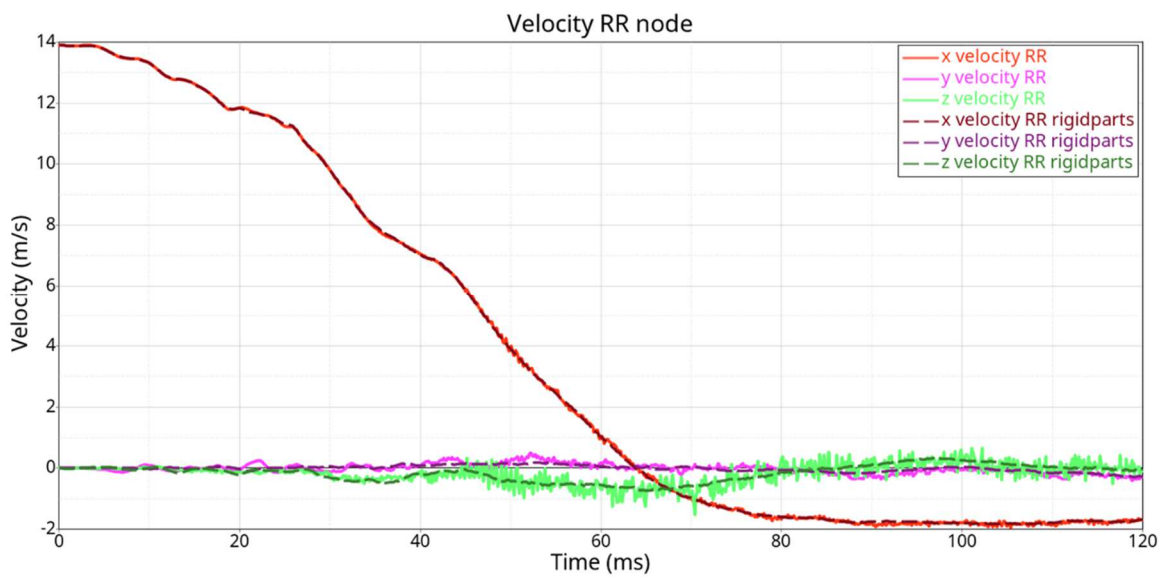


Figure 2.33 Original EuroNCAP model vs Rigidparts model - velocity RR node

As can be seen from the images, the velocity curves taken out from the Rigidparts model present fewer oscillations with a lower amplitude (less amount of numerical noise), therefore they are more suitable to be used in Sled kinematic definition. The differences of velocity found in different nodes of the same rigid sections are neglected.

2.2.4.2 Sled velocity curves

In the full-scale Rigidparts model, the vehicle has an initial velocity of 50 km/h (13.888 m/s) and it undergoes a heavy deceleration during the collision with the wall whereas, the Sled model starts from a standstill and it accelerates in order to represent the proper condition from the driver point of view over the crash test. For this reason, the equations of motion are not directly implemented on the Sled model, but they must be suited to simulate a reverse-firing motion. However, to represent the reality as faithfully as possible, the velocity curves in X direction taken out from the full-scale model are translated down to provide an initial velocity equal to 0 m/s, applying an offset of 13.888 m/s. On the other side, the other curves are kept unchanged. The velocity profiles applied at the four rigid sections in Sled model are exposed in the following figures (Figure 2.34-2.37).

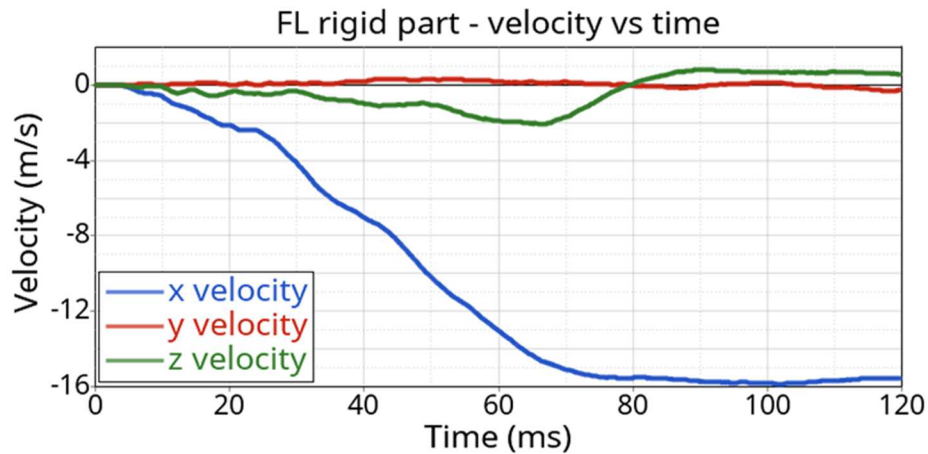


Figure 2.34 Rigidparts model - FL rigid section velocity

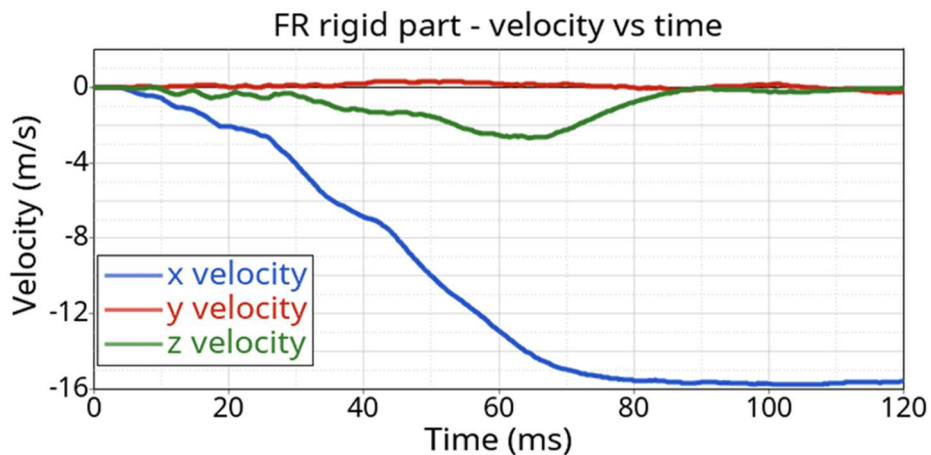


Figure 2.35 Rigidparts model - FR rigid section velocity

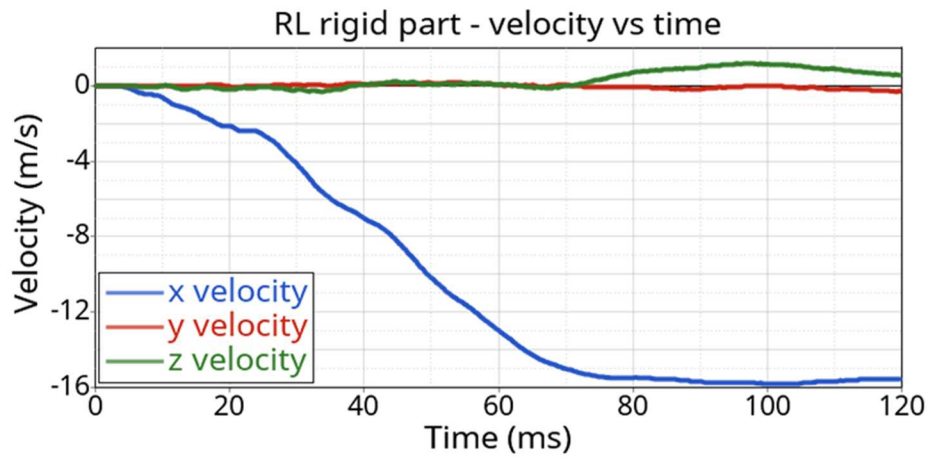


Figure 2.36 Rigidparts model - RL rigid section velocity

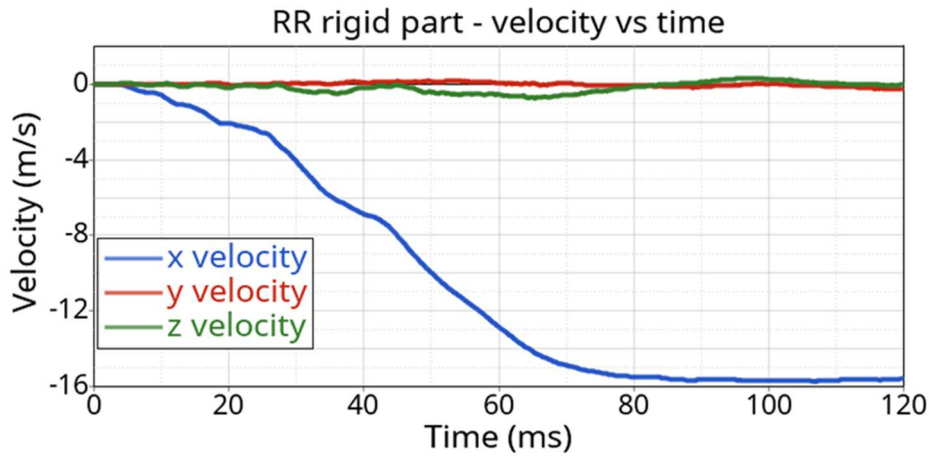


Figure 2.37 Rigidparts model - RR rigid section velocity

It is important notice that the values of the x velocity curves implemented in the sled model as pulse are negative because the velocity is applied with opposite direction with respect to the x axis, providing a backward motion of the structure. The velocity curves are applied to the model through *BOUNDARY_PRESCRIBED_MOTION_RIGID. This command allows to define the motion on a rigid part specifying the curve, therefore the velocity profiles in x, y and z direction are implemented on each rigid section.

2.2.5 Sled set-up

To complete the Sled model other entities must be modelled in order to ensure a proper crash test simulation. A several *CONTROL_option commands (the same implemented in full-scale vehicle model) are included to keep under control some parameters such as the time step, the energy etc. To take out from simulations the proper data, few *DATABASE_option commands are used, allowing to plot the energies values and nodes kinematic during the test, provide the 3D plot, etc. However, to manage the interactions between the parts surfaces over the whole simulation, *CONTACT_AUTOMATIC_SINGLE_SURFACE entity is defined for each component of the Sled as in complete vehicle model. A very important component implemented into the model is the accelerometer which is the same used in full-scale model and it is located. This part is located under the driver seat to compute the accelerations in that area, allowing to perform a comparison between the Sled and the original vehicle. In the Figure 2.38 is shown the position of the accelerometer.



Figure 2.38 Sled model - Driver accelerometer

2.3 Human Body Model

2.3.1 Introduction [12]

In the last century, the spread of car market led to the need to improve the safety system included in motor vehicles, and therefore to verify their effectiveness. Cadavers, animals, volunteers, and human surrogates (crash dummies) were used in crash test to reproduce different casualties in real-world road accidents. Although crash dummies are high-precision anthropomorphic instrument used to evaluate human injuries during vehicle crashes, they are built for repeated use thus their structure shows different responses with respect to the real occupant body. Nowadays, the necessity of study a high number of collision scenarios and the costs of testing campaigns have allowed the diffusion of Finite Element simulations in this field. In order to represent faithfully the traffic accidents, the FE models have become even more complex and precise, leading to the development of Human Body Models which are now an increasingly important tool in the study of injury biomechanics. The HBM are Finite Element (FE) computational model of the human body designed to replicate its biomechanics and kinematics in a variety of scenarios, where all their parts are represented realistically in both the geometry and the material properties. The models include detailed head (face, skull, brain, and spinal cord), the skeleton, internal organs (heart, stomach, liver, etc.), and air cavities (including the lung). Their purpose of these model is to accurately acquire the stresses developed in the human body under various loading conditions. The information gets from simulations with HBM allow to evaluate body injuries, fracture locations and internal organ trauma. There are many models, designed in order to simulate male or female human being with different sizes as shown in Figure 2.39. In this thesis a HBM provided by Toyota and called THUMS is adopted.



Figure 2.39 Different models of HBM [13]

2.3.2 THUMS model [13]

Total Human Model for Safety (THUMS) is a human FE model jointly developed by Toyota Motor Corporation and Toyota Central R&D Labs., Inc. The model aims to simulate human body kinematics and injury responses in car crashes. The geometries of the human body parts are represented by detailed FE meshes and their material properties are defined assuming constitutive laws. In this thesis, an average size adult male (AM50%ile) model which has a height of 175 cm and a weight of 77 kg is used to simulate the driver occupant in a mid-size passenger sedan during a crash test. It has an initial sitting posture in order to represent a car occupant, but this configuration is adjusted to fit properly into the Vehicle environment (Positioning §3.1) before testing. The THUMS in the original position is reported in Figure 2.40.



Figure 2.40 THUMS - initial sitting position [13]

The model provided was obtained through a high-resolution CT scanning process in order to digitize the interior of the body and to generate precise geometrical data for each model part. The HBM reflects the anatomical features of each organ, tissue, and bones in a human body, associating the proper material properties to each body part as reported in literature. Therefore, the model is able to simulate brain and internal organ injury at a tissue level, as well as skeletal fractures and ligamentum injuries. The THUMS contains approximately 760,000 nodes and 1.9 million elements. The whole body model was generated by integrating component models (head, torso and extremity models). The boundaries between component models were carefully connected so as to match the meshes without making geometrical discontinuity. The head is modelled in detail and it includes the epidermis (skin), skull, mandible, eyeballs, teeth, meninges,

cerebrum, cerebellum, brainstem, CSF etc. (Figure 2.41). The inferior part of the head model is attached to the torso through the neck in which muscle are modelled with 1D elements.

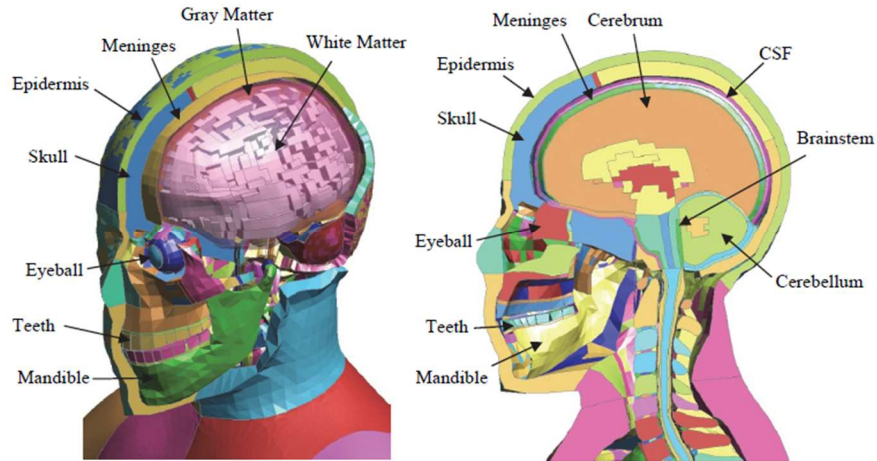


Figure 2.41 THUMS - head model [13]

All the skeletal parts and the major soft tissues are included. The hard tissues are ribs, sternum, spine vertebrae spine, clavicles, scapulas, sacrum and pelvis. The connective tissues such as costal cartilages, intervertebral discs and pubic symphysis are also modelled. Figure 2.42 shows the skeletal structure.

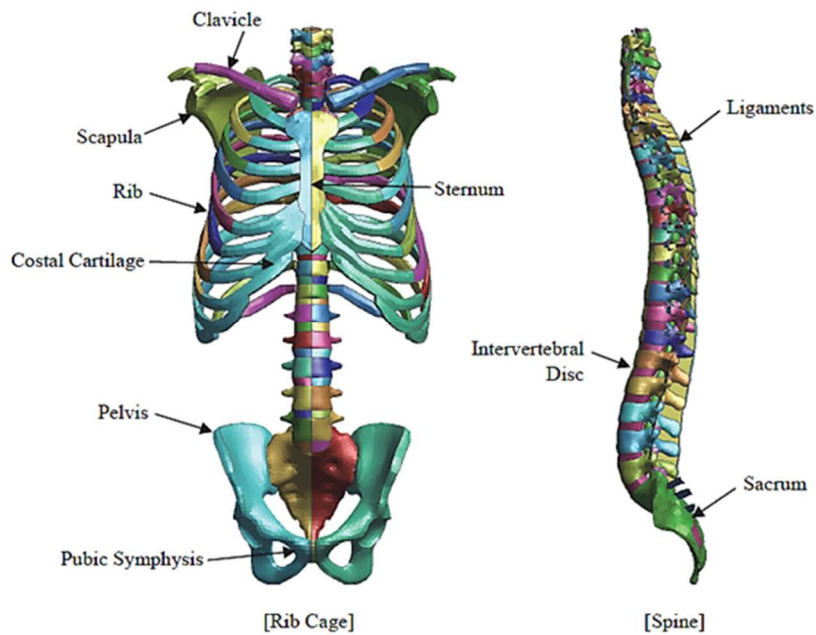


Figure 2.42 THUMS - Skeletal parts in torso model (with Neck Model) [13]

The internal organ tissues represented are heart, lungs, liver, kidneys, spleen, pancreas, gall bladder, bladder, esophagus, stomach, duodenum, small intestine, and large intestine. The major soft tissue parts are shown in Figure 2.43.

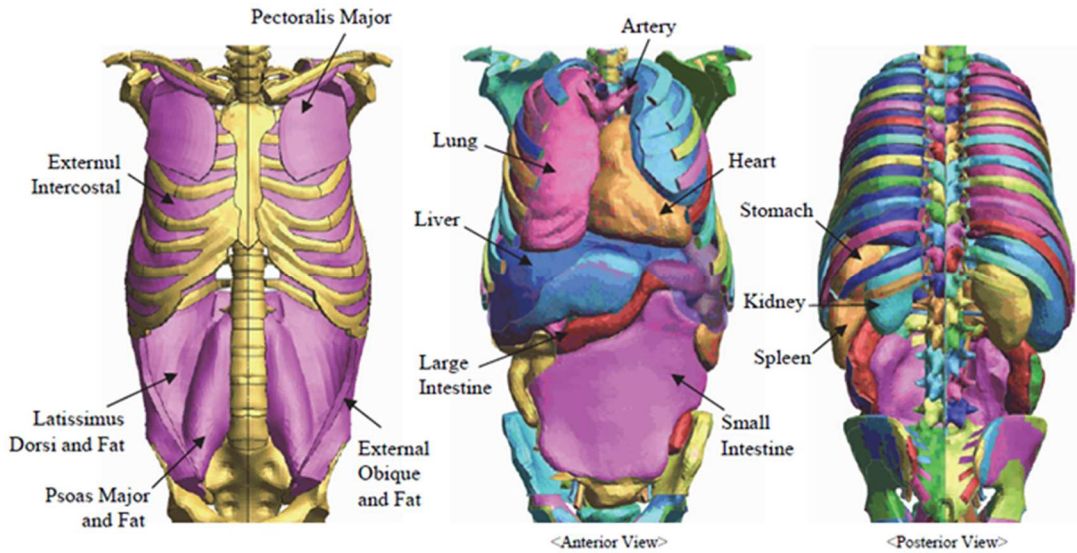


Figure 2.43 THUMS - Soft tissue parts in torso model [13]

The bones of the extremity models are surrounded by flash parts which simulate the extensor and flexor muscle (Figure 2.44). The skin (modelled with shell elements) fully covers the whole body.

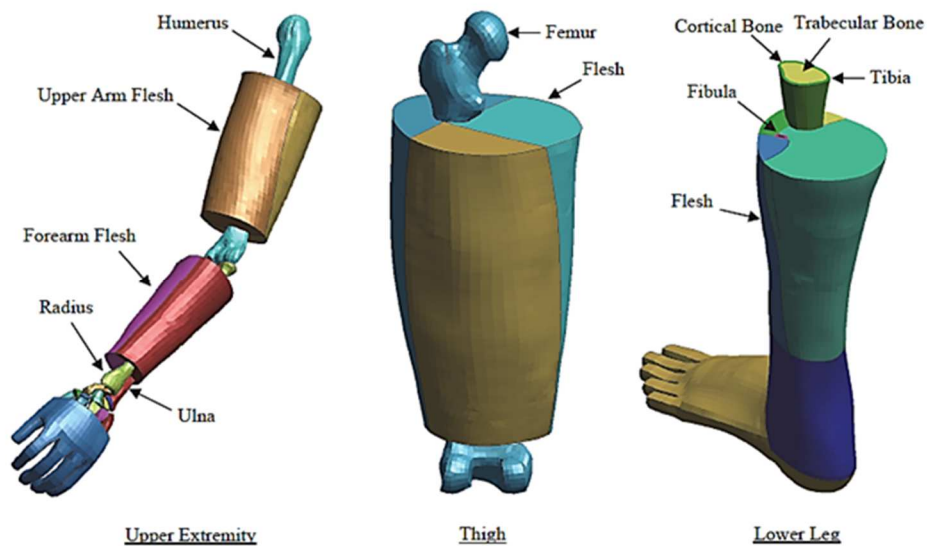


Figure 2.44 THUMS - Extremity models [13]

Joints are modelled as bone to bone connection with ligaments and no kinematic joint element is used (Figure 2.45).

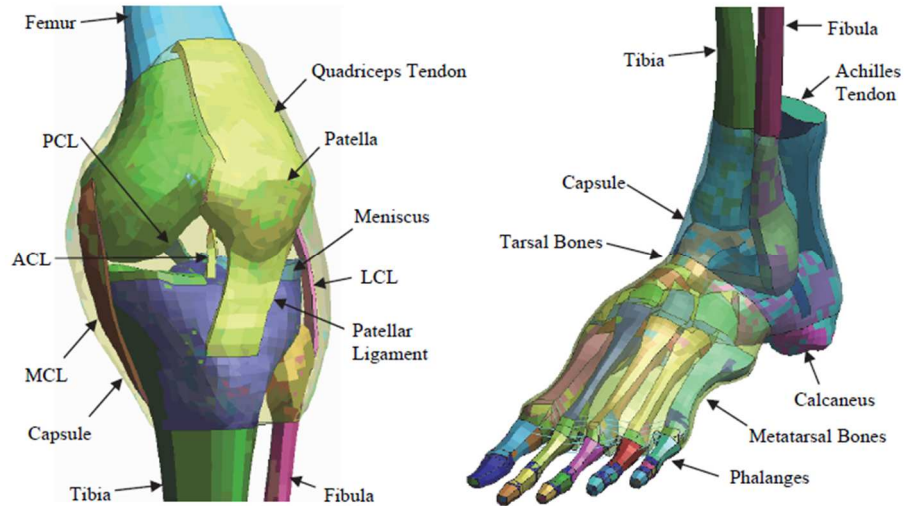


Figure 2.45 THUMS - Joint model [13]

2.3.3 THUMS instrumentation [14]

The original THUMS version is not provided with database definitions therefore it is necessary integrate the instrumentation such as accelerometers and cross-sections to the model in order to compute the biomechanical data. The version provided by Polytechnic of Turin, on the other hand, include several sensors which allows to perform a complete analysis of the human body behaviour over the crash simulation.

The biomechanical data measured in this work are:

- Head linear acceleration in x, y, z direction
- Head angular acceleration in x, y, z direction
- Linear acceleration in x direction of the T1, T4, T12
- Pelvis linear acceleration in x direction

HEAD SENSOR

The model is equipped with an accelerometer located inside the brain region. This sensor is defined directly on THUMS soft tissues, changing some elements into rigid parts (LS-DYNA requests a rigid part in order to define an accelerometer element). The head accelerometer is shown in Figure 2.46.

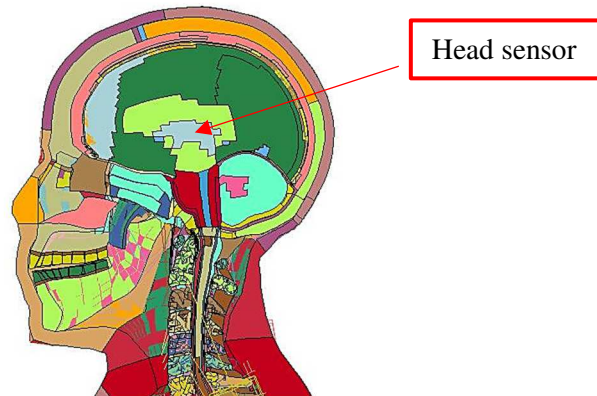


Figure 2.46 Head accelerometer

TORSO SENSORS

In order to describe the upper part of the human body, the THUMS is equipped with three accelerometers in vertebrae T1, T4 and T12. In this model for each vertebra, the whole part is modelled as a rigid component, allowing the definition of the sensor, and getting a good output signal. The figure 2.47 shows the location and few details about vertebrae sensors.

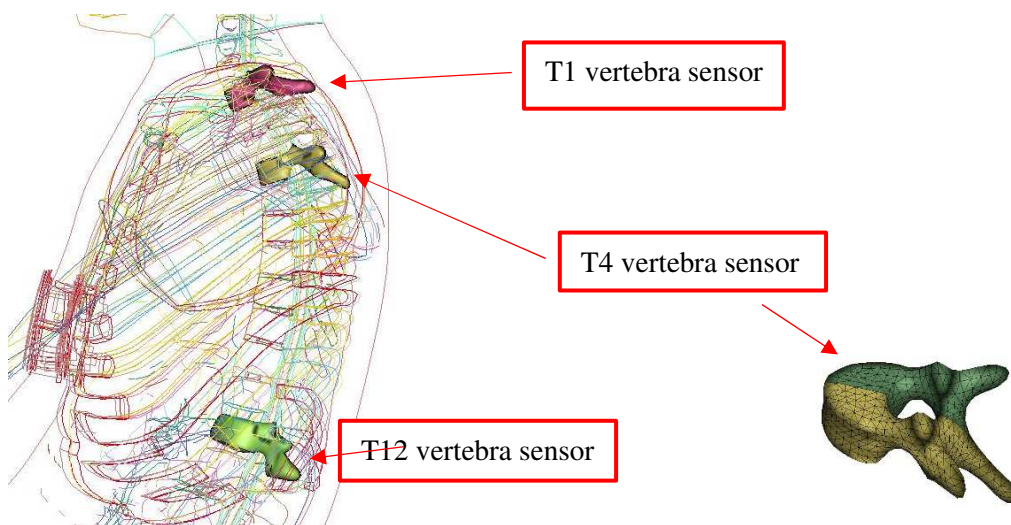


Figure 2.47 Vertebrae accelerometers and detail of the T4 vertebra

PELVIS SENSOR

This accelerometer is based on the same concept of the head sensor, i.e. in some elements belonging to hip bone, the rigid material is set. This stiffening of the skeletal structure allows to get clear acceleration signals. In Figure 2.48, the rigid elements of the accelerometers are exposed.

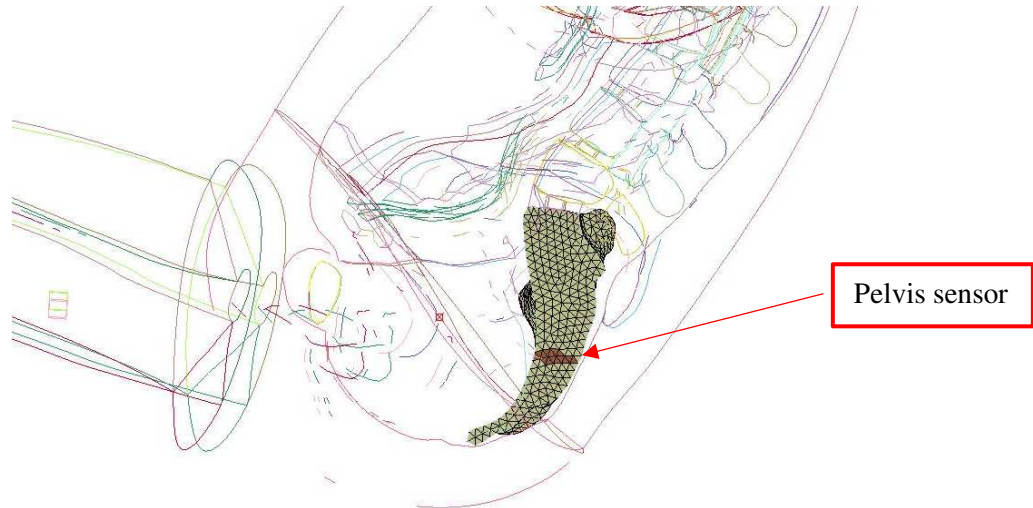


Figure 2.48 Pelvis accelerometer

2.4 Seatbelt model

2.4.1 Introduction

Seatbelts (also known as safety belts) are vehicle passive safety devices designed to secure vehicle occupants against harmful movement that may occur during a collision or a sudden braking. No other safety product has saved as many lives of car occupants, thus because of their vital role in driver and passenger safety they are considered Primary Restraint Systems (PRS). Before a crash occurs, occupants are travelling at the same speed of the vehicle and their motion do not change when the car stops suddenly due to a collision with another object. In this scenario, secondary impacts with interior strike hazards could occur and, in that case, serious injury or also likelihood of death could result after the crash. If seatbelts are installed on the seats, they apply an opposing force to the driver and passenger body reducing their speed, keeping occupants positioned correctly for maximum effectiveness of the airbag and preventing them to contact with interior parts or to be ejected from the vehicle.

2.4.2 FE seatbelt

In this thesis, the virtual restraint system was included in the finite element model of 2012 Toyota Camry Sled in order to secure the occupant as specified in Euro NCAP protocol. Since only the driver human body model is considered in this work, the complete FE seatbelt model is added on the driver side. It consists of a modern three-point seatbelt composed by:

- Anchors
- D-ring
- Buckle-tongue lock system
- Retractor (retractor pyrotechnic pretensioner and load limiter are included)
- Seat belt sensors
- Webbing

When the driver seatbelt system is included in simulation environment, the belt wrap THUMS body and the locking tongue is inserted into the buckle, representing the usage configuration as shown in Figure 2.49.

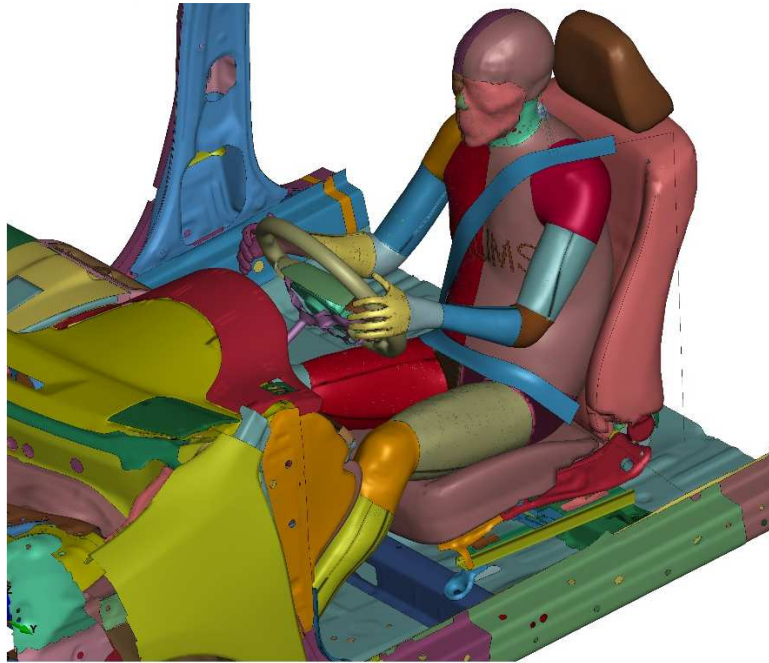


Figure 2.49 Seatbelt model

To model the whole seat belt system, several steps are taken:

1. Anchors modelling
2. Webbing modelling and routing process
3. Retractor, pretensioner, slip ring modelling

The anchor points are CNRB which link the belt components, such as retractor, slip rings and end belt, to vehicle frame. The webbing is divided in 3 segments:

- B-pillar belt, which runs near the B-pillar, from the retractor to the D-ring
- Shoulder belt, which wraps the driver chest, running from the D-ring to the tongue long hole
- Lap belt, which goes over the waist, from the tongue long hole to the end belt anchor

Since the B-pillar belt do not run over the human body, it is simulated as a segment belt which is made of several linear elements connected each other. On the other hand, the shoulder belt and the lap belt are more complex parts since these portions run over the occupant's chest and pelvis area, interacting with the THUMS. Therefore, in order to simulate properly the real seatbelts, they are made of two different webbing type: segment and fabric belts. Where the HBM comes in contact with the restrain system, the fabric belts are adopted. These belt portions are modelled as

a ribbon with proper width and thickness in order to simulate in a realistic way the pressure of the webbing on the occupant body. On the contrary, the segment belts cannot simulate suitably the contact interaction but describe properly the tensile behaviour, therefore they are placed near the slip rings. Adopting the segment webbing, the seatbelt model results lighter from the computational point of view moreover, it is possible to model the D-ring, the tongue long hole and the retractor as a node element in which all properties are defined.

Overall, this mixed model allows to:

- reduce the complexity of the restrain system
- simplify retractor, pretensioner and slip rings modelling
- require a single point to link the belt to the anchors
- simplify the belt management
- compute the belt forces in easiest way
- make it user-friendly if THUMS must be repositioned or model must be modified

On the other hand, the model is less detailed than a virtual restrain system with complete fabric webbing.

2.4.2.1 Seat belt anchors modelling

Due to the absence of the seatbelt model in original full-scale vehicle model, the anchors must be created properly in FE environment before modelling other components of the safety device. In a modern three-point seatbelt, four anchors are present, in particular, where retractor, end of the webbing, D-ring and buckle are located. Pictures of real 2012 Toyota Camry cockpit with typical installed restrain system were observed to estimate the anchors position. Since each component is modelled as a point with certain properties, a node is added at defined position and it was constrained thanks to a CNRB (which is the anchor) to the appropriate vehicle part.

END WEBBING:

The FE sled model provide the hole where the end of the seat belt must be fixed to the lower part of the frame, just left to the seat base. To simulate the bolted webbing, a node which will be the end node of the 1D seat belt was constrained to the hole edge in central position using a CNRB. The Figure 2.50 shows the real anchor system and the FE model.

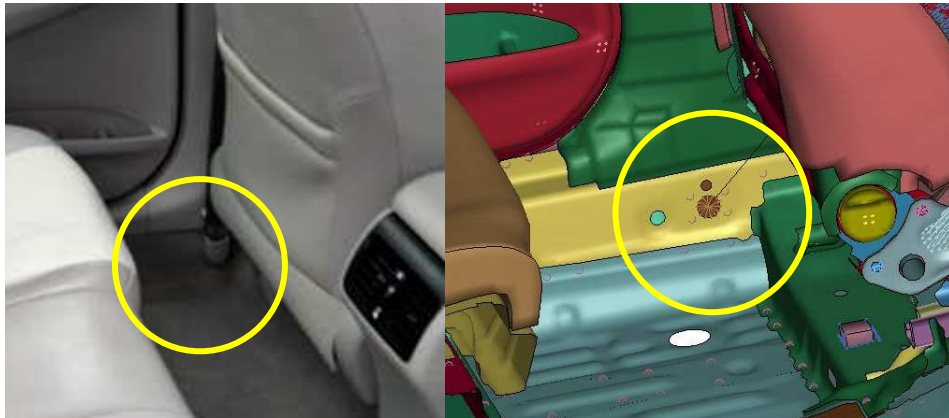


Figure 2.50 Comparison between actual and FE end belt anchor

BUCKLE

For the driver restrain system, the buckle is attached to the right side of the seat frame. Considering an indivisible buckle-tongue lock system for the finite element simulation, a node was added to simulate the belt sliding point. The coordinates of this node were defined considering the real position of the tongue long hole and the need to avoid 1D belt contacts with positioned THUMS. A CNRB was included to connect the point where the webbing runs to the appropriate seat frame part. Figure 2.51 exposes the comparison between real buckle-tongue anchor and simulated one.



Figure 2.51 Comparison between actual and FE buckler position

D-RING

In a real Toyota Camry, the D-ring is located on a sliding system which allows to regulate the height of the point where the seat belt runs. This regulation system is fixed on the B-pillar with

two bolts and their threaded holes are present in FE models as well. Considering the D-ring cover present in original model and the THUMS dimensions, an approximative middle position of the D-ring is taken into account in this thesis. The coordinates of the D-ring node were estimated observing real D-ring configuration and it is constrained with CNRB to the fixing hole edges on the B-pillar. Figure 2.52 shows the D-ring anchor in a real Toyota Camry and in FE environment.



Figure 2.52 Comparison between actual and FE D-ring position

RETRACTOR

In a real car, the retractor is located in the lower part of the B-pillar, fixed with a mounting bracket. In finite element model the bracket is not included but a simple anchor was created observing where the webbing come out from a real retractor. Then, a node was added to represent the automatic locking apparatus and it was constrained to the interface where the real bracket is installed through a CNRB. Figure 2.53 shows the anchor system.



Figure 2.53 Comparison between actual and FE retractor position

2.4.2.2 Webbing modelling [15][16]

The webbing is the flexible part of the seat belt system that is pulled around the person and is tightened to support the occupant body upon impact. It is made from polyester which is a soft material but highly resistant to cuts and scratches and has a tensile strength to support more than 28 kN. As mentioned previously, the webbing model is composed by different seat belt:

- Segment belt or single-Line belt (1-D Beam)
- Fabric belts (2-D Shells)

The segment belt elements are characterized by:

- *SECTION_SEATBELT
- *MAT_SEATBELT

The *SECTION_SEATBELT is a keyword that allows model single-line belt elements. Linear density, minimum allowable length for belt elements, load curve for loading and unloading are inputs specified for belt material. The minimum length is an important parameter for elements passing through D-rings, retractor, and tongue long hole. In LS-DYNA, when these belt elements go from one side of the slip ring to the other, it might be numerically necessary to reduce their lengths from the modelled state to do so. The value represents the dimension of the belt beam beyond which it cannot be reduced. As suggested by LSTC[x], the minimum allowable length for segment belt elements is set to 3 mm. The single-line belts operate mainly through the load curves which are force-engineering strain curves describing the belt behaviour. In this thesis the curves for loading and unloading are equal and the trend is showed in Figure 2.54

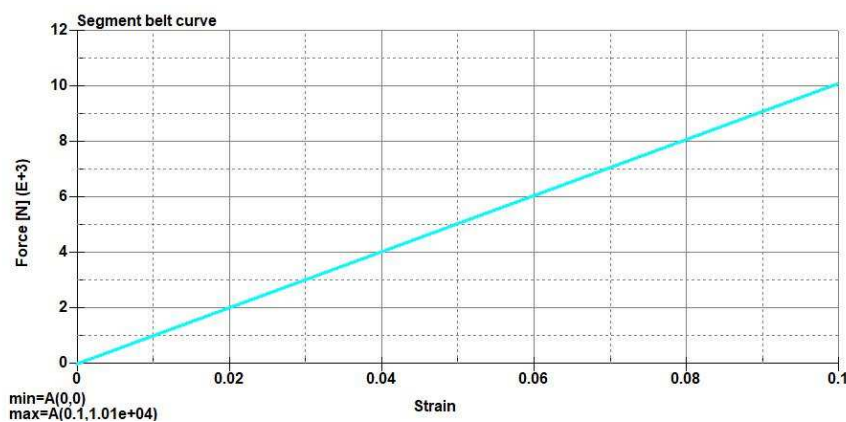


Figure 2.54 Segment belt curve

The fabric belts are modelled with a width of 46 mm and that are composed by triangular shell elements (*ELEMENT_SHELL).

These elements are characterized by:

- *SECTION_SHELL:
- *MAT_FABRIC

In *SECTION_SHELL, the thickness of the belt is set to 1.2 mm as in real webbing. It is usually found during testing that the strength of the belt in the lateral direction is only half that of the strength in the longitudinal direction, therefore to set correct properties, flag for orthotropic/anisotropic layered composite materials is activated in *SECTION command, allowing to define “fabric angles” which characterize longitudinal and lateral direction. The Figure 2.55 exposes the main axis (the arrows) of each shell element that compose the webbing. Thanks to the previous setting, the longitudinal direction is rotate of 90° with respect to main axis (lying on the shell plane) while the lateral direction coincides with it. In the *MAT_FABRIC, it is specified the mass density, the young’s modulus in transverse, longitudinal and normal direction, the Poisson’s ratio, and the shear modulus. Also, the material axes option is defined, allowing to model locally orthotropic properties.

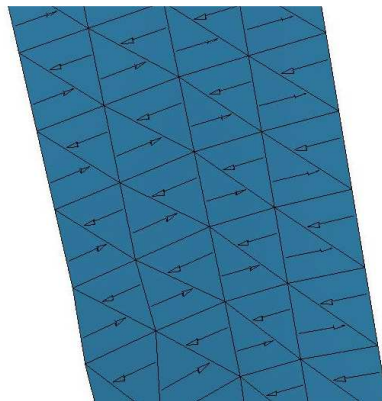


Figure 2.55 Main axes of the mesh element in fabric belt model

Another important setting is the activation of flag to modify membrane formulation which needs load curves definition in longitudinal and transverse direction for belt strain properties. These curves are determined from physical component tests with the belt and are provided by LSTC [15]. In this thesis, the segment belt load curves are used to describe tensile properties but whereas single-line belts use force-strain curves, fabric webbing needs stress-strain curves, therefore the force axis is multiplied by an Y-scale factor.

To obtain the stress value, the force must be divided by the cross-section area of the seat belt therefore:

$$\text{Section Area} = 46 * 1.2 = 55.2 \text{ mm}$$

$$Y\text{Scale Factor} = \frac{1}{\text{Section Area}} = 0.01812 \text{ mm}^2$$

The Figures 2.56 and 2.57 show the load curves and it is important notice that the strength of the belt in the lateral direction is half that of the strength in the longitudinal direction as previously reported.

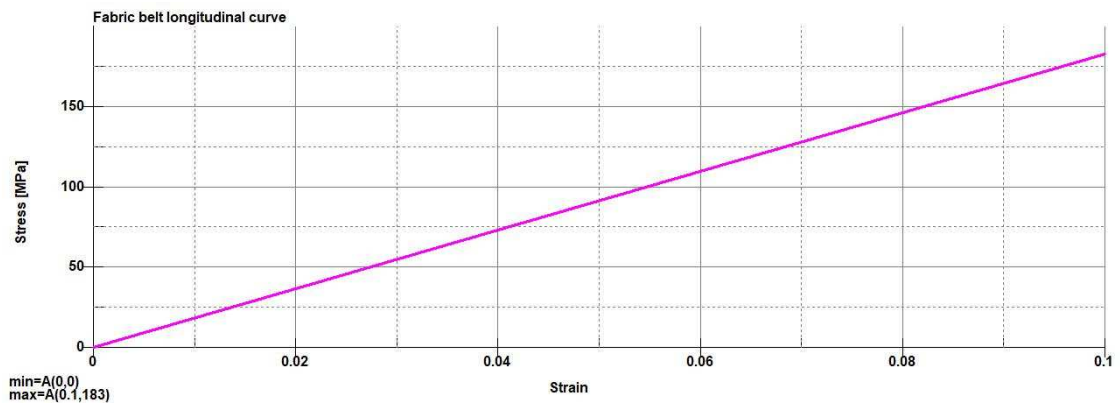


Figure 2.56 Longitudinal curve of the fabric belt model

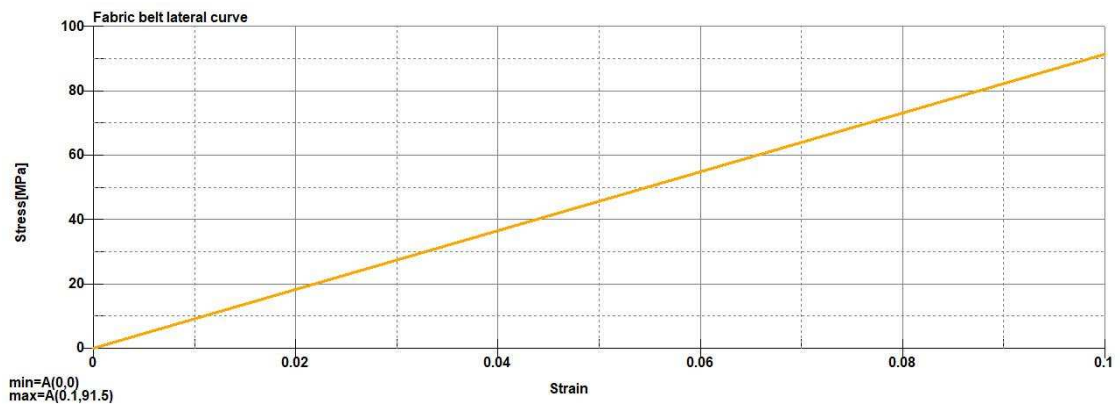


Figure 2.57 lateral curve of the fabric belt model

The routing of the belt system is performed thanks to *Seatbelt Fitting* command, but this process is better described in section §3.4 because several steps are required before.

2.4.2.3 D-ring and buckle-tongue lock system [15][16]

The D-ring is a metal ring shaped as D letter that is used to guide the webbing over the shoulder and across the chest of the occupant. It is installed in the upper part of the B-pillar (front passengers) and C-pillar (rear passengers). The buckle is the component of the seat belt system that secures and releases the tongue, which is attached to the webbing. This part is designed to hold the tongue firmly and allow the seat belt to be fastened and unfastened with very little force, also after a crash. The tongue is the piece that is connected to the webbing and fits into the buckle to secure the seat belt. The Dynamic Locking Tongue could be integrated in order to reduce loads on the occupant's chest. In LS-DYNA, to simulate the seat belt sliding behaviour at D-ring or tongue long hole, the *ELEMENT_SEATBELT_SLIPRING is used for each component. To define this command, must be identified:

- A node as “SLIPRING” element (node that represent D-ring or tongue long hole)
- The two seat belt elements that have a common node on the relative slipping
- The Coulomb dynamic friction coefficient at the ring

As previously described, the D-ring and the buckle-tongue lock system are represented as a node where the 1D seat belt slips through and after the routing process of the webbing, they are connected to two segment belt elements each. However, the most important and often confusing thing here is the node which is defined as slip ring does NOT belong to the two belt segments and it is constrained to the vehicle. Obviously, after the routing, the belt segments themselves have a common node which is coincident with the slip ring at Time=0 (they are coincident only at the beginning of the simulation). During the test, when the belt is pulled by the human body motion, the belt element which is pushed in the D-ring or long hole, pass through, and go to the other side. At this instant, the other node which characterizes the 1D belt element rises to the slipping location and instantaneously become coincident with the slipping node. Hence the belt node on slipping position is transient, being quickly replaced by the different nodes of the belt as it slips through. This process continues over the whole the crash test, with the belt going back and forth based on whether the retractor or the THUMS pull it. The dissipation of energy due to the friction between ring and webbing is considered through the Coulomb dynamic friction coefficient at the ring which has a value of 0.15 as specified in LSTC occupant modelling workshop.

2.4.2.4 Retractor and load limiter [15] [16]

This component allows every occupant to adapt the seat belt to his/her body dimensions, sacrificing some restraining ability in the early phase of a frontal crash, to get the belt comfortable in the daily usage. The retractor is an automatic locking apparatus and its main function is to pull in excessive webbing and thereby eliminate the worst of the slack in the belt. However, the rewinding spring force has to be rather weak otherwise the belt will be too uncomfortable to wear but, on the other hand, the rewinding capacity of the retractor has to be sufficient to “clean up” the belt, when is un-buckled. Also, it acts to prevent any further protraction of the belt strap, constraining occupant body on the seat during a collision. The system has two sensors: one sensor locks the webbing when it is pulled out of the retractor at a faster rate than normal, the other sensor locks the belt when the car brakes or accelerates quickly. This safety device is installed in the lower part of the B-pillar of the car. Another important component of the seatbelt system is the load limiter. This device is designed to allow the seat belt force applied upon the chest to rise only to a point where serious injury of the rib cage is unlikely. The seat belt is then allowed to extend in a controlled manner, maintaining a constant restraining force to absorb energy. To include the retractor into the FE sled system, LS-DYNA provide an appropriate command, *ELEMENT_SEATBELT_RETRACTOR, which allows to model it and set all functions as a real component. This command line needs some inputs:

- A node as “RETRACTOR” element
- The identification number of first belt element that is just outside the retractor
- A sensor which activates the retractor during a collision
- The time delay after sensor triggers
- The amount of pull-out between time delay ending and retractor locking
- Load curve for loading
- Load curve for unloading
- The fed length

As previously described, the retractor is represented as a node in which the segment belt is pull-in or pull-out depending on the condition. After the routing process, the B-pillar seatbelt is linked to the D-ring and the automatic locking apparatus, so this means that there is a 1D belt element which has a node characterized by the same coordinates of the retractor node. It is the same principle behind the slipping definition process. At “Time-0”, the first belt element that is just outside the retractor has a node which is coincident with the rewinding system, but it does NOT

belong to that component. In fact, whereas the retractor node is constrained to the vehicle structure, the webbing can run through during the simulation. However, the belt node is “transient” just as in the slip ring, with other nodes quickly replacing it as more and more belt elements are pulled out from the retractor. As in real restrain system, the FE retractor model have to be activated when a crash occurs, therefore during the test simulation, a sensor determines the lock-up of the rewinding system (up to four sensors can be defined). This sensor is modelled using *ELEMENT_SEATBELT_SENSOR and it triggers at a given time (sensor fire time) which is usually considered to be within 1 ms after the bumper hits the rigid barrier. After the sensor triggers, there could be a physical time delay (based on the restrain system design) to retractor locking but in this thesis delay time is not considered. Another parameter that can be set up with LS-DYAN is the length of loose belt which spools out at a very low force value before the retractor locks up, but it is not taken into account over the simulations. When the system is locked, the amount of belt spool-out is dependent on the force-pull out curve (*DEFINE_CURVE) which is specified for loading condition. The first point of the load curve is $(0, T_{min})$, where T_{min} is the minimum tension which is applied to pull in excessive webbing, removing possible belt slack. The minimum tension in the belt is 28N. In this FE model, the force limiter is included into the retractor as in Energy Management Retractor (EMR). It is possible adopting a load curve which ramps up quickly and then maintains a constant force value. This device allows webbing to be pulled out of the retractor in a gradual and controlled manner in response to the body motion, limiting the load on the occupant. If the tension in the belt relaxes during the simulation, the load curve for unloading is followed but in this work the two curves are equal. The Figure 2.58 shows the load curve.

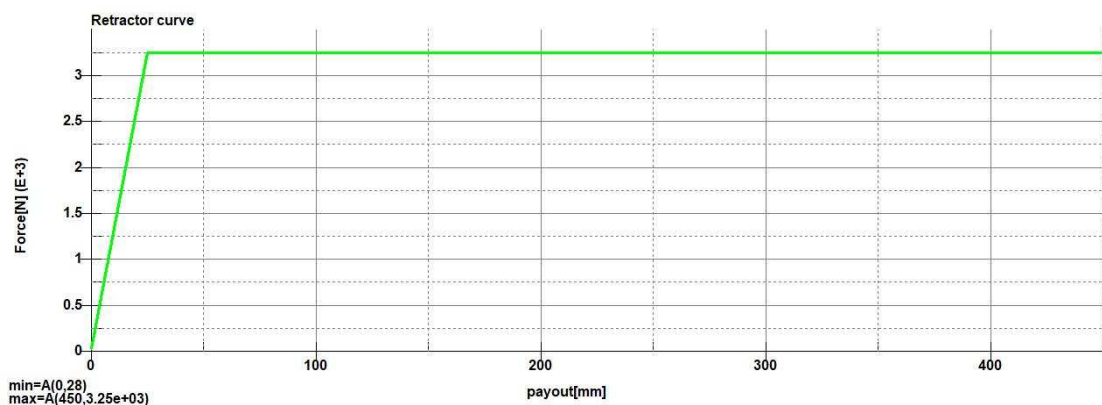


Figure 2.58 Retractor curve

The fed length is defined to set a typical initial length of element and it is at least three times the minimum length specified in belt properties. The maximum rate of pull out or pull in is given by $0.01 \times \text{fed length}$ per time step.

2.4.2.5 pretensioner [15][16]

This component aims to pre-tension the webbing when a collision occurs. There are two kind of devices: the retractor pretensioner and the buckle pretensioner. The retractor pretensioner is a device designed to retract some of the webbing seatbelt. A small pyrotechnic charge generates gas very quickly with a high pressure which then acts upon a pulling mechanism to rewind the retractor spool. Depending on the amount of slack present, up to 150-200 mm of webbing can be pulled in. The retractor pretensioner is fired by an electronic control unit sensing the vehicle crash pulse. The belt is tightened up significantly before the occupant has moved more than a few centimetres forward relative to the car during a frontal crash. If people wear a lot of clothing, a considerable amount of slack can be present in the belt system and especially in the lap belt, and this can increase the risk of abdominal injuries. In order to further improve the pre-tensioning of the lap belt, a pretensioner mounted on the seat belt buckle (buckle pretensioner) was developed. The first generation design was fully mechanical with a strong and fast acting spring but today with airbags commonly mounted into cars, the actuators of the buckle pretensioners are pyrotechnically driven. To model this component in FE environment, LS-DYNA provides the command `*ELEMENT_SEATBELT_PRETENSIONER`. This command line needs some inputs:

- The seat belt pretensioner type
- The identification number of the retractor
- A seat belt sensor which activates the retractor during the simulation
- The time between sensor firing and pretensioner acting
- The load curve for pretensioner
- The limiting force for retractor (beyond which it will not pull)

As in a real Toyota car, the component is a pyro pretensioner included into the retractor with limiting load system. During the simulation, the pretensioner is activated by a sensor (up to four sensors could be defined) which is modelled as `*ELEMENT_SEATBELT_SENSOR` and it triggers at a given time. In this work, a sensor fire time of 13 ms is used. After the sensor triggers, a time delay could occur before pretensioner acting but it has not been set. To model properly the

component in LS-DYNA, the retractor has a curve (*DEFINE_CURVE) that describes the webbing pull-in as a function of time, and over the whole simulation, the belt is drawn into the retractor exactly as specified. In Figure 2.59, the pretensioner curve shows a belt pull-in of 130 mm during the EuroNCAP test.

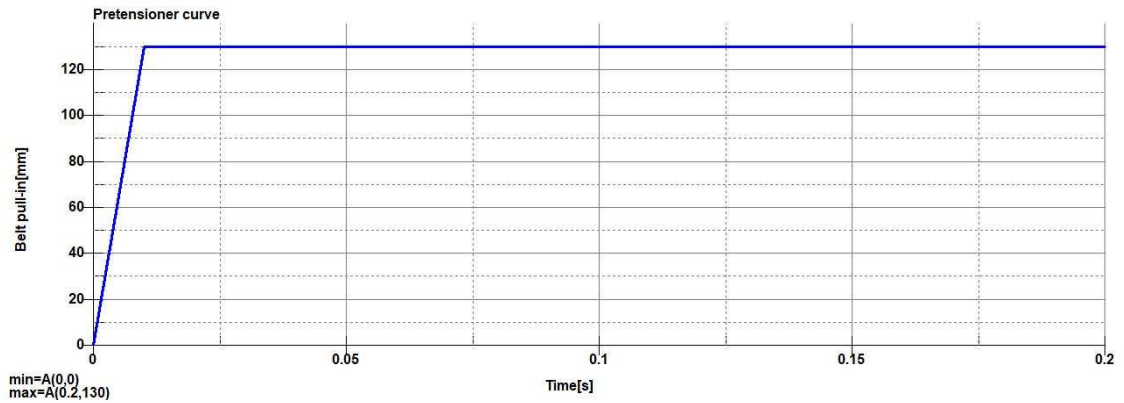


Figure 2.59 Pretensioner curve

However, if at any point the forces generated in the belt exceed the pretensioner load limit, then the pretensioner is deactivated and the retractor takes over.

Chapter 3

3 Pre-simulation processes

3.1 Introduction

In models where HBM is included some routine operation must be performed in order to realize properly the impact test according to EuroNCAP regulation. These operations allow to place the HBM into the vehicle and set the FE environment, providing more realistic impact simulations. As can be seen in Figure 3.1, if the original THUMS is inserted into the vehicle model, the body position do not represent adequately the conventional driving posture, detecting interpenetration between parts (e.g. the lower seat cushion and the HBM lumbar region). Therefore, it necessary modified the body configuration in order to respect the test standards.

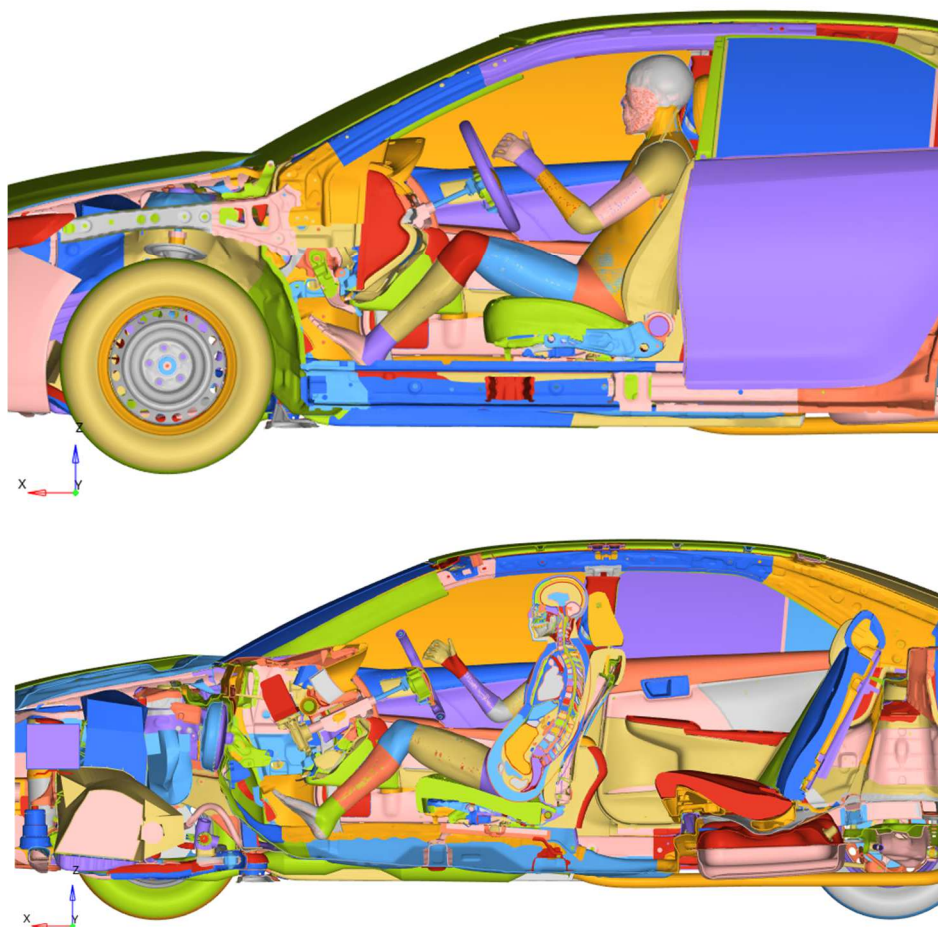


Figure 3.1 original THUMS in vehicle model - side (upper) and section (lower) views

The positioning process of the occupant body on its seat is very important for testing purposes and, as reported in frontal full-width impact protocol, few steps must be followed in order to respect test specifications. After the installation of the driver, the FE vehicle model must be modelled to interact properly with the THUMS, representing faithfully the test configuration.

The sequence of operations that are performed both for the sled and full-scale model is:

1. THUMS positioning

It allows to position the HBM in a standard configuration which represent the same set-up of an actual crash dummy during the test.

2. Sitting simulation

It allows to create the footprint left by the THUMS on the seat cushions when the occupant is placed into the vehicle.

3. Seat belt routing

It allows to wrap the seatbelt around the human body, securing it on the seat.

In the following section, detailed descriptions of the operations performed in this thesis are reported, underlining every step considered necessary to obtain a reasonable initial configuration of the models. The model in final configuration are assembled and showed in Figure 3.2. At the end of all these steps, contacts are defined in order to prepare the complete models to the simulations.

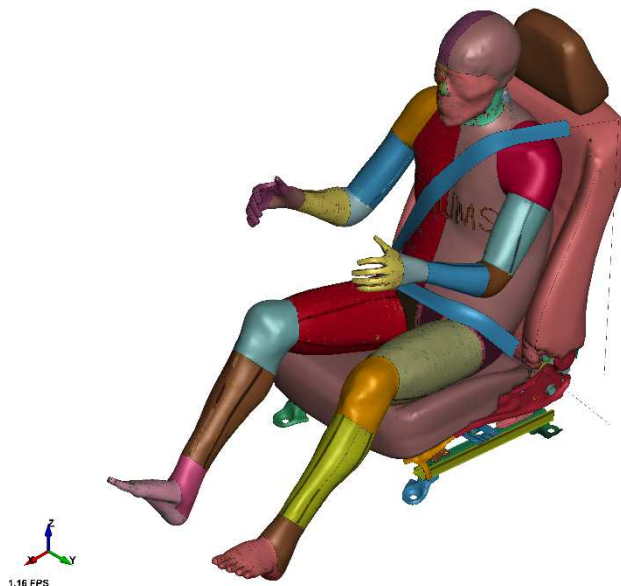


Figure 3.2 THUMS, seat and seatbelt in final configuration

3.2 Positioning

3.2.1 Introduction

The definition of the initial position of the occupant body model is an extremely important phase for crash test since it influences consistently, along with the restrain system configuration, the extent of driver injuries caused by the impact. Since the HBM are high complex FE models implemented in commercial explicit Finite Element (FE) codes, and they are typically available in one size and one posture, could be difficult or time consuming to change they initial configuration. In this thesis the initial posture of THUMS model is modified in order to emulate the initial configuration of a driver test dummy. The whole process requires two steps:

- Modelling in PIPER program
The HBM is load in PIPER environment to facilitate the positioning and at the end, LS-DYNA simulation files are obtained.
- Positioning simulation in LS-DYNA
It is a simulation that allows to modify the original human model, from the initial posture to the final one. Finally, the positioned model is exported.

3.2.2 Modelling with PIPER program [17] [18] [14]

In this Thesis work, the PIPER open-source program for HBM scaling and positioning is used to modify the original posture of the FE occupant body. This software framework is developed specifically to help with the personalization of HBM for injury prediction to be used in road safety. An important feature of this program is the possibility to associate some of the FE entities to anatomical concepts as these are useful for scaling or positioning (e.g. a bone is not expected to deform during positioning to the contrary of the skin). This association between the FE entities and anatomical entities is made by means of Metadata set for a given model. The Metadata are input information describing what needs to be interpreted by PIPER modules (e.g. anatomy, relationships, mesh) and they must be imported with the THUMS within the software in order to convert a complex human model into a simplified model with restricted number of degrees of freedom. The simplified HBM result very intuitive to handle during the posture setting. First of all, to start performing the positioning process, the original THUMS and its metadata are load into the PIPER program. Since the posture of the HBM is influenced by the dashboard dimensions

and obstructions into the cockpit, the vehicle environment is included into the modelling software, in order to detect possible interpenetration between models. Only the strictly necessary FE components of the car interior are considered so that high computational cost is avoided. The Figure 3.3 shows the vehicle component included into the modelling area.

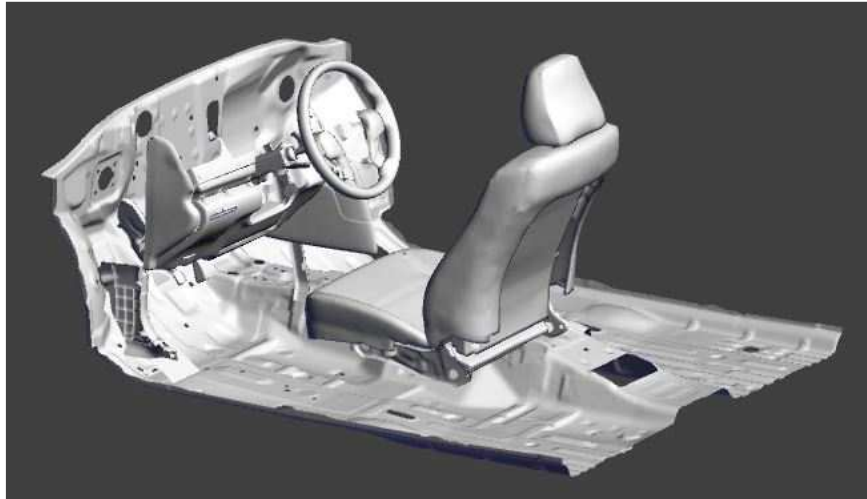


Figure 3.3 Vehicle environment for positioning in PIPER

Before starting with the actual handling of the THUMS, the original HBM is positioned on the driver seat in order to lay down the lumbar region and the gluteal muscles on the cushions. As can be seen from the Figure 3.4, the THUMS posture need to be fitted to simulate the correct driver position.

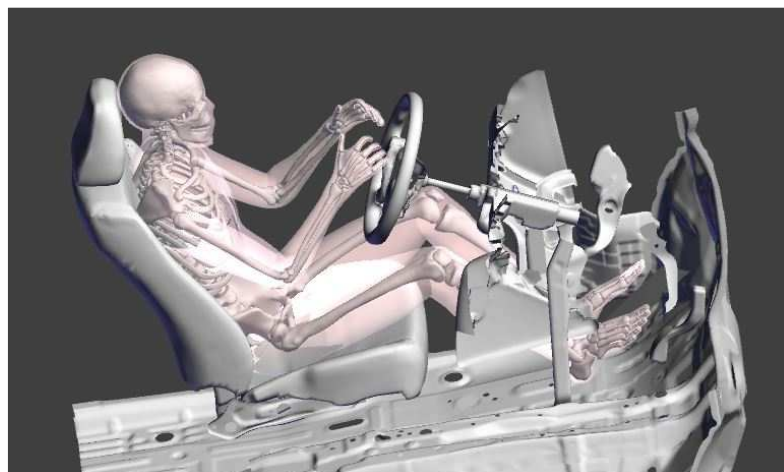


Figure 3.4 THUMS and vehicle environment

To correctly place the different body parts of the THUMS in the FE environment, three main functions are used:

- Landmarks positioning

The landmarks are nodes associated to bone entities, and usually positioned on their extremities, in order to manage easily the skeletal structure during the posture setting (Figure x). They can be moved manually defining their coordinates in *pre-positioning* module and it is possible to export their position in a dedicated file to save the body setting.

- Definition of joint rotations

It is possible specify in the FE model the angles of the main human body joints to perform the positioning.

- Fixed bones command

This command allows to fix the bone entities in order to keep their position when other body parts are moved towards a new location, facilitating the posture setting

The Figure 3.5 shows fixed bones in red and the landmarks of the THUMS model.

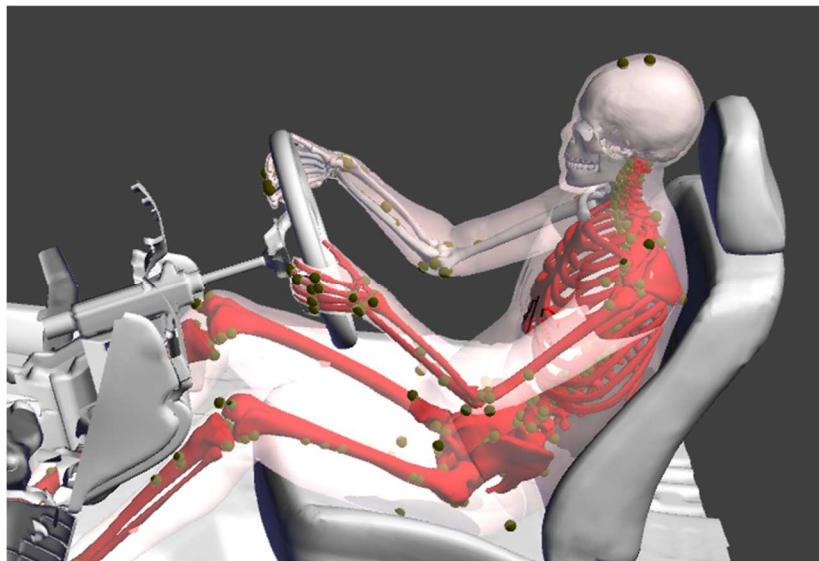


Figure 3.5 Positioning of the THUMS

The adjustment of the HBM posture is performed by following geometrical considerations provided by EuroNCAP protocol. The THUMS must reproduce the typical driving posture assumed by the dummy in a real crash test.

As reported in the testing protocol [6], the following requirements must be satisfied to represent correctly the standard driver posture:

- The occupant's backs should be in contact with the seat backrest and the centre line of the HBM should be lined up with the centre line of his respective seats.
- The driver's hands shall have their palms placed against the steering wheel at a position of a quarter to three.
- The upper legs of the occupant shall be in contact with the seat cushion as far as possible.
- The legs of the occupant should be in vertical longitudinal planes as far as is possible.
- The driver's right foot shall be placed on the undepressed accelerator pedal with the heel on the floor. The right foot should overlap the accelerator pedal with at least 20mm.
- The left foot should be placed on the footrest, located on the left side of the pedals

In order to achieve the final posture, the body parts are positioned in the following order:

1. Left and right lower limbs
2. Hips
3. Lumbar region and thorax
4. Left and right upper limbs
5. Head

The Figure 3.6 shows the final position assumed by the human model.

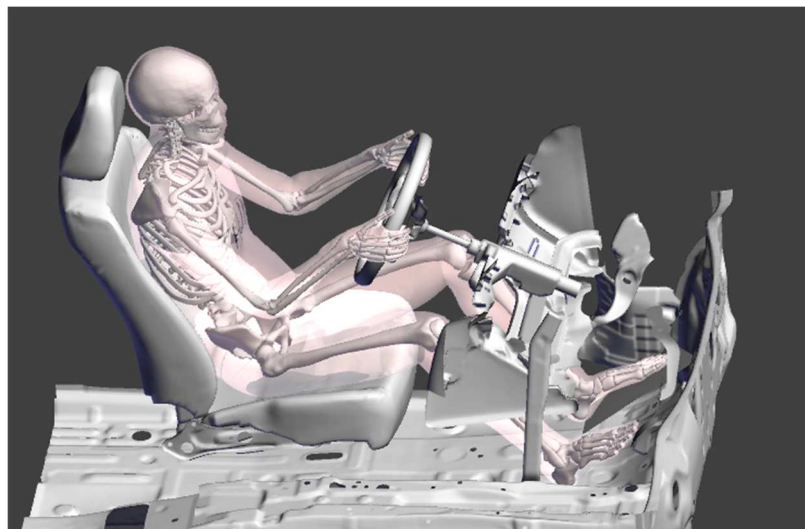


Figure 3.6 THUMS final posture

It is important to understand that when a body part is moved thanks to the definition of new landmark positions (targets), the software perform a simple simulation to transform directly the original human model, changing its configuration. When it occurs, the simplifications often produce a degradation of element quality but in this phase only the definition of the landmark coordinates of the positioned THUMS is relevant. Once the final posture is defined and all landmarks are in proper position, it is possible to export from the software a LS-DYNA simulation which allows to transform the original model in the positioned THUMS.

3.2.3 Positioning simulation and final THUMS model

The most common approach used for positioning FE HBM is to perform a full FE simulation between the original and target position [17]. The simulation files can be generated automatically using the *Scripting* module in PIPER software. This process allows to obtain a positioned model characterized by a good mesh quality, avoiding unrealistic skin folds or other artefacts which could be developed in PIPER *pre-positioning* module. The simulation allows also to respect internal entities of the HBM (such as constrains, contact entities, etc.) during the positioning, and it is performed in LS-DYNA program. Since only the final configuration of the model is relevant, the time step of the simulation is increased from 1 (set in file simulation as standard) to 10 ms in order to reduce the computational cost of this operation. The final posture of the THUMS complies with the EuroNCAP regulation and it ensures a well-positioned model in the vehicle environment. In Figure 3.7 is exposed the positioned HBM.



Figure 3.7 THUMS final position

Some details of the upper and lower limbs are shown in Figure 3.8 with respect to the vehicle environment.

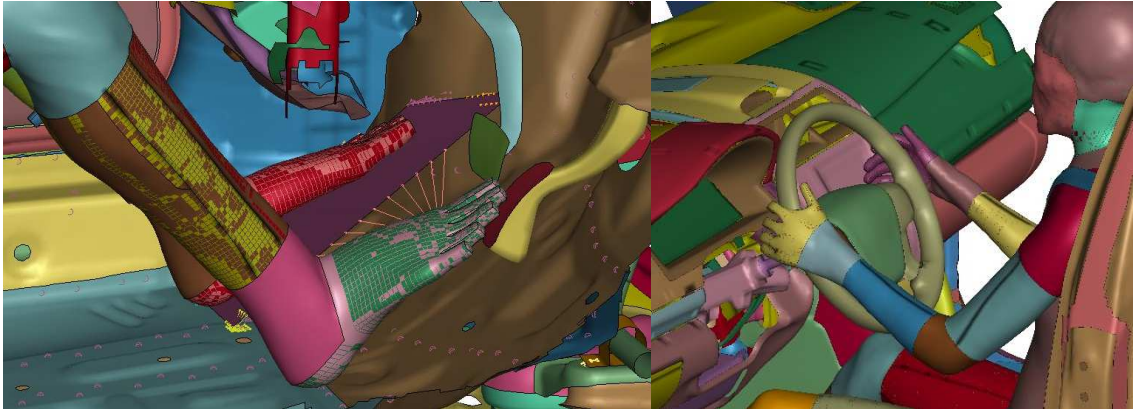


Figure 3.8 Details of positioned THUMS in vehicle environment

As can be notice, the parts of the THUMS do not contact to the vehicle component surfaces in order to avoid computational errors during the simulations. Some physical parameters are reported in Figure 3.9 in order to characterize in detail the final posture, while an overlapped view of the original and positioned model is reported in Figure 3.10

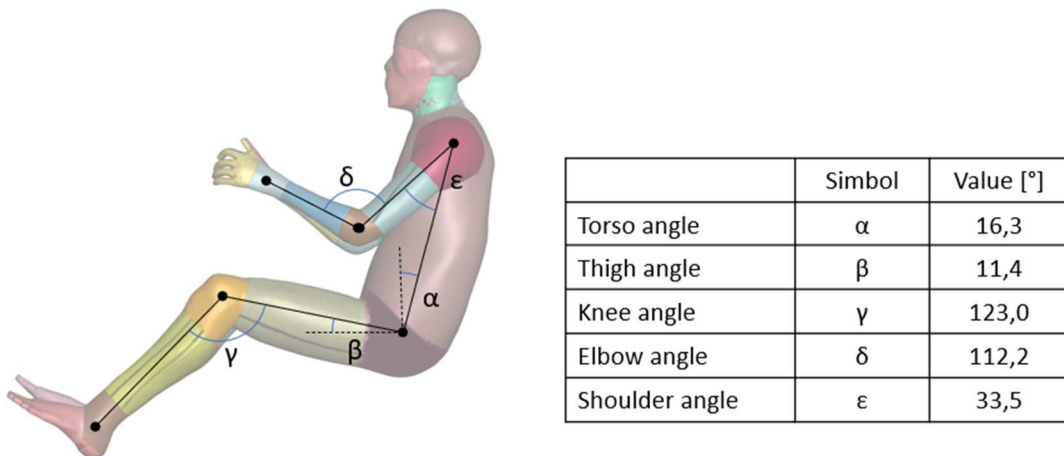


Figure 3.9 Details of the final posture

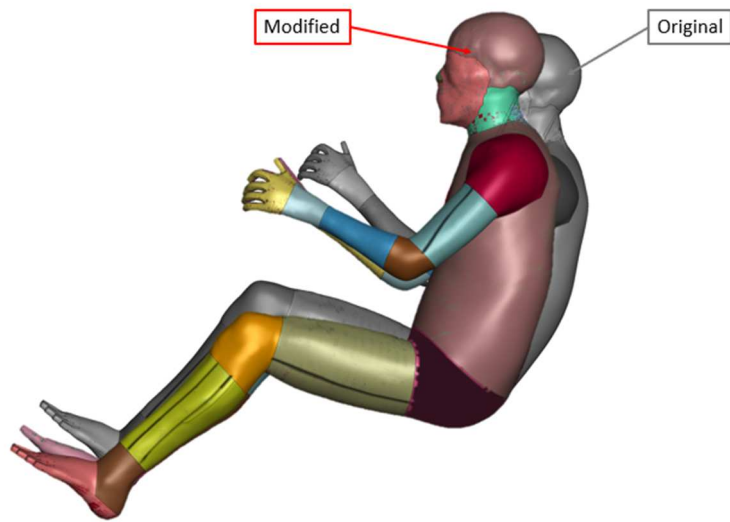


Figure 3.10 Initial vs final THUMS position - overlapped view

3.3 Sitting simulation

3.3.1 Introduction

When an occupant gets on a vehicle, his weight deforms the seat cushions and the spring frames as well. On the other side, if the FE human model is positioned inside the FE vehicle environment it can be notice that there are penetrations between the human body and the seat components (Figure 3.11).



Figure 3.11 Penetration regions between THUMS and driver seat

In order to represent faithfully the reality and a sitting simulation is performed at the end of which deformed driver seat is taken out. This final seat model can be easily included into the crash test simulation, avoiding penetrations and/or intersections between body parts and seat components.

3.3.2 Sitting simulation set-up and final seat model

This phase is necessary to simulate the pressure of the driver body on the seat foams with the aim of obtaining a deformed seat model. In order to perform the sitting simulation, the following models are involved:

- Simplified HBM

Since the deformation of the THUMS are negligible in this process, a simplified model of human body is used in order to reduce computational costs and facilitate the simulation setting. This model is obtained exporting the only skin parts of the original HBM which come in contact with the cushions. Even though the thickness and the original properties of the skin are kept, a rigid material is assigned to shell elements of the model, avoiding surface distortion over the whole simulation. The Figure 3.12 shows a comparison between the original THUMS and the simplified model.

- Driver seat

The FE model of undeformed driver seat is described in the previous section §2.2

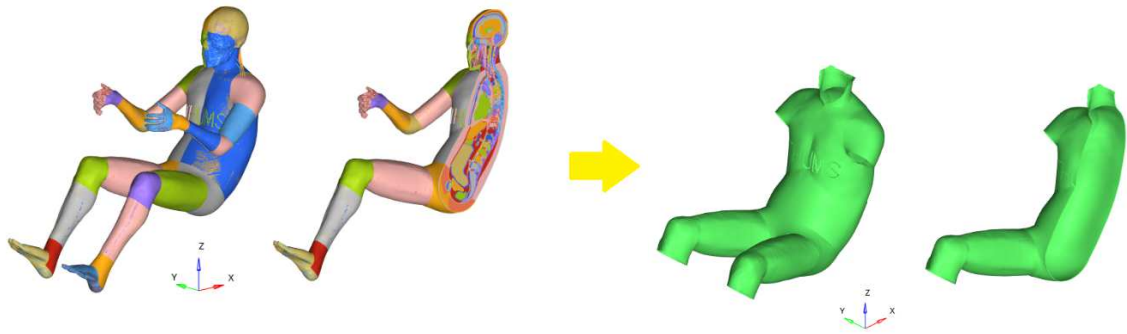


Figure 3.12 Comparison between THUMS and simplified skin model

During the simulation, the seat is constrained avoiding translations or rotations of the model thanks to `*BOUNDARY_SPC_SET` whereas, the rigid human skin performs a prescribed displacement in xz plane. This rigid translation is characterized by a displacement of 50 mm in x axis and 80 mm in z axis starting from the initial position and allowing to press the body surface against the seat cushions. Those values are the ones usually used for those kinds of activities in automotive company [14]. The motion is provided using the command `*BOUNDARY_PRESCRIBED_MOTION_RIGID`. The final position of the simplified skin model with respect to the seat is the same obtained at the end of the positioning described in

previous sections. In order to simulate the proper interaction between the surfaces of the models involved, *CONTACT_AUTOMATIC_SURFACE_TO_SURFACE command is used. The Figure 3.13 shows the initial and final simulation step.

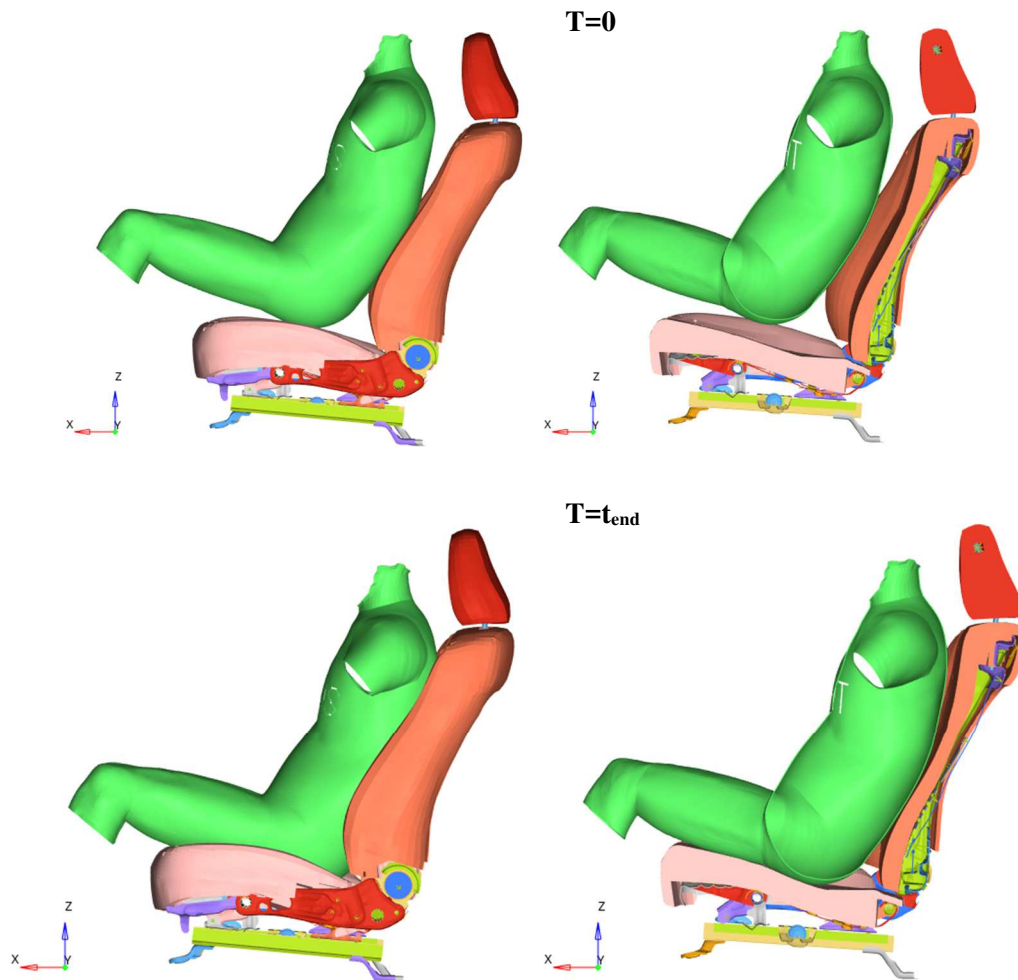


Figure 3.13 Sitting simulation - initial (upper) and final (lower) simulation step - side and section views

By means of this procedure, however, the residual stresses of the deformed seat are not considered. The preloads contribution on the deformed components has, in fact, negligible influence on the obtained biomechanical signals [14] and in crash test simulation. At the end of the simulation the deformed seat model is exported, and it is ready to be included into the vehicle environment for crash test simulations. Some details of the simulation are provided in Figure 3.14

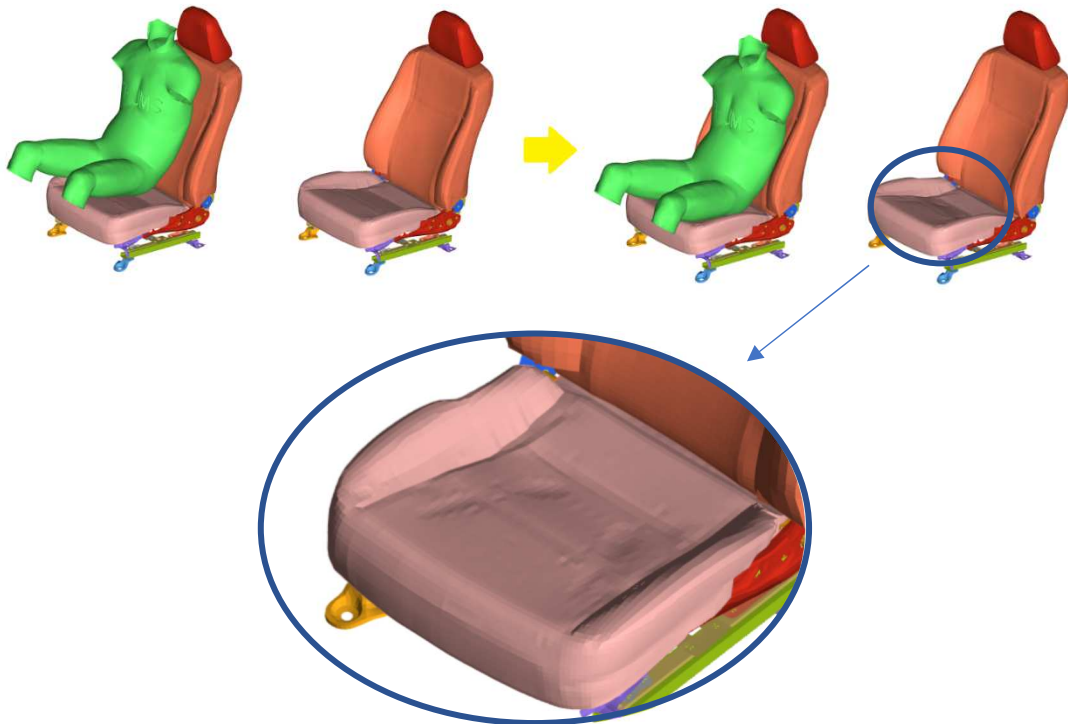


Figure 3.14 Sitting simulation and detail of the deformed seat cushion

Checking the penetration between HBM and seat model, as can be notice in Figure 3.15, no interpenetrate parts are found.

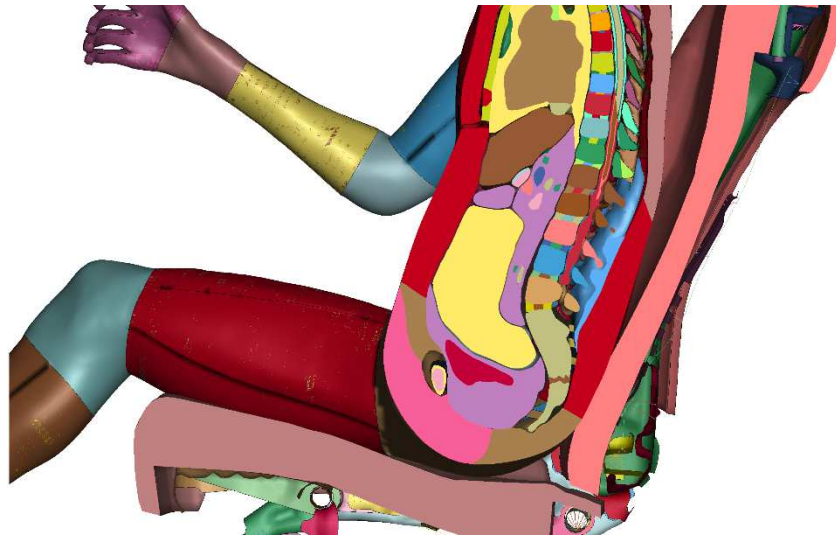


Figure 3.15 THUMS and seat - section view

3.4 Seatbelt routing

3.4.1 Introduction

In order to comply the EuroNCAP protocol, the occupants must be secured on their seat during the crash test, therefore a model of a driver seatbelt is included into the simulations. This passive safety device is a complete system modelled in LS-DYNA and described in detail in section §2.3. To reproduce faithfully the real test, the safety belt must be fitted precisely around the occupant body after his positioning inside the vehicle. This process is performed in LS-DYNA environment thanks to a proper application in *Occupant Safety* module.

3.4.2 Seat belt routing with LS-DYNA

The routing process allows to generate the webbing part of the seatbelt model. It is the main component of this safety device and it wraps the driver body in order to keep it in position during a collision. The model developed in this thesis is a three-point seatbelt composed by:

- B-pillar belt
- Shoulder belt
- Lap belt

Each of this webbing portion are created independently (resulting as different seatbelt) through a specific command provided in LS-DYNA. The B-pillar belt is modelled as a segment belt, while the other two webbing part are characterized by a mixed structure (they are made up of segment belt portion and a fabric one). As specify in belt model section, whereas a segment belt allows to reduce the computational cost of the simulation, the fabric belt ensures a more realistic behaviour where the webbing comes in contact with the occupant skin. In order to perform the routing process, some model must be load on LS-DYNA FE environment:

- The positioned THUMS
- The deformed driver seat exported from the sitting simulation
- The vehicle structure where the belt anchors are included (the sled structure is used to simplify the process). The anchors simulate:
 - The point where the belt comes out from the retractor
 - The D-ring
 - The buckle hole where the belt slip
 - The point where the belt is bolted constrained to the vehicle frame

In Figure 3.16 is shows the FE model before the routing.

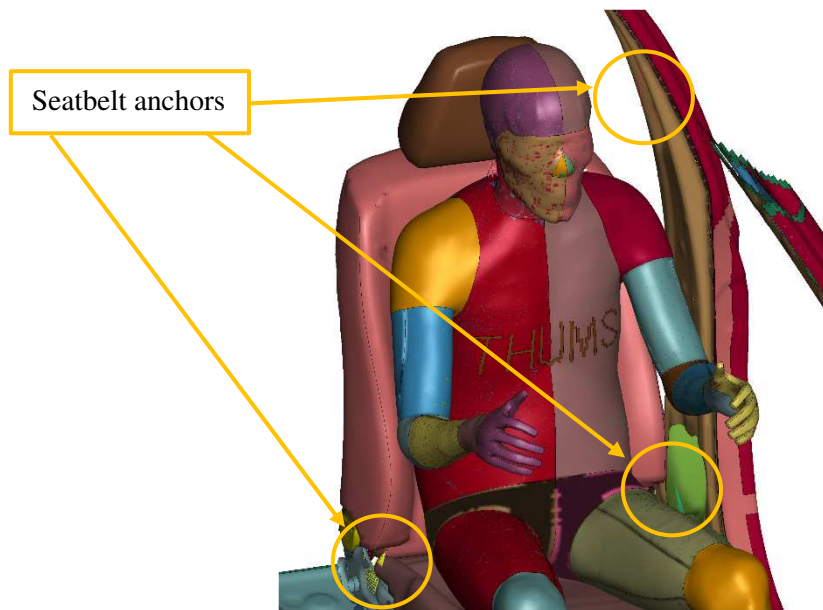


Figure 3.16 Structure, seat, THUMS and seatbelt anchors - FE configuration before routing

In LS-DYNA the *Seatbelt Fitting* command is supplied in *Occupant Safety* module to easily execute the process. The graphic interface of the used application is shown in Figure 3.17. In order to wrap precisely the webbing around the THUMS model, it is necessary to define the proper part as Contact Segment for each belt part:

- For shoulder belt, the left shoulder, the torso, and the right side of pelvis region are specified.
- For lap belt, the torso, the pelvis region, the legs upper part and some components on the right side of the seat are specified.
- No parts are defined for B-pillar belt.

Once defined the parts to wrap, the belt path must be drawn approximately, specifying a node sequence (the nodes can be picked directly on the model). To set up the parameters of the seatbelt the lower part of the application interface must be filled in. It is possible set the element size, the belt width (and for fabric belt the number of elements across width), the offset between the belt and the wrapped part surfaces, and the length of segment belt portion. In this work triangular shell elements (adopting the mesh parameters suggested by LS-DYNA) are used to mesh the fabric belt whereas, the length of the segment seatbelts is shown in Figure 3.18.

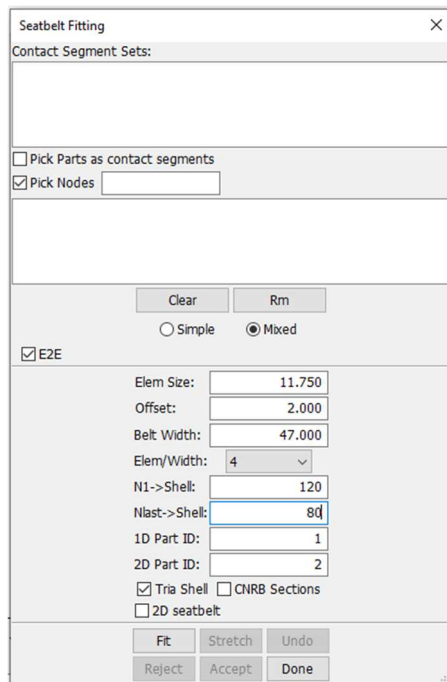


Figure 3.17 Graphic interface of the Seatbelt Fitting command

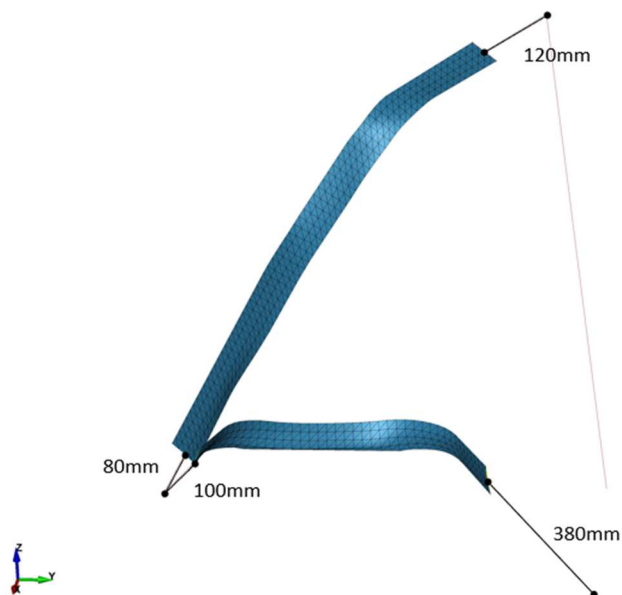


Figure 3.18 Seatbelt details

Running the *Fit* command, a rough webbing model is created but by means of *Stretch* command, the seatbelt is adjusted in order to fit properly to the human body. Once the routing process is completed, the final webbing model cannot be already imported in test simulation. The materials

and other element properties (described in detail in section §2.3) are defined manually, and the other safety components are included into the model at the end of the process. The Figure 3.19 shows the complete seatbelt model.



Figure 3.19 Seatbelt model at the end of the routing

0-length belt elements

The routing process performed with the LS-DYNA *Seatbelt Fitting* command allows to create only the seatbelt that runs between two points (anchors), but it cannot model the webbing wrapped inside the retractor. In order to simulate the belt spool-out some 0-length elements must be modelled manually. The 0-length elements are segment belt elements characterized by the same coordinates for the end nodes. This means the linear elements are condensed in a single point and in this case that position represents the retractor location. The belt sliding in and out the retractor is ruled by the retractor modelling and the tensile condition of the webbing during the test.

Chapter 4

4 Impact test simulation results

4.1 Comparison between full-scale and sled model without occupant

This simulation aims to compare the sled behaviour with respect to the full-scale vehicle model during the front full-width impact test (detailed in Chapter 1). Following the energy analysis, the accelerations of the structures and the visual comparison between models are reported.

4.1.1 Visual comparison

In order to observe the behaviour between full-scale and sled model, a visual comparison is given. The two models are represented at the same simulation time instants in the following Figures 4.1-4.7. The time step used to capture the simulation frames is equal to 20 ms until 120 ms. As expected, the models show a very similar behaviour during the simulation.

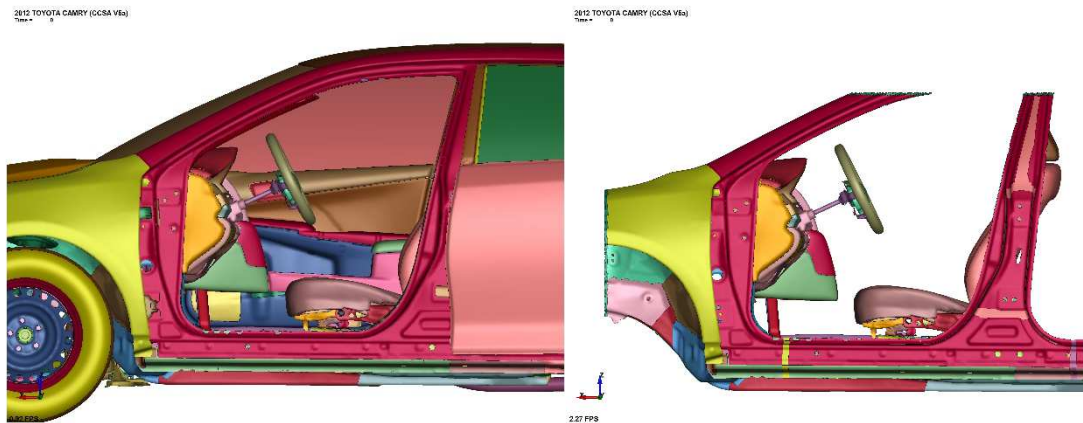


Figure 4.1 Full-scale and sled model - side view - 0 ms



Figure 4.2 Full-scale and sled model - side view - 20 ms



Figure 4.3 Full-scale and sled model - side view - 40 ms

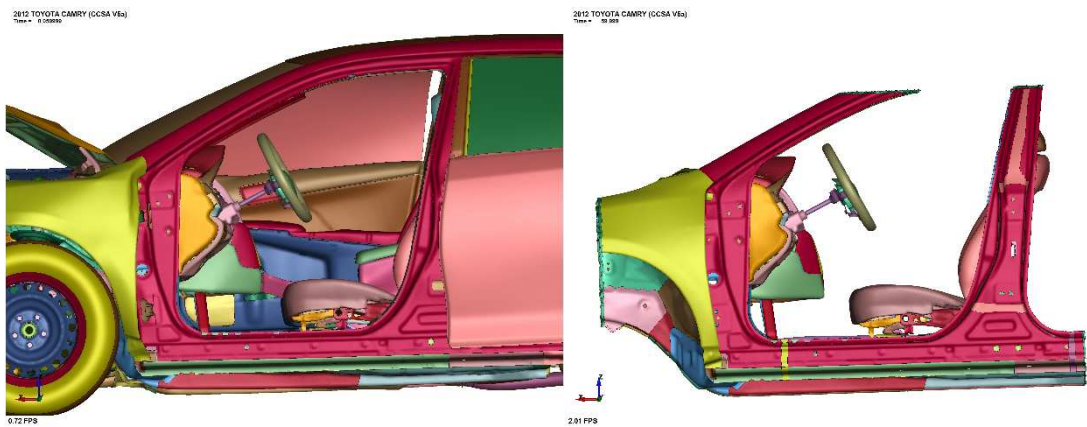


Figure 4.4 Full-scale and sled model - side view - 60 ms

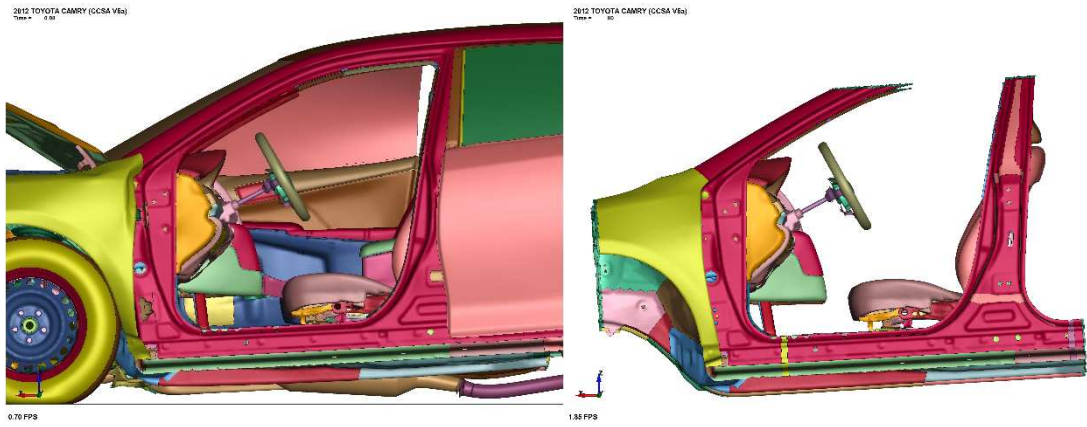


Figure 4.5 Full-scale and sled model - side view - 80 ms

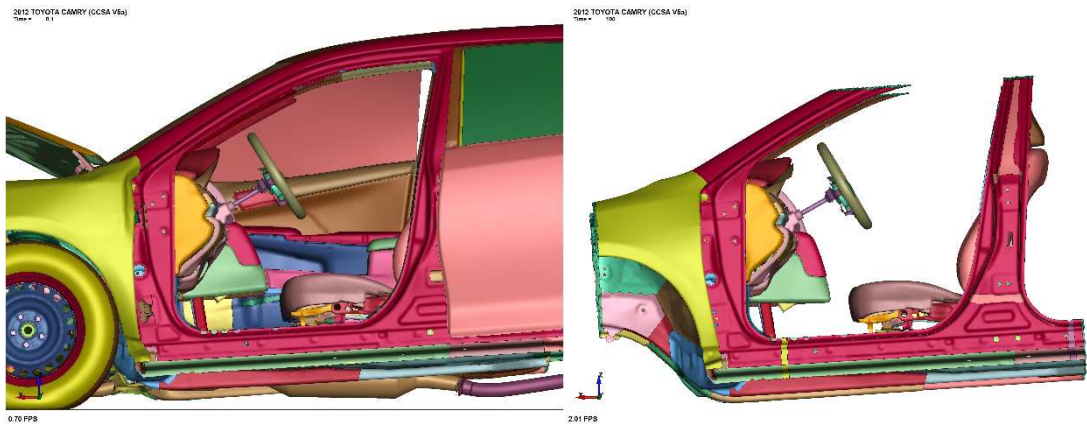


Figure 4.6 Full-scale and sled model - side view - 100 ms

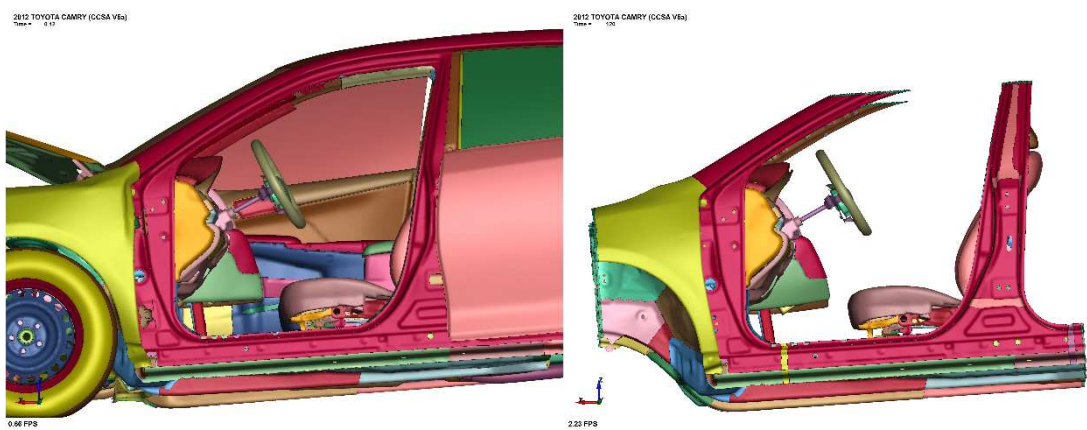


Figure 4.7 Full-scale and sled model - side view - 120 ms

4.1.2 Energy balance

In this analysis, the energies considered are:

- Total energy
- Kinetic energy
- Internal energy
- External work
- Sliding interface energy
- Hourglass energy

The global energy plot of the full-scale vehicle simulation is reported in Figure 4.8.

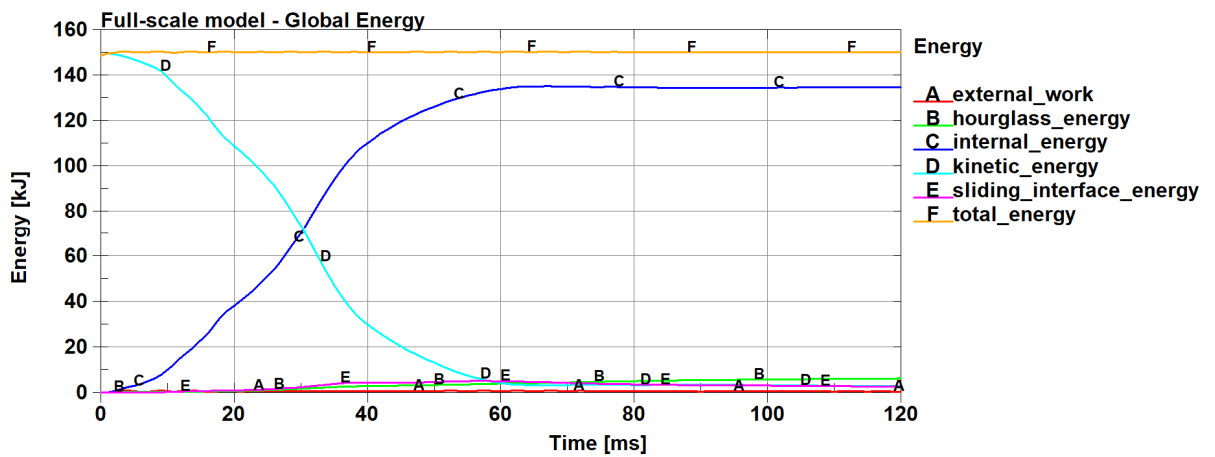


Figure 4.8 Full-scale model - Global energy plot

The global energy plot of the sled test simulation is reported in Figure 4.9.

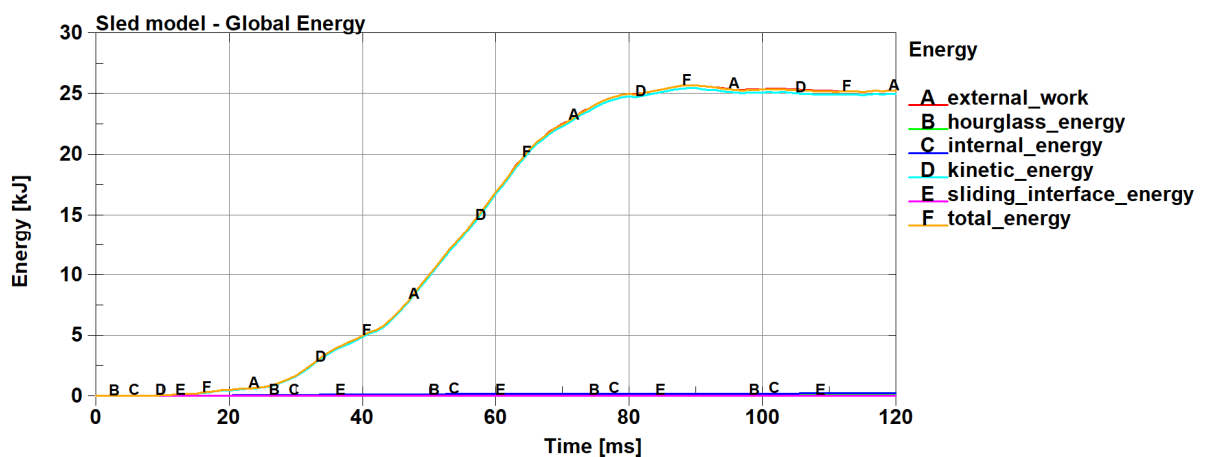


Figure 4.9 Sled model - Global Energy plot

It can be seen, there is energy balance throughout the simulation in both models. In full-scale model the simulation starts with an initial kinetic energy and no external work is applied. As the simulation progressed, the kinetic energy decreased, and the internal energy increased due to structure deformation of the vehicle. Sliding interface and hourglass energy increase slightly over the whole simulation. The total energy remains constant since no external work is applied to the system. On the other hand, the sled model is characterized by a rise in total energy trend. The external work provided to the system allows the kinetic energy to increase over the simulation. The internal, hourglass and sliding interface energy keep their values near to 0J. The Table 4.10 facilitates the comparison between two models.

	Full-scale model	Sled model
Initial Kinetic Energy [kJ]	148,439	0
Maximum Total energy [kJ]	150,343	25,681
Hourglass Energy Rate (with respect to the total energy)	4,10%	0,184%

Figure 4.10 Table energy comparison

4.1.3 Acceleration comparison

In order to compare the kinematic of both models, an accelerometer (described in section §2.1.3) is positioned under the driver seat at the same x coordinate of the B-pillar. In the following Figure 4.11-4.13, the x, y, and z acceleration in full-scale and sled model are showed. All signals are filtered with a SAE 60 filter.

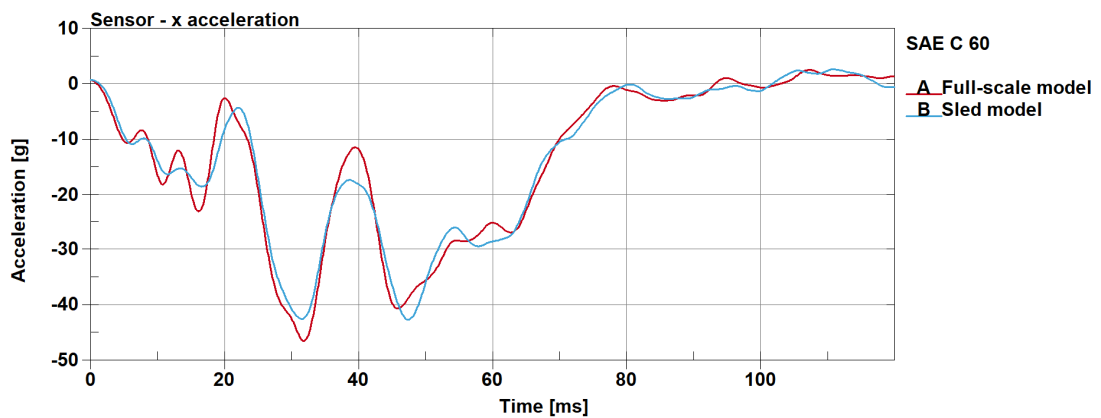


Figure 4.11 Sensor - x acceleration

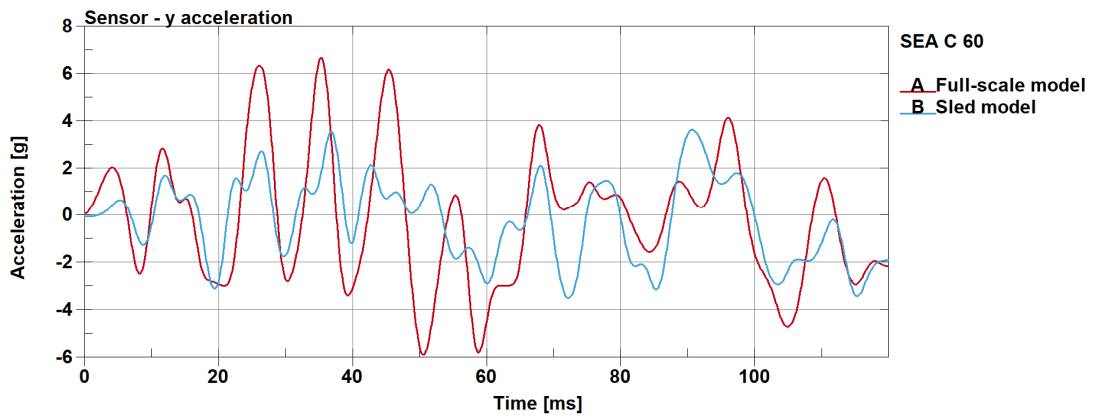


Figure 4.12 Sensor - y acceleration

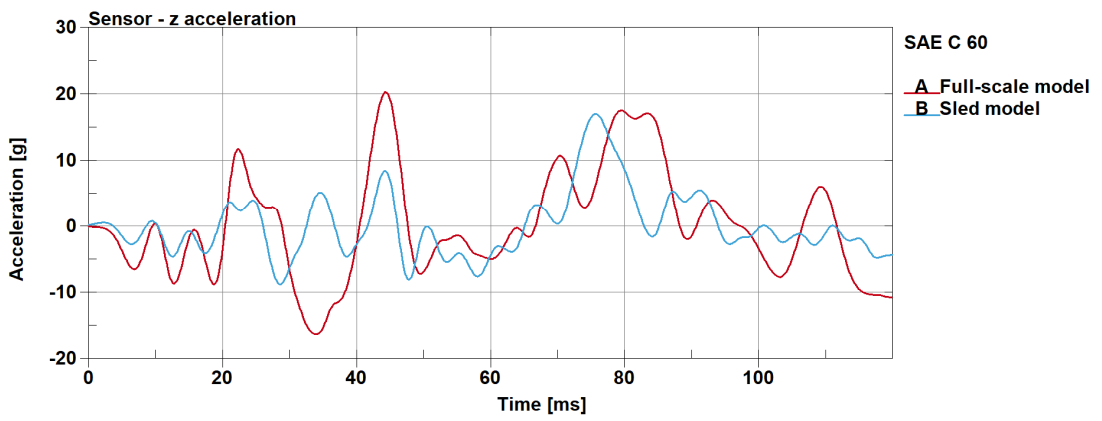


Figure 4.13 Sensor - z acceleration

Observing the curves profile, it is possible to notice the similarity between the two models. Few slight difference between full-scale and sled acceleration are due to the approximation of the velocity curves applied to the rigid sections.

4.2 Comparison between full-scale and sled model with HBM

This simulation aims to compare the sled behaviour with respect to the full-scale vehicle model during the front full-width impact test, including the THUMS secured on driver seat with the seatbelts. In Figure 4.14, the final configuration of full-scale and sled model is shown. In this section the following parameters are reported for both models:

- Energy balance
- Vehicle kinematics
- THUMS accelerations
- Seatbelt forces

The visual comparison between the model simulations are reported as well.

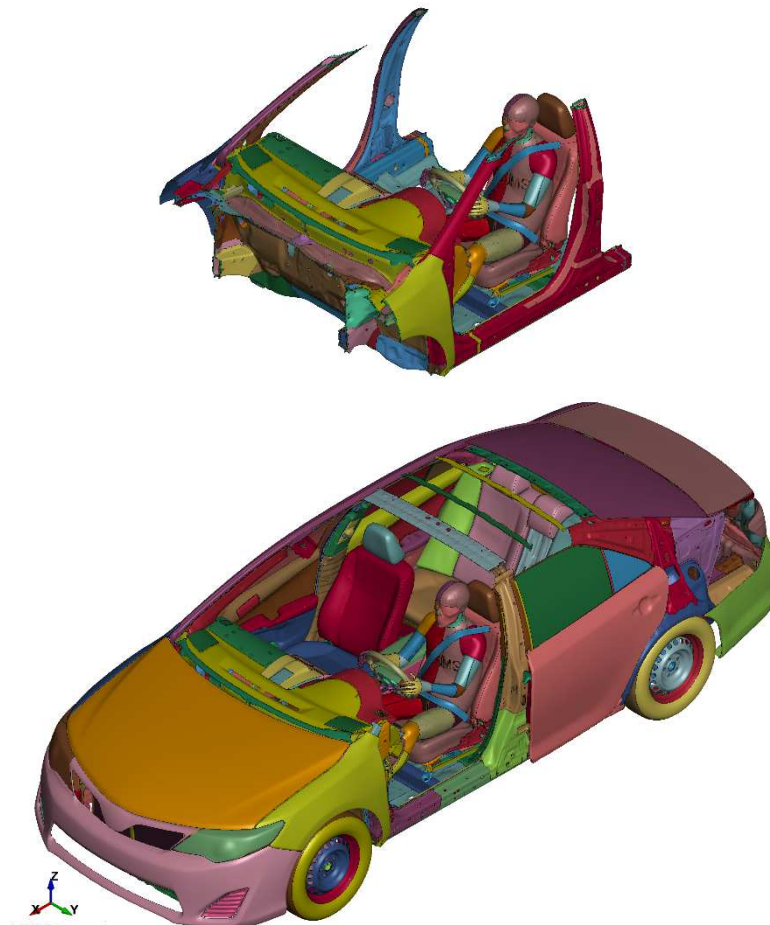


Figure 4.14 Sled (upper) and full-scale (lower) model with THUMS

4.2.1 Visual comparison

In order to observe the behaviour between full-scale and sled model, a visual comparison is given. The two models are represented at the same simulation time instants in the following Figures 4.15-4.21. The time step used to capture the simulation frames is equal to 20 ms until 110 ms. Some little differences are detected between the two model, especially in upper limbs. The lack of the windshield in sled model allows hands to protract beyond the dashboard more than in the complete vehicle model. In particular, it can be seen that in full-scale vehicle the right arm shows a more significant rebound. During both the simulations a deformation of the driver seat is detected, lifting and rotating the cushion.

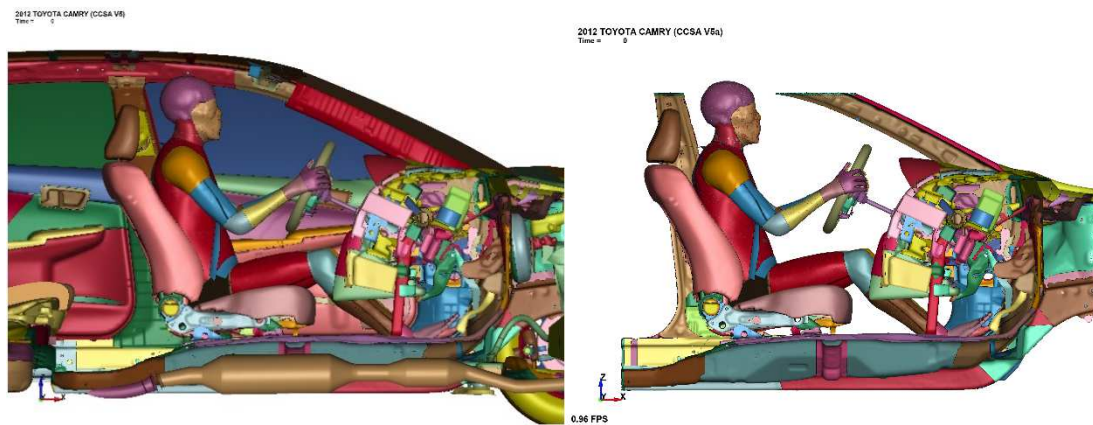


Figure 4.15 Full-scale and sled model with THUMS - side section view - 0 ms



Figure 4.16 Full-scale and sled model with THUMS - side section view - 20 ms



Figure 4.17 Full-scale and sled model with THUMS - side section view - 40 ms



Figure 4.18 Full-scale and sled model with THUMS - side section view - 60 ms



Figure 4.19 Full-scale and sled model with THUMS - side section view - 80 ms



Figure 4.20 Full-scale and sled model with THUMS - side section view - 100 ms



Figure 4.21 Full-scale and sled model with THUMS - side section view - 110 ms

4.2.2 Energy balance

In this analysis, the energies considered are:

- Total energy
- Kinetic energy
- Internal energy
- External work
- Sliding interface energy
- Hourglass energy

The same consideration made in the previous comparison (section §4.1.2) are also valid in this case, but the energy related to the THUMS is accounted for in the energy balance.

The global energy plot of the full-scale vehicle simulation is reported in Figure 4.22.

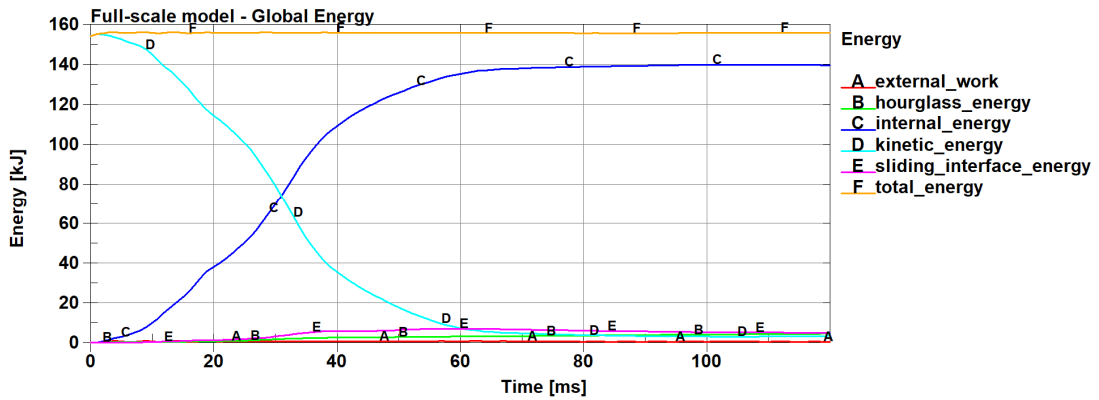


Figure 4.22 Full-scale model - Global energy plot

The global energy plot of the sled test simulation is reported in Figure 4.23.

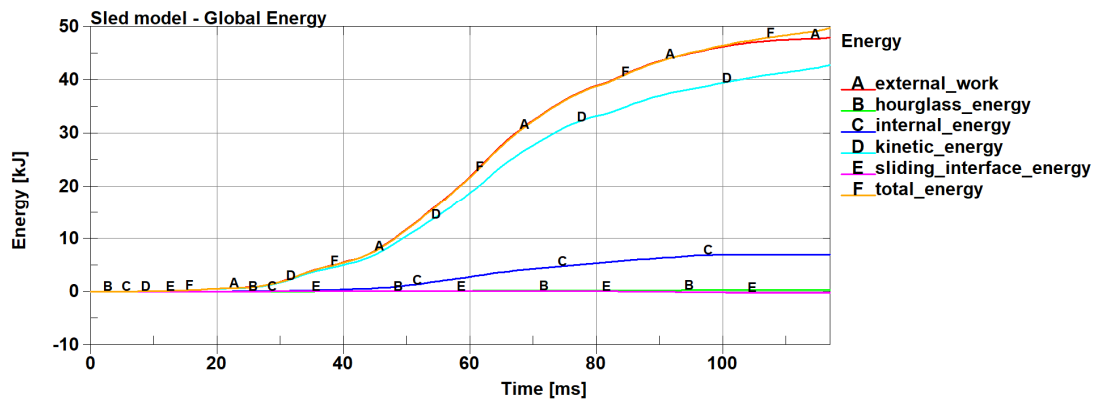


Figure 4.23 Sled model - Global energy plot

The Table 4.24 facilitates the comparison between two models.

	Full-scale model	Sled model
Initial Kinetic Energy [kJ]	154,139	0
Maximum Total energy [kJ]	156,036	49,631
Hourglass Energy Rate (with respect to the total energy)	2,871%	0,961%

Figure 4.24 Table energy comparison

4.2.3 Vehicle kinematics comparison

Since the sled kinematics are obtained from the full-scale model without considering the occupant presence, the comparison between the following parameters are reported:

- The velocity curves of the rigid sections in sled model and the velocity of the nodes in the same area in full-scale vehicle (Figure 4.25-4.28). In order to facilitate the comparison, an offset of 13.888 m/s is given to x velocity in full-scale model.
- The accelerations measured by the accelerometer placed under the driver seat in both models (Figure 4.29-4.31).

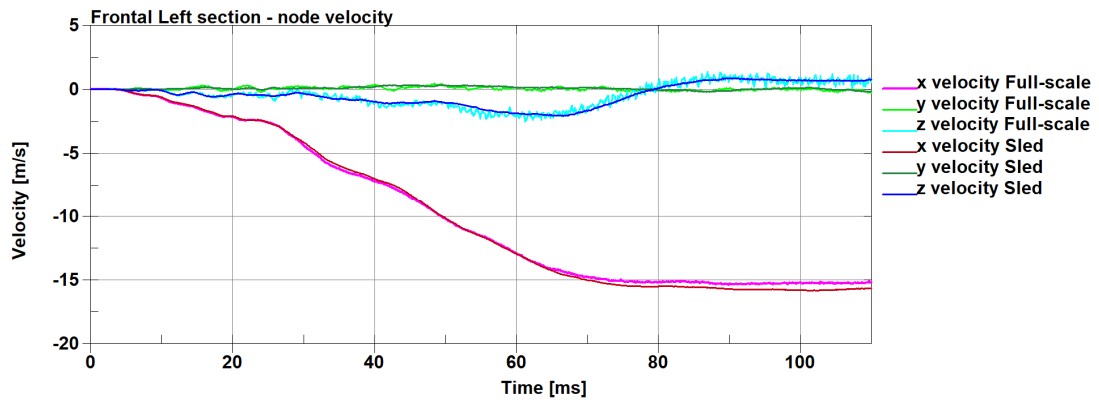


Figure 4.25 Velocity in Frontal Left section area

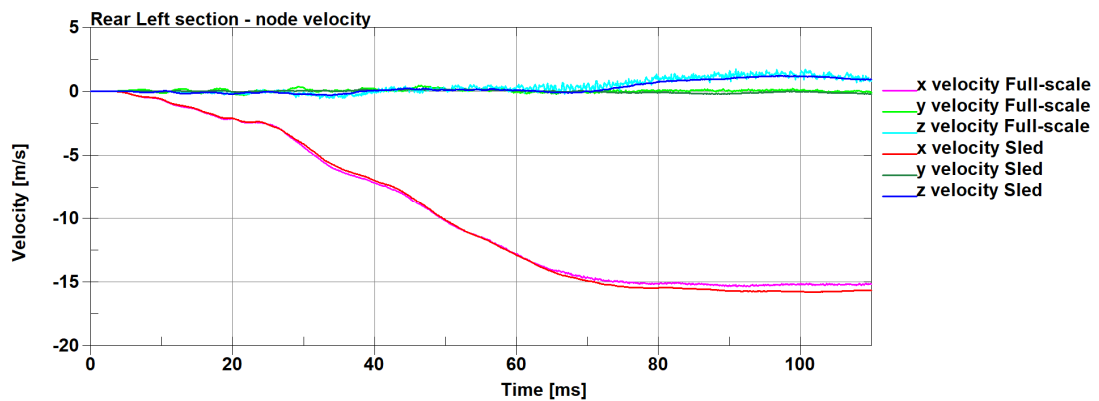


Figure 4.26 Velocity in Rear Left section area

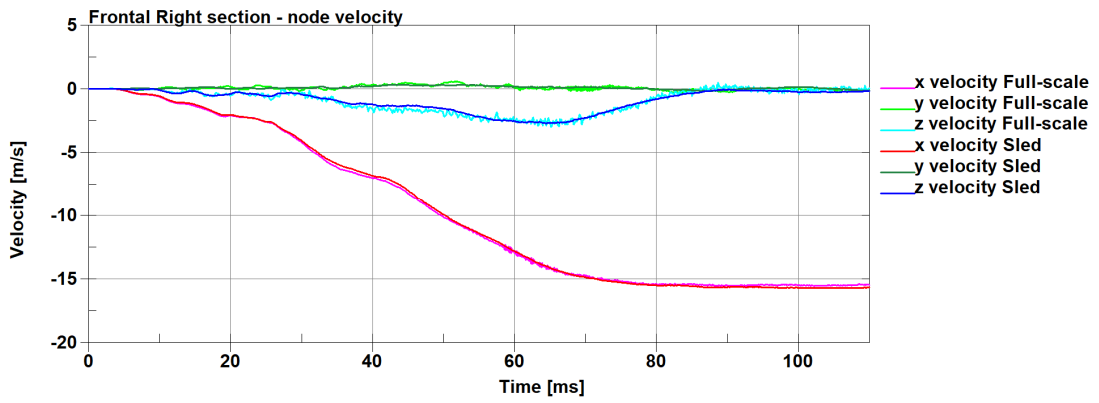


Figure 4.27 Velocity in Front Right section area

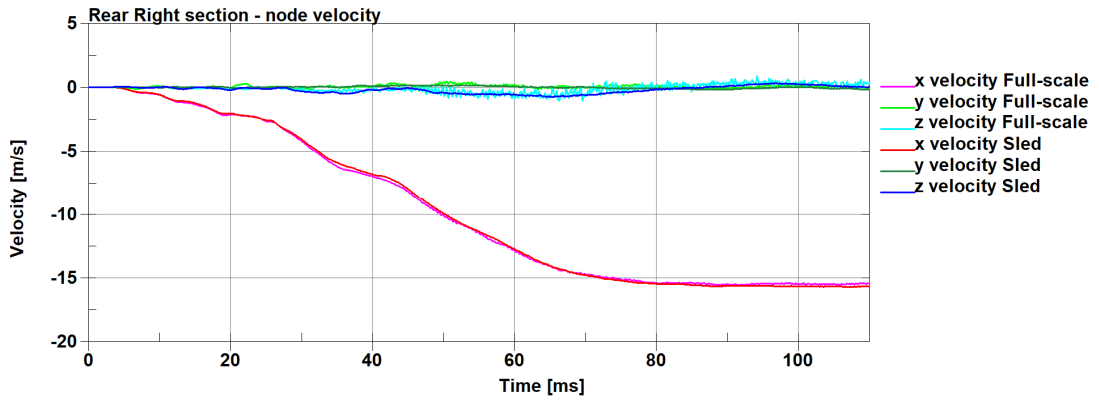


Figure 4.28 Velocity in Rear Right section area

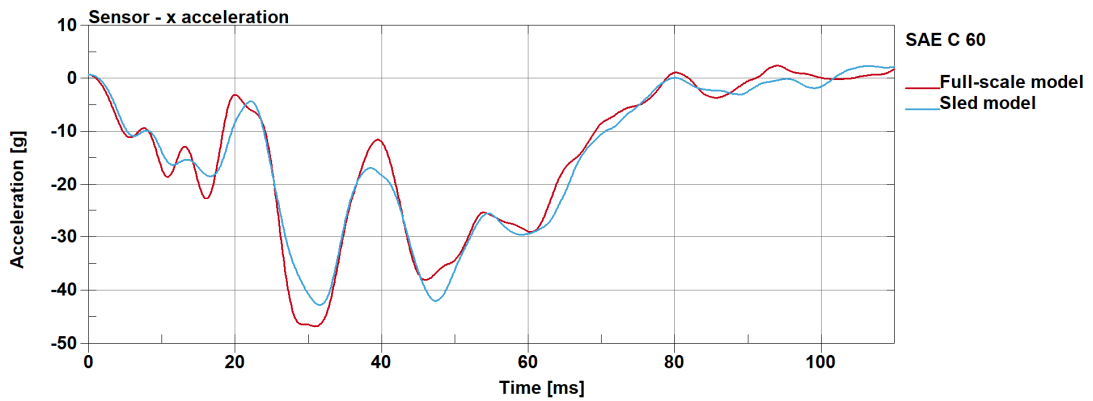


Figure 4.29 Sensor - x acceleration

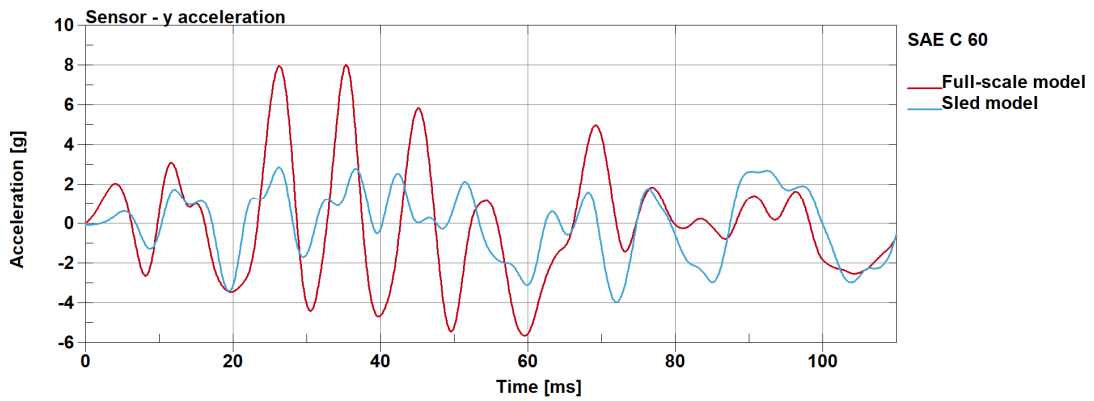


Figure 4.30 Sensor - y acceleration

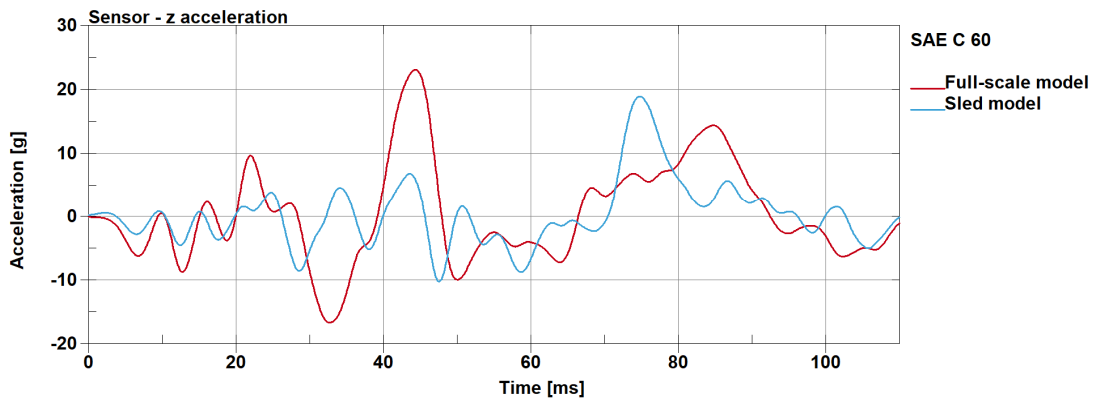


Figure 4.31 Sensor - z acceleration

Since the velocity curves applied on the sled system derive from the full-scale crash simulation without the occupant, it is natural to detect some discrepancies between model under consideration. The presence of the HBM influences slightly the simulation as can be seen in velocity curve plots, especially on the left side of the vehicle. On the other hand, observing the acceleration of the structure in driver seat, it is clear that there are not substantial differences, but it can be notice in the sled model, the oscillations of the accelerations are characterized by lower amplitude. This is due to approximation of the input velocity curves for the motion and the low mass structure of the sled.

4.2.4 THUMS acceleration comparison

Since the THUMS is equipped with several sensors described in section §2.3.3, the acceleration of the head, thorax (vertebrae T1, T4 and T12) and pelvis region is reported in the following Figure 4.32-4.43. All signals are filtered using the filter SAE C 180.

THUMS head signals

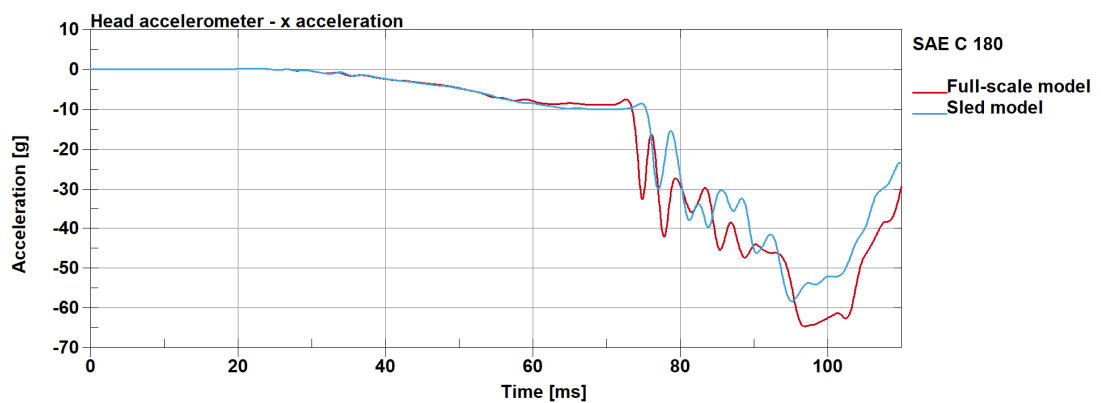


Figure 4.32 Head accelerometer - x acceleration

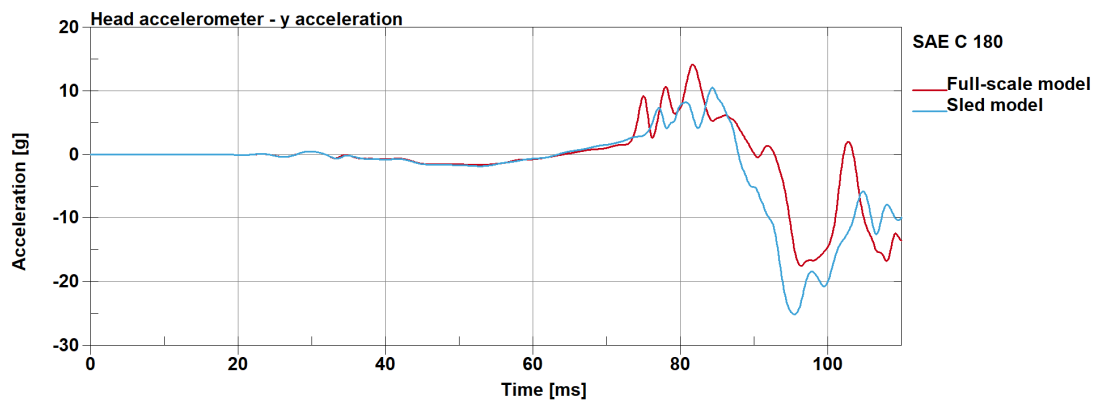


Figure 4.33 Head accelerometer - y acceleration

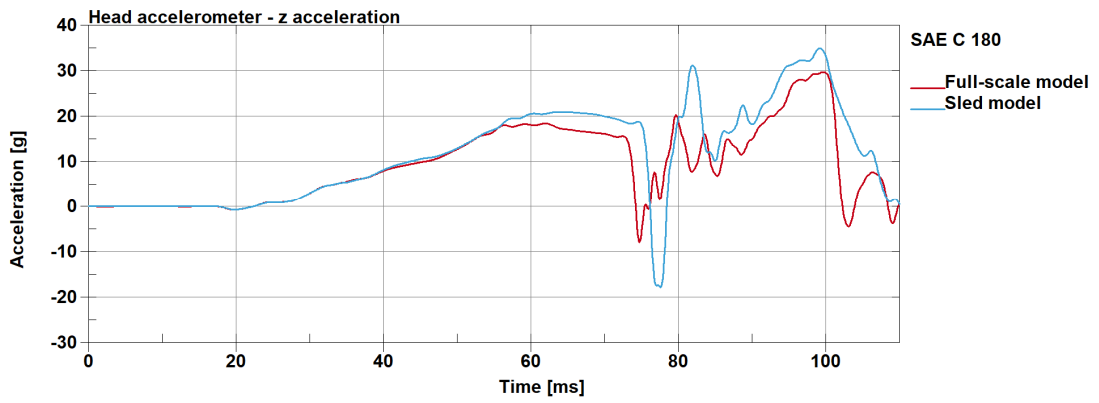


Figure 4.34 Head accelerometer - z acceleration

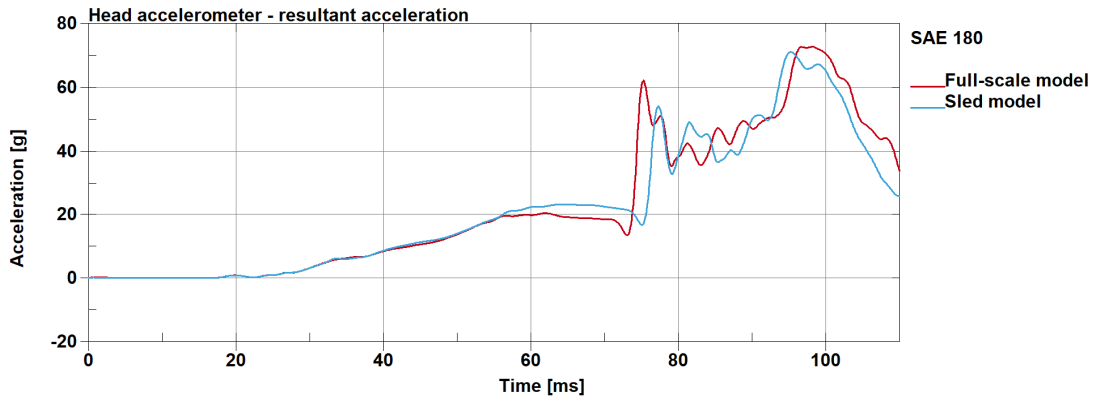


Figure 4.35 Head accelerometer - resultant acceleration

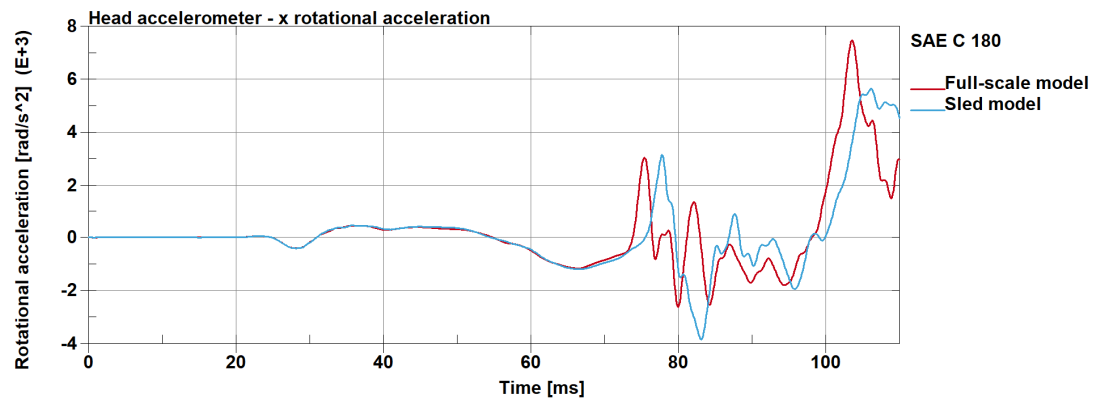


Figure 4.36 Head accelerometer - x rotational acceleration

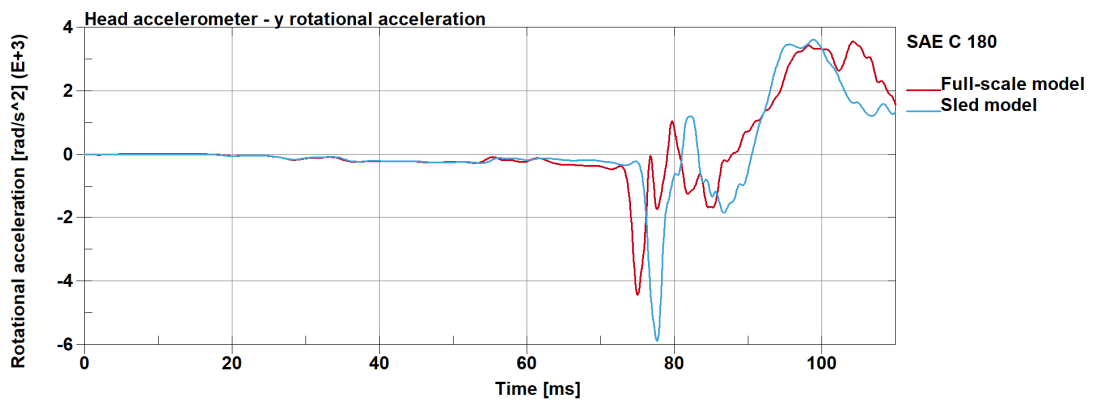


Figure 4.37 Head accelerometer - y rotational acceleration

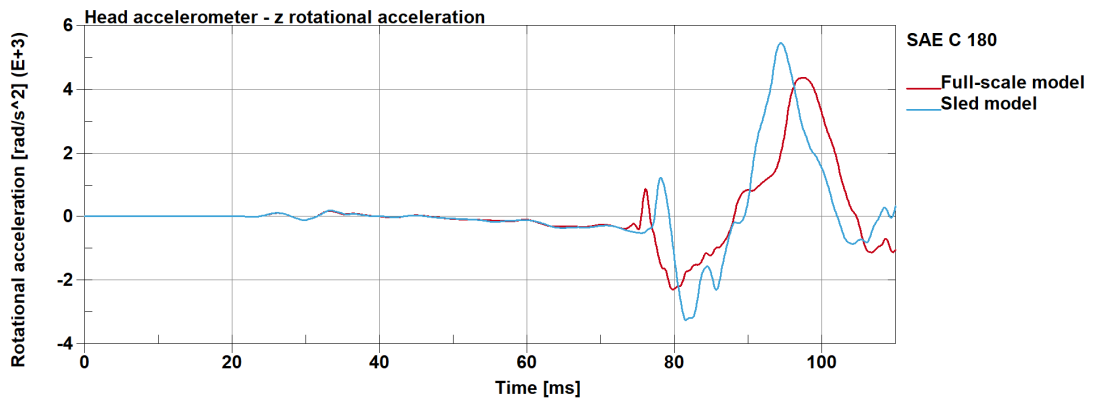


Figure 4.38 Head accelerometer - z rotational acceleration

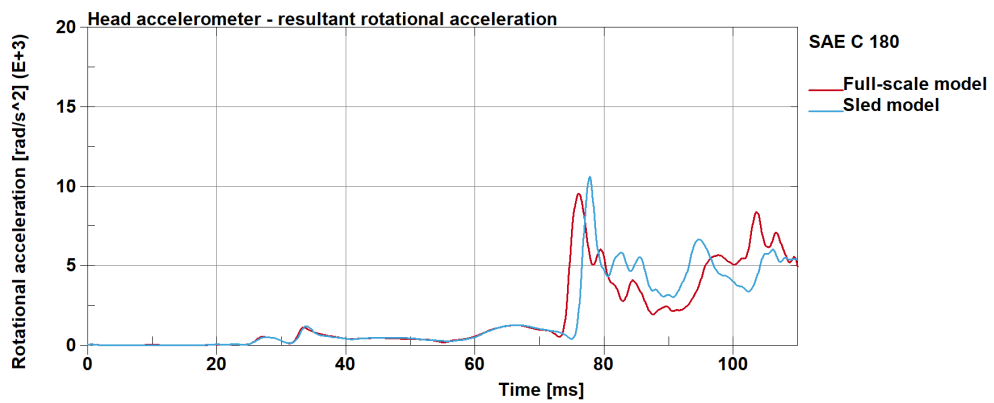


Figure 4.39 Head accelerometer - resultant rotational acceleration

THUMS thorax signals

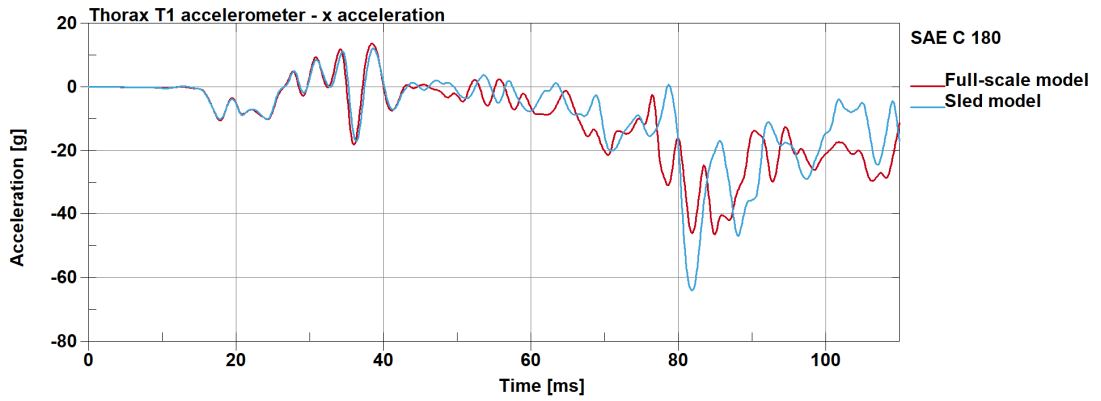


Figure 4.40 Thorax T1 accelerometer - x acceleration

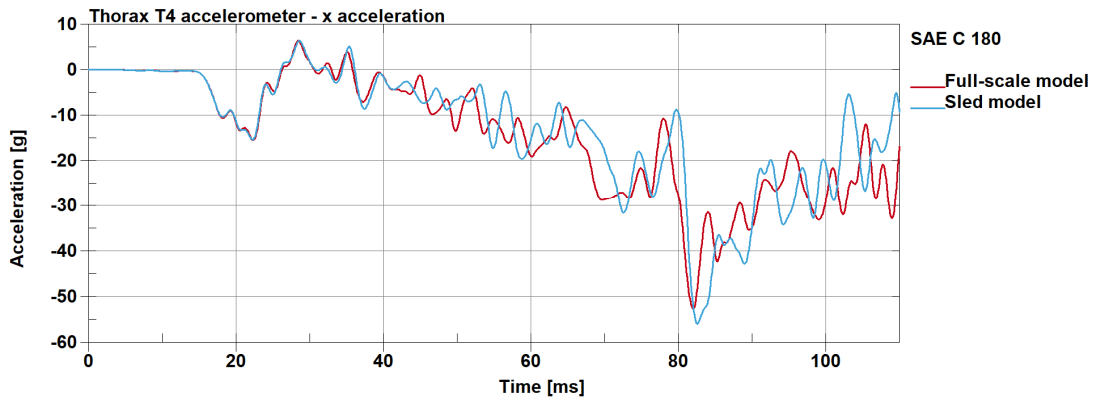


Figure 4.41 Thorax T4 accelerometer - x acceleration

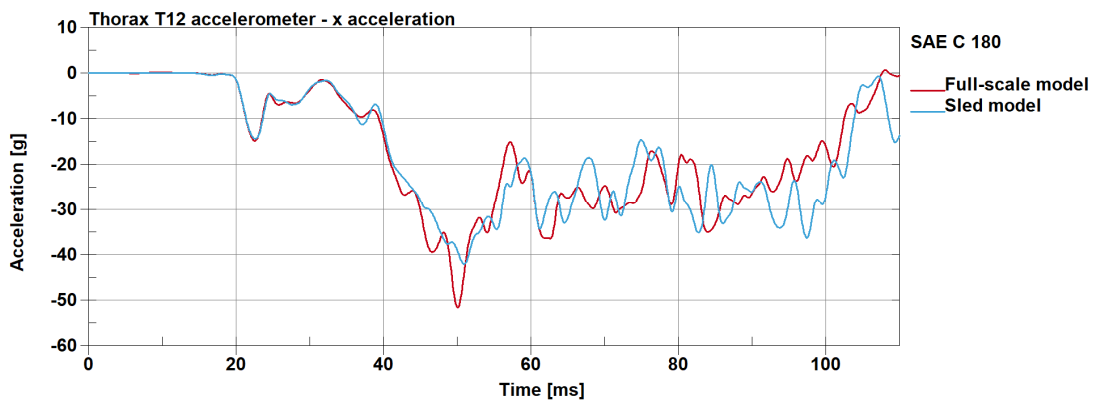


Figure 4.42 Thorax T12 accelerometer - x acceleration

THUMS pelvis signal

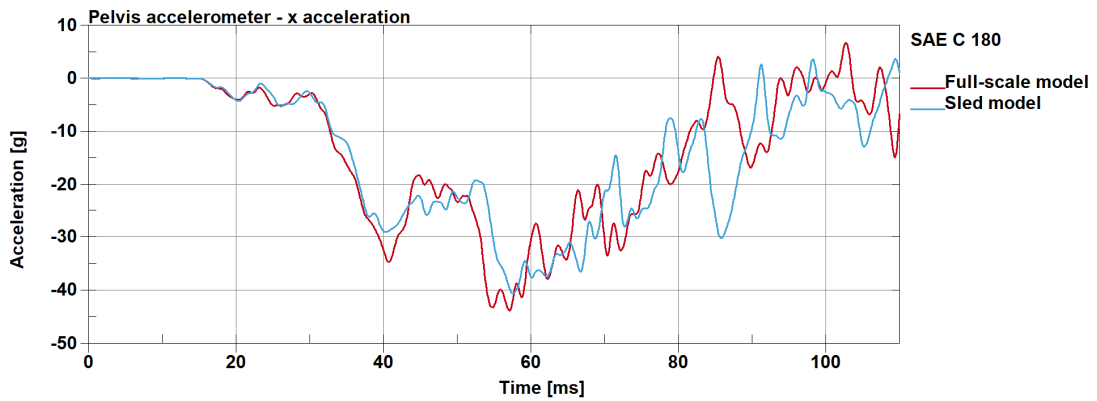


Figure 4.43 Pelvis accelerometer - x acceleration

The two model presents well overlapped accelerations for the first 40 ms, 60 ms for the head accelerometer. After this initial time step, the signals measured on the THUMS during the test indicate that the body motion of models follows a similar pattern, but several dissimilarities are present. First of all, in complete vehicle model the driver head impacts with the steering wheels few milliseconds before it occurs in sled model as can clearly be seen in head, T1 and T4 accelerometer (at about 74-78 ms).

4.2.5 Seatbelt forces comparison

The load on the shoulder belt is computed observing a segment belt element near the THUMS shoulder whereas the force on the lap belt is taken out from another segment element near the left hip. The signals are filtered using SAE C 108 and the curves are exposes in Figure 4.44 and 4.45.

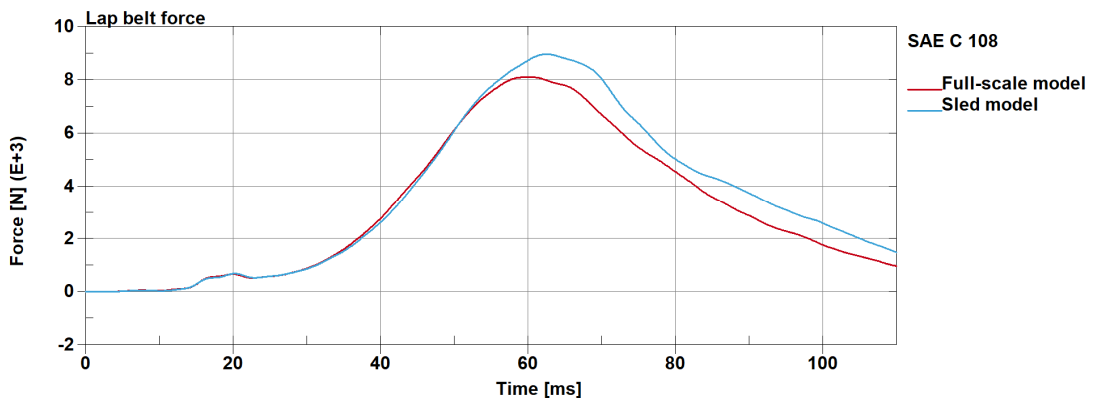


Figure 4.44 Lap belt force

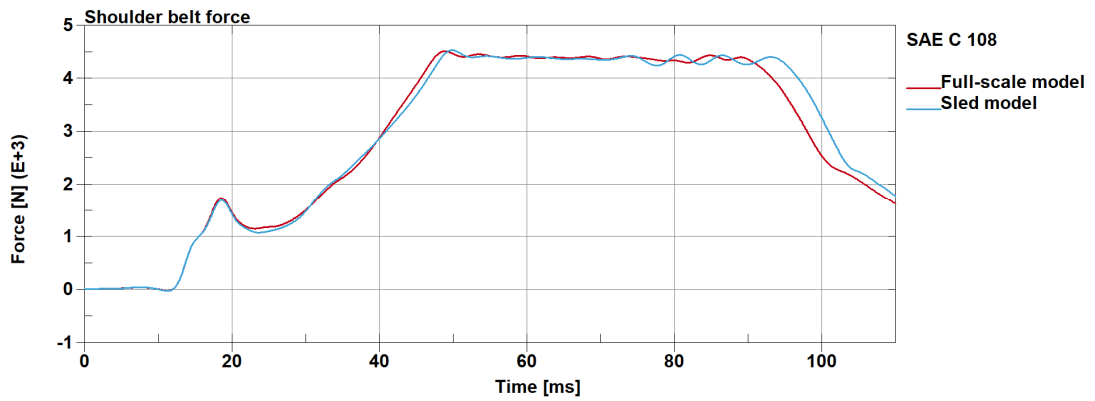


Figure 4.45 Shoulder belt force

In the seatbelt system, the retractor fires at 1 ms while the pretensioner is activated at 13 ms. In shoulder force plot, the load peak caused by the pretensioner can be easily noticed between 13 and 19 ms. Then, during the simulation the load increase gradually until the load limit of the retractor is reached (constant load limiting, 50-95 ms). The differences in belt forces between sled and full-scale model are due to the kinematics of the human body (in full-scale model the THUMS impacts before to the steering wheel than in sled simulation).

Conclusions

In this thesis, a simplified FE model which is able to reproduce the internal environment of a mid-size passenger sedan was created starting from a full-scale 2012 Toyota Camry validated against several NCAP test. The original model was modified, disassembling and cutting several components, leaving only essential parts for the interior car representation. The model (inspired by an actual model adopted in a well-known car manufacturer) is set in order to perform a frontal FW impact, according to the EuroNCAP protocol. Its pulse motion was obtained monitoring the kinematics of the full-scale vehicle frame over the crash test without occupants and extrapolating the velocity curves in four designed regions of the sills: two frontal one (left and right) near the A-pillar and other two in rear position with respect the driver seat close to the B-pillar. These velocity profiles were used to prescribe the motion of four rigid sections which allow to transfer the pulse on the sled frame appropriately. The validation of this sled system was carried out comparing the model with respect to the full-scale vehicle. Two comparisons were performed:

- The first one was based on monitoring the crash behaviour of the structure in both models, without including the driver occupant into the simulation.
- The last one was performed placing a HBM (THUMS) in driver configuration into the vehicle environment and confronting the biomechanical parameters resulted from the simulations.

In order to properly set the simulations where the THUMS was involved, the occupant was positioned in standard driver posture and then, the sitting footprint of the human body on the seat was created. At the end, the seatbelt was fitted to secure the driver during the test.

The results obtained from the first comparison were as expected. The reduced mass of the sled environment and the presence of the rigid sections incorporated into the frame have allowed to represent accurately the pulse motion on the structure. On the other hand, slight differences between accelerations of sled and complete car model were detected. These discrepancies are due to the approximation of the velocity profiles since the full-scale vehicle presents a high number oscillation with very small amplitude (numerical noise, elastic phenomena, vibration of the structure, etc.). No substantial differences are detected between models.

On the contrary, more dissimilarities are found adding the occupant model. Since the pulse motion of the sled model are referred to the complete vehicle without driver, some little differences are encountered comparing the velocity curves of the rigid sections with the kinematics of the full-

scale frame in respective regions. On the other hand, the effect of the occupant presence in the vehicle environment do not influence seriously the accelerations of the structure in driver area. The accelerations measured by the sensors included into the THUMS show a well overlapped profile for the first instants, then the curves follow the same trend but with slightly different oscillations.

It is important notice the simulation presents some irregularities. The seatbelt system is not yet calibrated to constrain properly the driver, observing the submarining phenomenon in abdominal region. Another anomaly is the deformation of the driver seat which cause rotation and lift of the cushion, reducing the effectiveness of the restrain system and altering the occupant position.

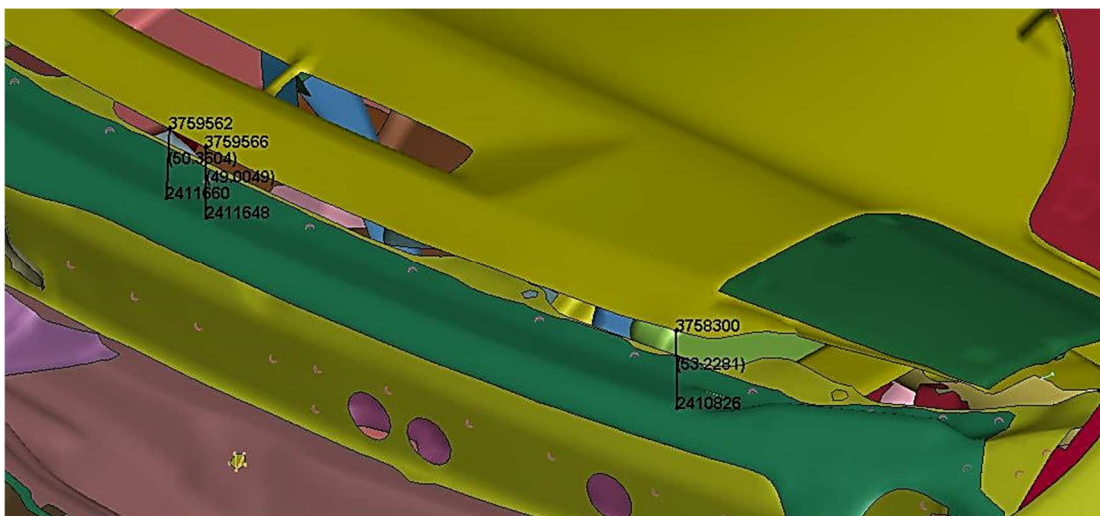
Overall, the sled model reproduces quite good the internal environment of a passenger sedan, but some adjustment could be done. The first step could be introducing the kinematics for the rigid sections obtained monitoring the full-scale model with THUMS on board over the simulation. This adjustment will make the simplified model more realistic, reducing the discrepancies between models. Another adaptation could be represented by the inclusion of the windshield into the model in order to detect eventually the interactions between its surface and the HBM. In addition, a driver airbag could be included into the FE environment, improving the effectiveness of the restrain system.

In the next future, this simplified model could be used to test different passive safety devices in a large variety of configurations, evaluating the effects on the human body. Since in the last few years the interest and the necessity to analyse crash tests involving autonomous vehicle is increased, several simulations must be performed in order to cover a large variety of scenarios. The computational lightness of the system and its ease of use could make this FE model a helpful tool for researches in safety field of future vehicles

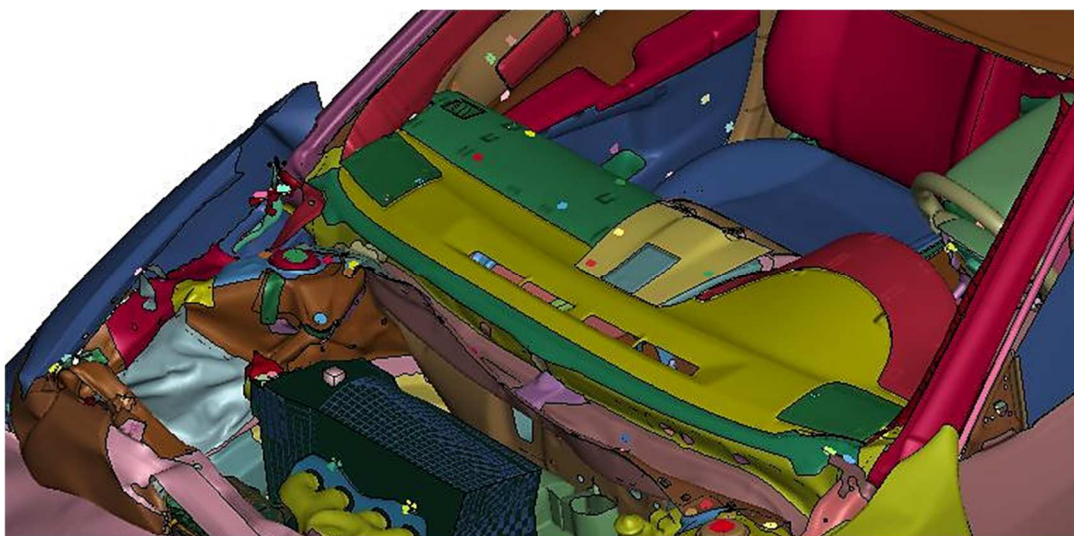
Appendix A

Dashboard constraining

During the comparison between the sled and the full-scale vehicle an unrealistic behaviour is detected in the dashboard of the simplified model. When the test is in progress, the upper part of the dashboard rises, and a huge displacement of the surface free edge is measured (about 50 mm, Figure 1) at the end of the simulation. The behaviour of the dashboard in full-scale model at 120 ms is exposes in Figure 2.

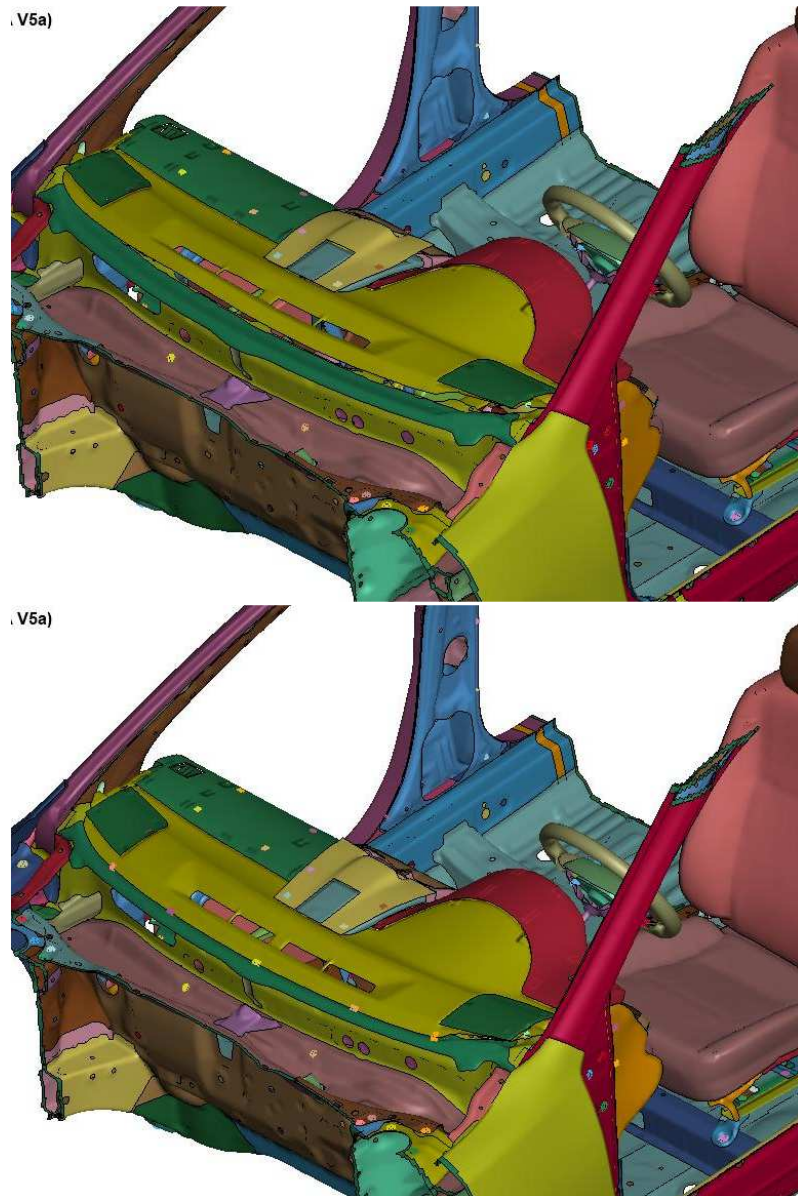


Appendix A 1 Detail of the dashboard free edge displacement in sled model at 120 ms



Appendix A 2 Detail of full-scale vehicle at 120 ms (windshield and hood are blanked)

This behaviour is due to the absence of vehicle windshield which limits the displacement of free edge in the z axis. In order to solve this problem, five CNRB are included, fixing properly the dashboard to the vehicle frame. In Figure 3, the comparison between the unconstrained sled and the constrained sled model is shown.



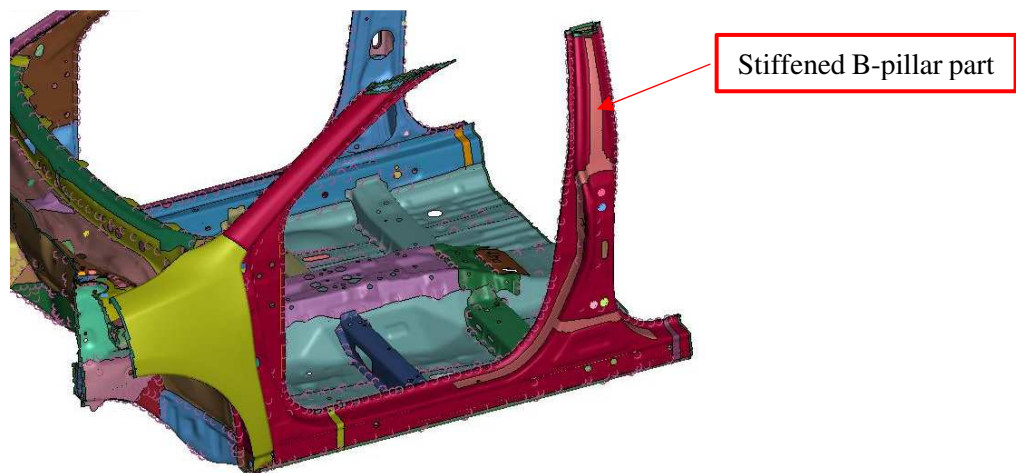
Appendix A 3 Comparison between unconstrained and constrained dashboard in sled model at 120 ms

B-pillar stiffening

During the modelling and cutting process the vehicle frame underwent a considerable weakening from the structural point of view, considerably reducing its rigidity. In particular, removing the roof of the car leads to a structural problem on pillars, especially on the top area. Since the D-ring is connect to the upper part of the B-pillar, excessive deformation could cause an important displacement of that belt anchor, leading to a different restraint configuration with respect to the full-scale model. In order to avoid this problem a stiffening process of the pillar is performed, obtaining a structure reinforcement incorporated in car frame. The properties of some elements in the pillar are changed to:

- *SECTION_SHELL with a thickness of 1 mm
- *MAT_RIGID where $\rho=7.89 \cdot 10^3 \text{ kg/m}^3$, $E=210\,000$, $\nu=0.3$ (as a structural steel)

The 1-millimeter thickness is applied because it is the same dimension found in the original unstiffened part whereas the material is considered as a structural steel for inertia properties and contact analysis (as the other structural parts). The final structure is shown in Figure 4.



Appendix A 4 Detail of the Stiffened B-pillar

References

- [1] Dekra, “Rapporto sulla Sicurezza Stradale,” 2018.
- [2] S. Alessandro, “Sicurezza passiva,” in *Costruzione dei Veicoli Terrestri*, 2019-2020.
- [3] “EuroNCAP,” [Online]. Available: <https://www.euroncap.com/en>.
- [4] “https://en.wikipedia.org/wiki/Euro_NCAP,” [Online].
- [5] A. N. H. Shinsuke Shibata, “Evaluation of Moving Progressive Deformable Barrier Test Method by Comparing Car to Car Crash Test,” Honda R&D Co., Ltd. Automobile R&D Center, Japan.
- [6] E. N. C. A. P. (EuroNCAP), “Full Width Frontal Impact Testing Protocol,” 2019.
- [7] e. a. L. Morello, “The Automotive Body, Vol. 2: System Design,” p. 463–558.
- [8] C. G. M. University, “Development & Validation of a Finite Element Model for the 2012 Toyota Camry Passenger Sedan,” May 2006.
- [9] D. B. H. P. C. K. a. K. O. D. Marzougui, “Development & Validation of a Finite Element Model for a Mid-Sized Passenger Sedan,” in *13th International LS_DYNA Users Conference*.
- [10] CCSA, “Vehicle modelling,” [Online]. Available: <https://www.ccsa.gmu.edu/models/>.
- [11] J. W. S. Brian J. Smyth, “Developing a Sled Test from Crash Test Data,” in *SAE World Congress & Exhibition*, 2007.
- [12] R. K. A. J. P. X.G. Tan, “A Comparative Study of the Human Body Finite Element Model Under Blast Loadings,” in *ASME-IMECE2012*, 2012.
- [13] T. C. R. L. I. TOYOTA MOTOR CORPORATION, “Total Human Model for Safety (THUMS) Documentation Academic Version 4.02_20150527,” 2015.

- [14] A. S. F. C. F. G. G. Belingardi, "Finite Element Simulation of Impact of Autonomous Vehicle with Human Body Model in Out-of-Position Configuration," 2019.
- [15] L. S. T. Corporation, "Occupant modelling workshop," 2015.
- [16] L. S. T. Corporation, "LS-DYNA user's manual," 2017.
- [17] Y. L. P. P. P. B. Thomas Janak, "Transformation Smoothing to use after Positioning of Finite Element Human Body Models," in *IRCOBI Conference*, 2018.
- [18] PIPER, "www.piper-project.org," [Online].
- [19] EuroNCAP, "The Car Selection Explained," [Online]. Available: <https://www.euroncap.com/en/about-euro-ncap/the-car-selection-explained/>.
- [20] C. A. o. R. S. Professionals, "Seat Belt Load Limiters," [Online]. Available: <http://www.carsp.ca/research/resources/high-tech-vehicle-safety-systems/seat-belt-load-limiters/>.

Acknowledgments

First of all, I would like to acknowledge my academic supervisor Eng. Scattina Alessandro for following me during this thesis work. In addition, I would like to thank Germanetti Filippo for sharing with me his experience and knowledge in the fields of crash test and Finite Element modeling. A thank you goes to Area IT of Polytechnic of Turin for their precious help in software and connection management. Finally, I would like to acknowledge the CCSA at GMU and the FHWA for shearing the FE car models and allowing so to develop this work.

Inoltre, vorrei ringraziare tutte le persone che mi sono state vicino durante questo percorso di laurea, sin da quando sono partito per Torino. Un particolare ringraziamento va alla mia famiglia; mia madre Regina, mio padre Ruggero e le mie sorelle Isabella e Sofia che mi hanno sempre sostenuto durante la mia permanenza al Politecnico. Un grazie molto speciale va a mio nonno paterno Francesco e mia nonna materna Marcellina che sempre mi hanno spronato a studiare e dare il meglio di me. Ringrazio gli zii Fabrizio, Daniela, Massimiliano e Giuseppe che hanno sempre creduto in me e mi sono stati vicini, portando gioia e risate. In fine vorrei ringraziare tutti gli amici, d'infanzia, di scalata, di studio, di festa, per il loro costante supporto e per aver condiviso con me, in questi anni, momenti indimenticabili che non scorderò mai scorderò. Grazie a tutti.